FERROHYDRODYNAMICS STUDIES THROUGH BROWNIAN DYNAMICS SIMULATIONS OF SPHERICAL NANOPARTICLE SUSPENSIONS

by

Denisse Soto-Aquino

A dissertation submitted in partial fulfillment of the requirements for the degree of

DOCTOR OF PHILOSOPHY
in
CHEMICAL ENGINEERING

UNIVERSITY OF PUERTO RICO
MAYAGUEZ CAMPUS
2012

Approved by:

Carlos Rinaldi, PhD President of the Graduate Committee	Date
Julio Briano, PhD Member, Graduate Committee	Date
Aldo Acevedo, PhD Member, Graduate Committee	Date
Stefano Leonardi, PhD Member, Graduate Committee	Date
Paul Sundaram, PhD Representative of the Graduate Studies	Date
Aldo Acevedo, PhD Interim Chairman of the Department of Chemical Engineering	Date

Ferrohydrodynamics Studies Through Brownian Dynamics Simulations of Spherical Magnetic Nanoparticle Suspensions

by Denisse Soto-Aquino
Submitted to the Department of Chemical Engineering
on May 1, 2012, in partial fulfillment of the requirements for the degree of
Doctor of Philosophy

ABSTRACT

In this contribution, Brownian dynamics simulations of spherical, thermally blocked, magnetic nanoparticles under applied shear and magnetic fields were studied. Equilibrium and dynamical properties as well as rheological properties and energy dissipation rates of a dilute system were obtained. The algorithm describing the change in the magnetization and magnetoviscosity of the suspension was derived from the stochastic angular momentum equation. Simulation results were compared with the predictions of suspension-scale models based on three magnetization relaxation equations for different situations: i) constant magnetic field and shear flow, ii) transient response of magnetic and shear flow, iii) oscillatory shear flow with constant magnetic fields, and iv) alternating magnetic field for energy dissipation rate determination. For all the conditions studied, excellent agreement is observed between simulation results and the predictions of an equation due to Martsenyuk, Raikher, and Shliomis. From simulation results at constant magnetic field over a wide range of conditions, master curves were obtained using a newly defined Mason number based on the balance of hydrodynamic and magnetic torques. From the transient response studies, both simulations and analysis show that the transient approach to a steady state magnetoviscosity can be either monotonic or oscillatory depending on the relative magnitudes of the applied magnetic field and shear rate. Simulations for the dynamic properties of ferrofluids under oscillatory shear and constant magnetic fields show an apparent elastic character to the rheology of these suspensions. Energy dissipation rates were obtained from the dynamical magnetization properties and compared with Rosensweig's energy dissipation model. Results show that Rosensweig's original analysis is strictly limited to low magnetic field amplitude and frequency. Finally, a Brownian dynamics simulation algorithm for interacting particles was developed. Simulation results for the equilibrium properties of magnetized particles show agreement with theoretical models, but fail to predict dynamic properties.

Ferrohydrodynamics Studies Through Brownian Dynamics Simulations of Spherical Magnetic Nanoparticle Suspensions

by Denisse Soto-Aquino
Submitted to the Department of Chemical Engineering
on May 1, 2012, in partial fulfillment of the requirements for the degree of
Doctor of Philosophy

RESUMEN

En esta contribución, simulaciones de dinámica browniana de partículas esféricas, con dipolos fijos en su estructura, bajo campos magnéticos y esfuerzos cortantes han sido estudiadas. Se obtuvieron propiedades magnéticas en equilibrio y dinámicas, así como las propiedades reológicas y la razón de disipación energética del sistema en el límite de dilución. El algoritmo que describe el cambio en la magnetización y magnetoviscosidad de la suspensión se deriva de la ecuación de momento angular estocástica. Resultados de la simulación fueron comparados con las predicciones de modelos a escala en suspensión sobre la base de tres ecuaciones que describen la relajación de magnetización en diferentes condiciones: i) flujo y campo magnético constante, ii) la respuesta transitoria del campo magnético y de flujo, iii) flujo de corte oscilatorio a campo magnético constante y iv) campo magnético alternante para la determinación de la disipación de energía. Para todas las condiciones estudiadas, un excelente acuerdo fue observado entre los resultados de la simulación y las predicciones de la ecuación desarrollada por Martsenyuk, Raikher y Shliomis. De los resultados de simulación en campo magnético constante en un amplio intervalo de condiciones, curvas maestras fueron obtenidas utilizando una nueva definición del número de Mason basado en el balance de torque hidrodinámico y magnético. De los estudios de respuesta transitoria, tanto simulaciones como el análisis matemático muestran que el estado transitorio a una magnetoviscosidad en estado estacionario puede ser monótona o oscilatoria en función de las magnitudes relativas del campo magnético aplicado y la velocidad de flujo. Simulaciones para las propiedades dinámicas de ferrofluidos bajo campos magnéticos constantes y esfuerzos oscilatorios muestran un carácter elástico aparente en las propiedades reológicas de estas suspensiones. La razón de disipación de energía fue obtenida de las propiedades dinámicas de la magnetización y fue comparada con el modelo de Rosensweig de disipación de energía. Los resultados muestran que el análisis original de Rosensweig es estrictamente limitado a campos magnéticos y frecuencia bajas. Por último, simulaciones de

dinámica browniana para partículas que interactúan fue desarrollado. Resultados de la simulaciones para las propiedades de equilibrio de las partículas magnetizadas muestran estar en acuerdo con los modelos teóricos, pero no para predecir las propiedades dinámicas.

DEDICATION

TO MY FAMILY

María A. Aquino, Janice Soto-Aquino, and Rafael J. Soto-Aquino

ACKNOWLEDGMENTS

From my family to friends, from the University to the staff of the Chemical Engineering Department; there are so many people to say thanks, people that in some way give me their guidance, support, make me laugh or gave me their help when I needed it. First, I want to thank God, for being with me every day of my life. Thanks to my family: my brother Rafael and sister Janice, especially to my mom, my hero, the wonderful woman who taught me that dreams can come true and that obstacles are just a hard way of learning in life. I am grateful to my boyfriend Leonardo Fernandez, for being my friend and support.

Thanks to the Chemical Engineering Department at the University of Puerto Rico, Mayaguez, for giving the opportunity to study the PhD. In addition, thanks to the staff that in various ways helped me with administrative stuff. Special thanks to Sr. Zapata for all the technical support that he gave me during these years. I am grateful to my advisor Dr. Carlos Rinaldi, for his support, guidance and faith in me which made possible the successful completion of this dissertation. Thanks to my committee members: Dr. Leonardi, Dr. Briano, and Dr. Acevedo. Special thanks to Dr. Gustavo Lopez from the Chemical Department at the University of Puerto Rico, Mayaguez, for his guidance and mentoring.

I am deeply grateful to my extended family, my friends: Edmarie Berrios, Ana G. Arevalo, Vivian Florian, Yeira Padilla, Victoria Calero, Jorge H. Sanchez, Maik Irrazabal, Isaac Torres, Misael Diaz, among others, for being with me in both good and bad times. Also thanks to my labmates: Roberto Olayo, Mar Creixell, Sergio Sierra, Adriana Herrera as well as my friends from the Department and my town: Amarilys Carde, Veronica Rodriguez, Lidiany Gonzalez, Corelis Zayas, Jennie Feliciano, Shirley Caban, Karian Perez, Rafael Ruiz, Josue Cruz, and my

best friend Erick Santiago. Thanks for their friendship and support, for making me laugh and all the good times that we had during years.

I want to thank to Dr. Juan de Pablo and Dr. Moreno-Razo, and the NSEC Program, from University of Wisconsin, Madison, for the support and help to accomplish my projects. I want to acknowledge the BDP-PR LSAMP Program, for their financial support.

CONTENTS

LIST OF FIGURES

1

1 INTRODUCTION

Fluids that can be effectively controlled by magnetic fields of moderate strength are a challenging subject for scientists interested in the basics of fluid mechanics as well as for practical applications in engineers. Due to the fact that no natural liquids offer these features, the starting point of the field of magnetic fluid research can be found in theoretical treatments of magnetically controlled heat transfer machines. Since these early ideas already showed that a liquid material with controllable magnetic properties would provide a wide range of development possibilities, significant efforts have been undertaken to synthesize such fluids. After the first stable synthesis of a magnetically controlled fluid in the early 1960's, the development of the so-called ferrofluids has provided a high potential for new research and the development of the field of ferrohydrodynamics. Several hundred scientific publications per year and thousands of patents document ferrofluid research as an emerging field, as shown in Figure 1.1. In this Chapter we present definitions and concepts to provide an understanding of the topic.

1.1 FERROFLUIDS

Ferrofluids are suspensions of magnetic nanoparticles in an ordinary non-conducting non-magnetic liquid. Typically, the fluid in which the particles are dispersed is water or an organic solvent. The particles in a ferrofluid typically consist of single magnetic domains and have an average diameter of ~10 nm (see **Figure 1.2**). In addition, they are coated with a surfactant to prevent the particles from aggregating due to magnetic and van der Waals attraction. The repulsion due to the surfactants must be strong enough to prevent agglomeration even when a magnetic field is applied. The magnetic nanoparticles in ferrofluids are commonly magnetite, maghemite (γ-Fe_2O_3), and magnetic ferrites, such as cobalt ferrite or manganese ferrite and the surfactants used vary depending on the application [1, 2].

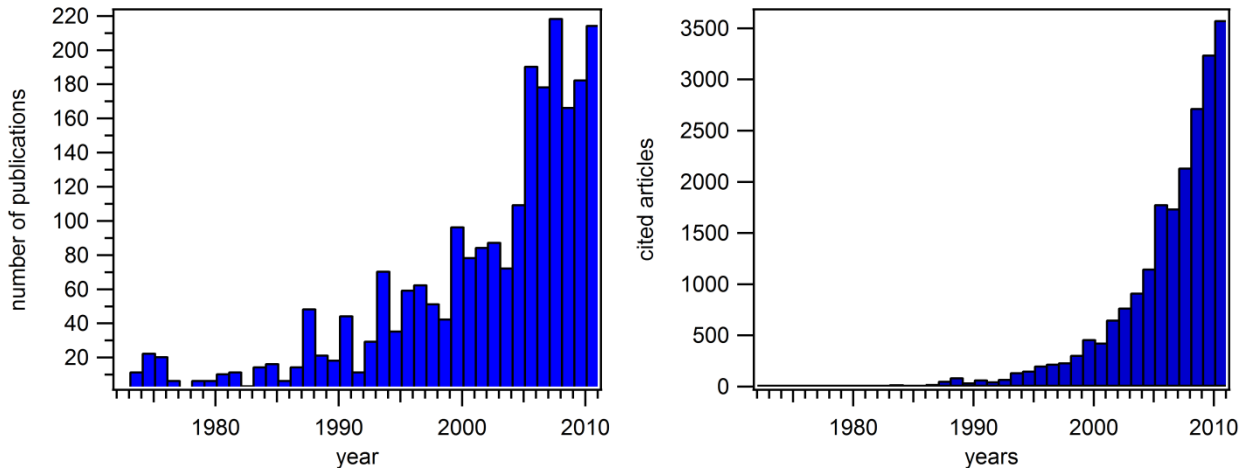

Figure 1.1 a) Papers per year and b) cited articles per year with the keyword ferrofluid according to Web of knowledge

Since the invention of magnetic fluids in 1964, ferrofluids have been considered as a promising material for many applications, ranging from mechanical applications such as dampers, seals, and heat transfer fluids [3-6], to biomedical applications such as cancer treatment by magnetic hyperthermia [7, 8] and drug delivery [9-11]. The use of magnetic fluids has attracted

attention over the last decades because they exhibit functional magnetic [12-14] and rheological properties [15-23], when subjected to an external magnetic field. Several phenomena such as viscosity increases in constant magnetic fields [24, 25], the so-called "negative viscosity effect" [26-29] in oscillating magnetic fields, and field induced flow in uniform rotating magnetic fields [30-33] have been observed, leading to open a wide range of possibilities in many applications in science and engineering, as is evident from the increment in publications during the last decades, as shown in **Figure 1.1**.

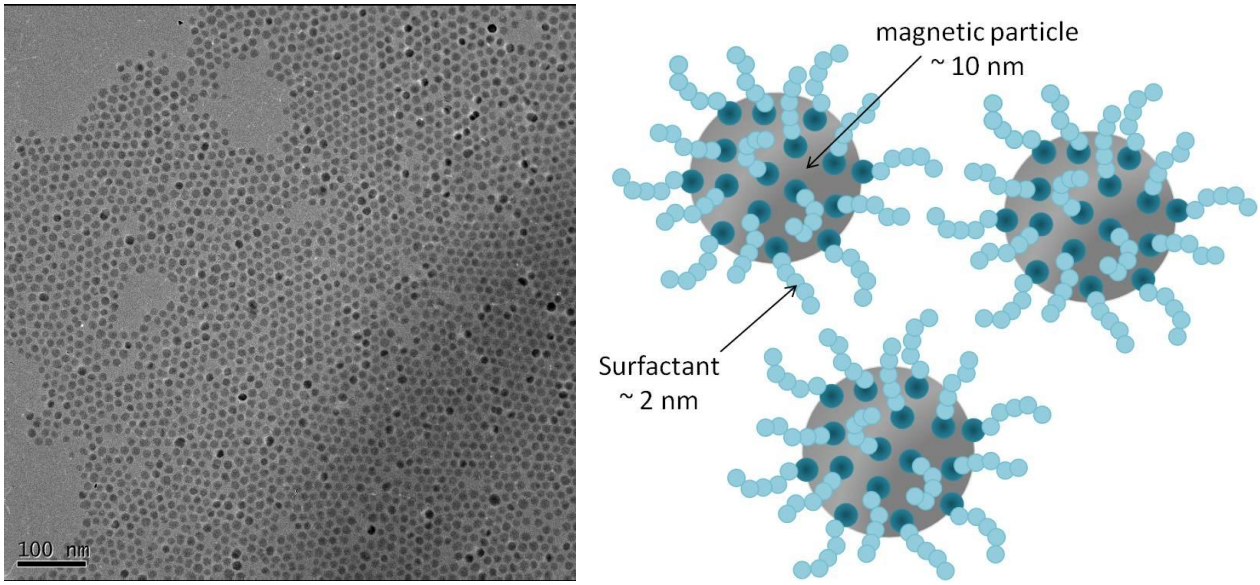

Figure 1.2 a) TEM image of cobalt ferrite particles. b) Sketch of the magnetic nanoparticles in the ferrofluid.

1.2 MAGNETIC PROPERTIES OF A FERROFLUID

When a constant magnetic field, **H**, is applied to a ferrofluid, it exerts a torque $\mathbf{T}_m = \mu_0(\boldsymbol{\mu} \times \mathbf{H})$, where μ_0 is the permeability of free space, tending to align the magnetic moments of the particles orient along the field direction. In a gradient field the whole fluid responds as a homogeneous magnetic liquid, moving to the region of highest magnetic flux. This implies that ferrofluids can be precisely positioned and controlled by external magnetic fields.

The torque exerted on the particles tends to align their magnetic dipole moment, **m**, which can be calculated from

$$\boldsymbol{m} = \frac{1}{V}\sum_{i=1}^{n}\boldsymbol{\mu}_i , \tag{1.1}$$

with the applied magnetic field. Here V is the volume of the suspension and n is the number of particles. In the absence of a magnetic field, the magnetic moments of the particles are randomly distributed and the fluid has no net magnetization. In order to describe the behavior of ferrofluids under certain conditions of magnetic and flow fields various theories have been developed such as the Langevin function, to determine the equilibrium magnetization of the suspension, and Debye's theory, which describes the dynamic magnetization of a suspension of spherical particles suspended in a Newtonian fluid. Because of their relevance in subsequent chapters, these theories are described below.

1.2.1 EQUILIBRIUM MAGNETIZATION AND THE LANGEVIN FUNCTION

In the absence of an applied magnetic field, the particles are randomly oriented and the suspension has no net magnetization. When the suspension is subjected to an external magnetic field the magnetic dipole moments of the particles tend to align along the direction of the applied magnetic field either by particle rotation or by dipole moment rotation within the particle. For low field strengths this tendency is partially overcome by thermal agitation, but as the magnetic field strength increases the magnetic dipoles of the particles become increasingly aligned with the field direction, until achieving a saturation state where the dipoles are almost completely aligned with the magnetic field.

Consider a collection of single domain magnetic particles suspended in a nonmagnetic carrier fluid. The magnitude of the torque on each particle exerted by an external magnetic field is given by

$$\mathbf{T} = \mu_0 \boldsymbol{\mu} \mathbf{H} \sin\theta . \tag{1.2}$$

In Eqn (1.2), θ is the angle between $\boldsymbol{\mu}$ and $\mathbf{H}$ in orientation space (which is represented by a unit sphere). The energy necessary to turn the dipole to an angle θ is

$$W = \int_0^\theta T d\theta = \mu_0 \mu H \left(1 - \cos\theta\right), \tag{1.3}$$

where W is the work stored as potential energy. Thermal agitation opposes this alignment, thus, Boltzmann statistics describes the number of dipoles having energy W as [1]

$$n_d\left(\theta,\phi\right) = \frac{N_d\,\alpha}{4\pi \sinh\alpha} e^{\alpha\cos\theta}, \tag{1.4}$$

where N_d is the total number of dipoles, $\alpha = {\mu_0 \mu H}\big/{k_B T}$, being k_B the Boltzmann's constant, and T the absolute temperature. We are interested just in particles with their dipoles forming an angle θ with the field; then, integrating (1.4) over ϕ, we get that

$$n_d\left(\theta\right) = \frac{N_d \alpha}{2\sinh\alpha} e^{\alpha\cos\theta}. \tag{1.5}$$

The effective magnetic dipole moment of a particle is its component along the field direction, i.e. $\mu\cos\theta$. Therefore, the average value of $\mu\cos\theta$ is given by

$$\left\langle \mu\cos\theta \right\rangle = \frac{\int_0^\pi \mu\cos\theta\, n_d\left(\theta\right)\sin\theta d\theta}{\int_0^\pi n_d\left(\theta\right)\sin\theta d\theta} = \mu\left(\coth\alpha - \frac{1}{\alpha}\right). \tag{1.6}$$

Let n be the number of particles in a unit volume of fluid, then, the magnetization m along the magnetic field direction is $m = n\left\langle \mu\cos\theta \right\rangle$, and its saturation value m_s, in terms of the dipole of

the particles, is $m_s = n\mu$. Therefore, from Eqn (1.6), the dimensionless magnetization of the suspension becomes

$$\tilde{m} = \frac{m}{m_s} = \coth\alpha - \frac{1}{\alpha} \equiv L(\alpha), \tag{1.7}$$

where $L(\alpha)$ denotes the *Langevin function* and α is the Langevin parameter. The magnetization curve, shown in **Figure 1.3** compare with simulations for equilibrium magnetization, saturates at high values of α where the magnetic field dominates the Brownian torque, resulting in particles with their magnetic dipole moments almost aligned in the field direction. On the other hand, at low α , the rotational Brownian motion dominates and the particles have random orientations as shown in **Figure 1.4**.

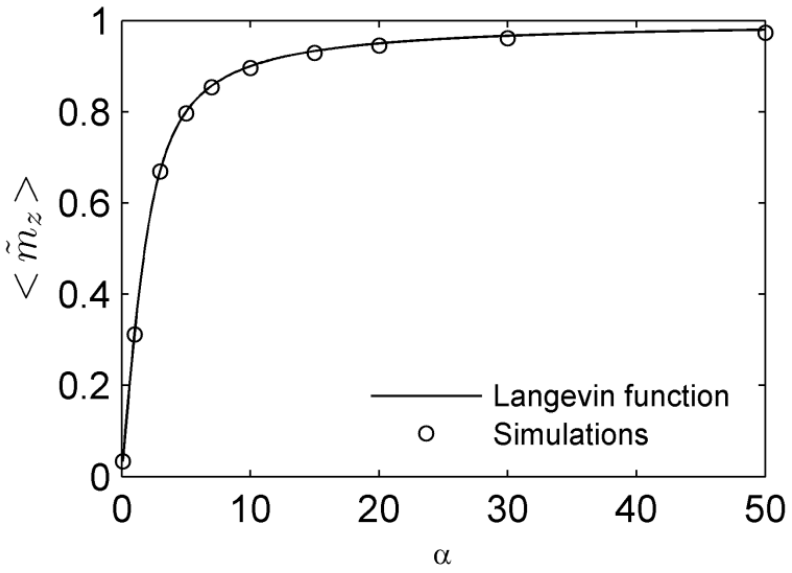

Figure 1.3 Dimensionless equilibrium magnetization as a function of Langevin parameter

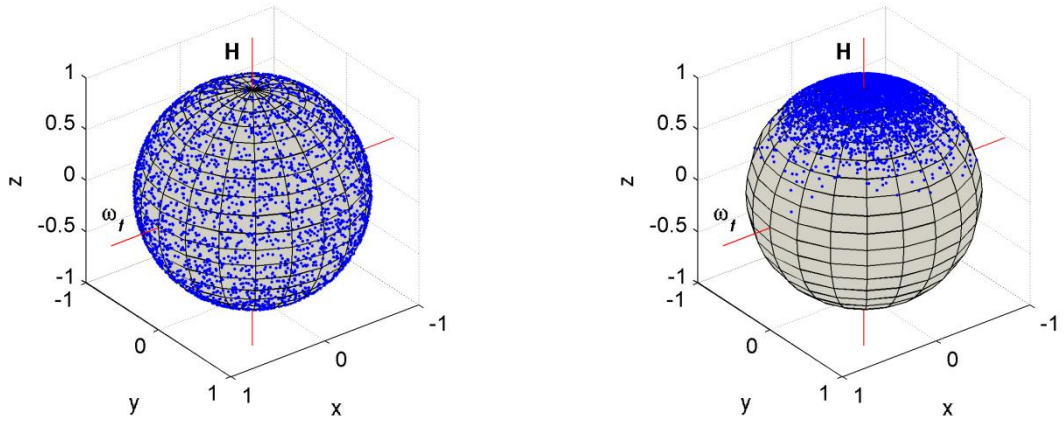

Figure 1.4 Orientation of the distributions of the magnetic dipole moments of the magnetic particles of a) $\alpha = 0$ and b) $\alpha = 100.0$. Each dot corresponds to a particle with its magnetic dipole aligned with the corresponding point in the unit sphere.

1.2.2 DYNAMIC MAGNETIZATION AND THE DEBYE MODEL

There are two mechanisms by which the particle's magnetic dipole moment may relax in a ferrofluid: Brownian relaxation and Néel relaxation [1]. Brownian relaxation occurs if the magnetic moment of the particle is fixed in its crystal structure while in Néel relaxation the magnetic moment may rotate inside the particle [34]. In Brownian Relaxation, particles imply rotation of the whole particle and is characterized by a Brownian relaxation time having hydrodynamic origin. In order to obtain a model for this relaxation mode of the magnetization, it is necessary to solve the Smoluchowski equation for the orientational distribution function *f* of the magnetic dipole moments, which in vectorial form is written as [35]

$$\frac{\partial f}{\partial t} = \nabla_{\Phi} \cdot \left(\mathbf{D}_r \cdot \nabla_{\Phi} f \right) - \nabla_{\Phi} \cdot \left(\mathbf{T}_m \cdot \zeta_r^{-1} \right) f \, . \tag{1.8}$$

In (1.8) ∇_{Φ} is the differential operator in orientation space, $\mathbf{D}_r$ is the rotational diffusion tensor given by the generalized Stoke-Einstein equation as $\mathbf{D}_r = \left(k_B T \right) \boldsymbol{\zeta}^{-1}$, and ζ is the rotational hydrodynamic resistance dyadic. We are only interested in solutions that are dependent on the

zenithal angle θ because it alone enters into the potential energy of the permanent dipole in the external field, as shown in Section 1.2.1. For the particular case of isotropic particles, the rotational hydrodynamic resistance is expressed by only one constant ζ_r. Thus, for a constant magnetic field $\mathbf{H} = H_0 \mathbf{i}_z$, and Eqn (1.8) would be written as

$$\frac{\zeta_r}{k_B T}\frac{\partial f}{\partial t} = \frac{1}{\sin\theta}\frac{\partial}{\partial \theta}\left(\sin\theta \frac{\partial f}{\partial \theta}\right) + \frac{\mu_0(\mu H_0)}{k_B T}\frac{1}{\sin\theta}\frac{\partial}{\partial \theta}\left(\sin^2\theta f\right). \tag{1.9}$$

Solving Eqn (1.9) for small values of the Langevin parameter $\alpha << 1$, the expression for the mean dipole of the system, $\langle \mu\cos\theta \rangle = \int \mu\cos\theta f \sin\theta d\theta$, is used to obtain the dimensionless magnetization of the suspension $\tilde{m}_z(t) = \langle \mu\cos\theta \rangle / \mu$. Two special situations are readily obtained: (i) relaxation upon switching off the field, and (ii) response to an oscillating field. In the first case, we assume that the system is at equilibrium with an external magnetic field at $t = 0$, and suddenly the field is turned off, $H_0 = 0$, for $t > 0$. At $t = 0$ the distribution function is given by Eqn (1.5)

$$f(t=0) = \frac{\alpha}{2\sinh\alpha} e^{\alpha\cos\theta}, \tag{1.10}$$

where (1.10) can be expanded to first order in the Langevin parameter as

$$f(t=0) = \frac{\alpha}{2\alpha}\left[1 + \alpha\cos\theta + O(\alpha^2)\right] = \frac{1}{2}\left(1 + \frac{\mu_0\mu\cos\theta}{k_B T}\right). \tag{1.11}$$

This suggests an orientation distribution function in Eqn (1.9) of the form

$$f == \frac{1}{2}\left(1 + \frac{\mu_0\mu\cos\theta}{k_B T} g(t)\right). \tag{1.12}$$

Since $H_0 = 0$ for $t > 0$, and substituting Eqn (1.12) in Eqn (1.9) we obtain that $g = e^{-t/\tau_B}$, where $\tau_B = \zeta_r / (2k_B T)$ is called the Debye (or Brownian) relaxation time. This result for the function g is then used to obtain the dimensionless magnetization, along the magnetic field direction, of the suspension

$$\tilde{m}_z = \frac{1}{3}\alpha \exp\left(-t/\tau_B\right). \tag{1.13}$$

In the case of a weak external oscillating magnetic field, $\mathbf{H} = H_0 \cos(\Omega t)\mathbf{i}_z$, the dipole moment of the particles follows the oscillations of the magnetic field with a phase lag between the field and the particles. The *z*-component of the dimensionless magnetization is then

$$\tilde{m}_z = \left(\frac{1}{3}\alpha\right)\mathrm{Re}\left\{\hat{\chi}e^{j\Omega t}\right\} = \left(\frac{1}{3}\alpha\right)\left[\tilde{\chi}'\cos(\Omega t) + \tilde{\chi}''\sin(\Omega t)\right], \tag{1.14}$$

where $\hat{\chi} = \tilde{\chi}' - j\tilde{\chi}''$ is the dimensionless complex susceptibility. Nondimensional in-phase and out-of-phase susceptibilities $\tilde{\chi}'$, $\tilde{\chi}''$ respectively are frequency dependent

$$\tilde{\chi}' = \frac{1}{1+(\Omega\tau)^2}, \quad \tilde{\chi}'' = \frac{(\Omega\tau)}{1+(\Omega\tau)^2}. \tag{1.15}$$

On the other hand, in Néel relaxation, the magnetic moment aligns without physical rotation of the particle. This kind of relaxation takes place if the thermal energy overcomes the energy barrier provided by the magnetocrystalline anisotropy of the magnetic material. The Néel relaxation time is typically modeled using the expression:

$$\tau_N = \tau_0 \exp\left(\frac{KV_c}{k_B T}\right), \tag{1.16}$$

where τ_0 is a decay time between 10^{-10} to 10^{-8} sec., K is the magnetocrystalline anisotropic constant, and V_c is the volume of the magnetic core of the particle. It is important to note that

both relaxation mechanisms are particle size dependent, and thus, for a monodisperse suspension, the effective magnetic relaxation time τ will follow the shorter process, according to

$$\tau = \frac{\tau_B \tau_N}{\tau_B + \tau_N}. \tag{1.17}$$

As shown in **Figure 1.5**, the transition from Néel to Brownian relaxation time may be considered to take place for particles with a size d_s obtained by equating τ_B and τ_N ; thus, $d_s = 8.5$ nm for iron and $d_s = 4$ nm for cobalt [1]. Although, the Néel mechanism is not considered further in this thesis (we assume a suspension of magnetic particles with particle-locked magnetic dipole moments), it is valuable to review some of the work on both mechanisms in the ferrofluid literature to obtain a better understanding of the relevance of the relaxation mechanism.

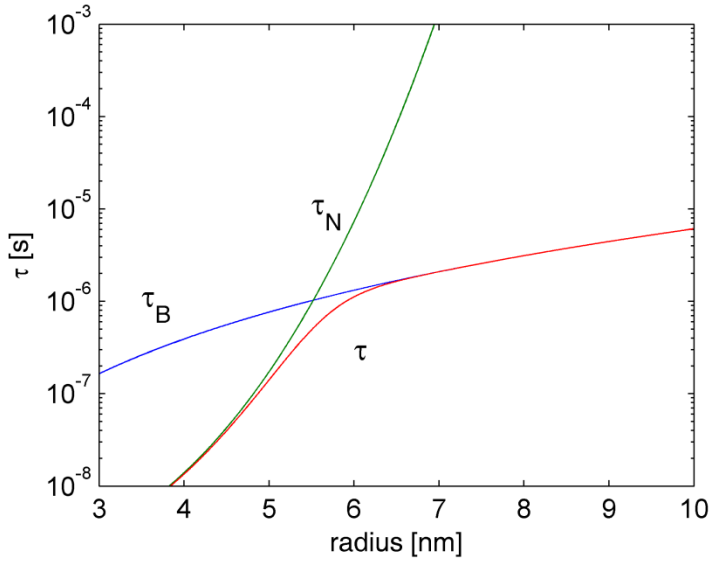

Figure 1.5 Relaxation times as function of the particle radius of magnetite for a anisotropy constant equal to 14 kJ m^{-3} and a water viscosity of 0.002 kg/m^2 s at room temperature of 298 K

1.2.3 ANALYSIS OF SIMULTANEOUS BROWNIAN AND NÉEL RELAXATION MECHANISMS IN FERROFLUIDS

A long-standing problem in the theory of magnetic relaxation of ferrofluids is how the Néel mechanism of relaxation (i.e. internal rotation of the magnetic dipole moment with respect to the crystalline axes inside the particle) and the Brownian relaxation (due to physical rotation of the ferrofluid particle in the carrier fluid) may be treated in the context of a single model comprising both relaxation processes [34]. This question was answered in part by Shliomis and Stepanov [36, 37], who showed that for uniaxial anisotropy, for weak applied magnetic fields and in the non-inertial limit, the equations of motion of the ferrofluid particle incorporating both the internal and the Brownian relaxation processes decouple from each other. Thus the reciprocal of the greatest relaxation time is the sum of the reciprocals of the Néel and Brownian relaxation times. Scherer and Matuttis [38] proposed another treatment using a generalized Lagrangian formalism; however, in the discussion of the applications of their method they limited themselves to a Néel and a Brownian mechanism independently. Coffey and Fannin [39] re-examined the Shliomis and Stepanov model taking into consideration the ratio between Néel and Brownian relaxation times. With this assumption they demonstrated that the Langevin equation for the Brownian rotational motion of the particle itself reduces to that describing Debye relaxation in the applied field but is coupled to the magnetic motion via the external field.

Because there is no full understanding of the relaxation mechanism, it is commonly accepted that the magnetization of a ferrofluid relaxes from one equilibrium value to another through a combination of Brownian and Néel mechanisms. If one assumes both processes occur in parallel the result is that the effective relaxation time is dominated by the faster of the two processes, as shown in Eqn (1.17). As the number of applications of ferrofluids in time varying magnetic fields increases it becomes increasingly important to understand, in a quantitative

manner, how the relaxation time of a suspension of magnetic nanoparticles depends on the intrinsic, nanoscale properties of the particles. Relaxation times of ferrofluids have been utilized for quantification of biological binding processes, efficiency of magnetic inductive hyperthermia, and magnetic resonance imaging. In addition, the rate of magnetization relaxation is a crucial parameter to consider feasibility in magnetic data storage applications [40, 41]. Simulations become an important tool to understand the relaxation mechanism.

Several simulation studies have explored relaxation mechanisms in ferrofluids using Brownian dynamics simulation [42-45]. In the modeled system, the nanoparticles are so diluted that the magnetic interparticle interaction is negligible. In general, these simulations assume that the effective relaxation time is due to contributions of Brownian and Néel mechanism; assuming that the dominant mechanism of magnetization of a particle will be that which has the shortest relaxation time. Otherwise they just assume that particles relax through just one mechanism.

1.2.4 MAGNETIZATION OF UNIAXIAL SWITCHING PARTICLES

As explained before the two mechanisms responsible for magnetic relaxation in nanoparticles are the physical rotation of the individual particles in the fluid (Brownian relaxation) and the collective rotation of the atomic magnetic moments within each particle (Néel relaxation). We have developed a Brownian Dynamics algorithm to model the Brownian and Néel relaxation mechanisms in a suspension of non-interacting magnetic nanoparticles by assuming that the time scale for the Néel mechanism is much faster than that for Brownian relaxation.

If it is assumed that the dipole within each particle switches instantaneously along the easy axis such that the dipole always has a positive component along the field direction, in the condition in which the external field is equal to zero the behavior of a collection of particles will

be discontinuous. For $\mathbf{H}=0$ the magnetization will be zero not yet for infinitesimal $\mathbf{H}$ it will not be zero. The orientation distribution of the particles is a function solely of the zenithal angle θ in a spherical coordinate system wherein the radial vector is $\mathbf{e_z}=\mathbf{e_r}$. Under such conditions one obtains

$$\frac{\delta f(\theta)}{\delta \underline{\phi}}=\hat{\underline{\phi}}\frac{\partial f}{\partial \theta} \qquad \frac{\delta E_m}{\delta \underline{\phi}}=\hat{\underline{\phi}}\frac{\partial E_m}{\partial \theta}, \tag{1.18}$$

where the magnetostatic energy E_m is given by

$$E_m=-\mu_0\mathbf{m}\bullet\mathbf{H}=\begin{cases}\mu_0 mH\cos\theta & if \quad \mathbf{e_z}\bullet\mathbf{i_z}>0\\ -\mu_0 mH\cos\theta & if \quad \mathbf{e_z}\bullet\mathbf{i_z}<0\\ 0 & if \quad \mathbf{e_z}\bullet\mathbf{i_z}=0\end{cases}. \tag{1.19}$$

The equilibrium orientation distribution must therefore be

$$f(\theta)=\begin{cases}c\exp(-\alpha\cos\theta) & for \quad \theta<\pi/2\\ c\exp(\alpha\cos\theta) & for \quad \theta>\pi/2\\ 0 & for \quad \theta=\pi/2\end{cases} \tag{1.20}$$

The normalization constant is obtained from

$$\int_0^{\pi} f(\theta)\sin\theta d\theta=1 \tag{1.21}$$

to obtain that

$$c=\frac{1}{2}\frac{\alpha}{(\exp(\alpha)-1)}. \tag{1.22}$$

The equilibrium orientation distribution is obtained as

$$f(\theta)=\begin{cases}\dfrac{\alpha}{2}\dfrac{\exp(\alpha\cos\theta)}{\exp(\alpha)-1} & for \quad \theta<\pi/2\\ \dfrac{\alpha}{2}\dfrac{\exp(-\alpha\cos\theta)}{\exp(\alpha)-1} & for \quad \theta>\pi/2\\ 0 & for \quad \theta=\pi/2\end{cases} \tag{1.23}$$

Then, the mean magnetization of a collection of particles is given by

$$\frac{\langle m_z\cos\theta\rangle}{m}=\frac{\exp(-\alpha)-(1-\alpha)}{(1-\exp(-\alpha))\alpha}. \tag{1.24}$$

In the limit that $\alpha\to\infty$ the model agrees with Langevin at high fields.

If Eqn (1.24) is compared with the Langevin function as shown in **Figure 1.6**, it is seen that the magnetization curve saturates at high field, $\alpha > 10$, where the magnetic field dominates the Brownian forces resulting in particles with their magnetic dipole moments almost aligned in the field direction.

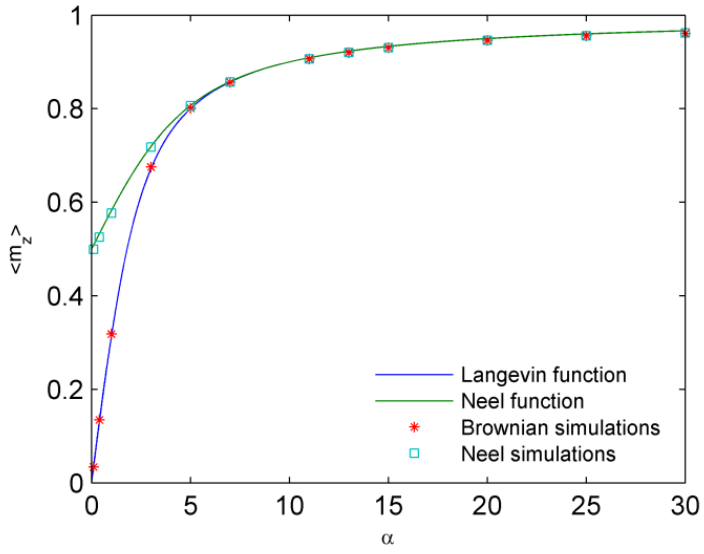

Figure 1.6 Dimensionless equilibrium magnetization from simulations of Néel and Brownian particles as function of the Langevin parameter compared with Langevin function and Eqn (1.24)

1.3 THE MAGNETOVISCOUS EFFECT

One of the most attractive properties of ferrofluids is the possibility of exerting an influence on their flow and physical properties by means of moderate magnetic fields. So long as there is no external magnetic field and the particle concentration is not too high the properties of the suspension are close to the properties of the suspending liquid, and the viscosity satisfies the formula obtained by Einstein

$$\eta = \eta_0 \left(1 + \frac{5}{2} \tilde{\phi} \right). \tag{1.25}$$

Here η_0 stands for the viscosity of the carrier liquid, η for the viscosity of the suspension in the absence of a magnetic field, and $\tilde{\phi}$ denotes the volume fraction of all suspended material. If a magnetic field is applied to the suspension the particles will rotate relative to the fluid resulting in a change in viscosity and the Einstein result is no longer applicable.

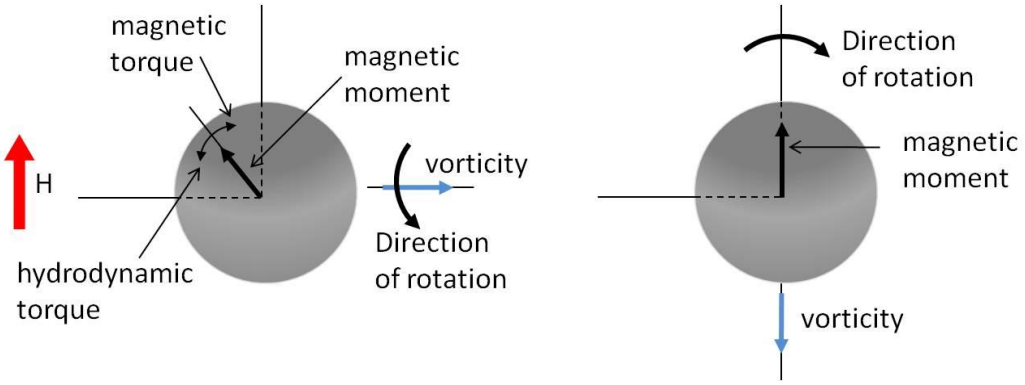

Figure 1.7 Schematic diagram of the origin of rotational viscosity in a ferrofluid

In a suspension of magnetic particles with particle-locked magnetic dipole moments, i.e. particles relaxing by the Brownian relaxation mechanism, if a magnetic field is applied to the suspension under shear, there are two situations of interest (see **Figure 1.7**). First, we can consider that the applied field is perpendicular to the vorticity of the flow. In this situation the magnetic

field will tend to align the magnetic moment with the field direction while the viscous torque exerted by the flow tends to rotate the particle and thus will produce a misalignment of magnetic moment and field. This misalignment will give rise to a magnetic torque to realign the moment and thus counteracting the viscous torque preventing the free rotation of the particle in the flow and giving rise to an apparent increase of the fluid viscosity. The second case has the field applied collinear with vorticity. In this case the magnetic moments will be aligned in the direction of the field and because it is identical to the axis of rotation of the particle no field influence on the rotation of the particle will be observed.

The first experimental report of changes in viscosity due to a magnetic field was published by Rosensweig *et al.* in 1969 [46], who carried out experiments over a wide range of variables such as solvent viscosity, ferric induction, particle diameter, temperature, applied field, shear rate, and number concentration. They observed viscosity increments in ferrofluids under shear and magnetic fields. The viscosity of the fluid in a magnetic field was also estimated by dimensional analysis and verified experimentally. Subsequently, McTague [47] described the magnetoviscosity of a highly dilute colloidal suspension of cobalt particles with a mean diameter of at least 6 nm in a Hagen-Poiseuille flow. Shortly thereafter, a theoretical explanation of the magnetoviscosity as well as the basis of ferrohydrodynamics was developed by Shliomis [48-51]. These theories, formulated several decades ago, neglect any kind of particle interaction; hence these theories are used only in the highly dilute limit. In addition, these models often differ in the assumptions made for the so-called magnetization relaxation equation. These theories will be discussed in detail in Chapter 2. Regarding the magnetoviscous effects we only mention the results of Rosensweig and McTague but alert the reader of books [1, 52] that give a detailed treatment of the rheology of ferrofluids in a magnetic field. Other books [53-55] have been published as a series of lecture

notes that cover specific areas and theories. Besides these references no general treatment of the whole field of ferrofluids is currently available.

Despite all the research in the past decades, the controversy surrounding the equation describing the rate of change of ferrofluid magnetization has not been settled preventing deeper understanding of the magnetoviscous effect. Computational simulations [42, 56-63] can play a valuable role in explaining the response of ferrofluids to DC and AC magnetic fields. As such, this is the focus of the present work.

1.4 LANGEVIN DYNAMICS SIMULATIONS

There are several formulations for the stochastic equations of motion that may be used to perform non-equilibrium, Brownian and Hydrodynamics simulations. However, here we will only cover a small part of this area that is particularly useful for simulating the dynamic behavior of dilute and semidilute ferrofluids.

The Langevin equation is a stochastic differential equation describing the motion of Brownian particles in which two force terms have been added to Newton's second law to approximate the effects of neglected degrees of freedom. These two forces experienced by the Brownian particle are a systematic force (viscous drag) and a rapidly fluctuating force (thermal drag). The systematic force represents the hydrodynamic friction experienced by the particle. The random or fluctuating force is due to random collisions of the molecules of the liquid on the particle, also called white noise.

For a spherical particle, physical and magnetic properties are most naturally written in a cartesian coordinate system with axes aligned with the principal axis, (primed axis), rather than relative to the coordinate axes of the laboratory space, (unprimed axis), as shown in **Figure 1.8**.

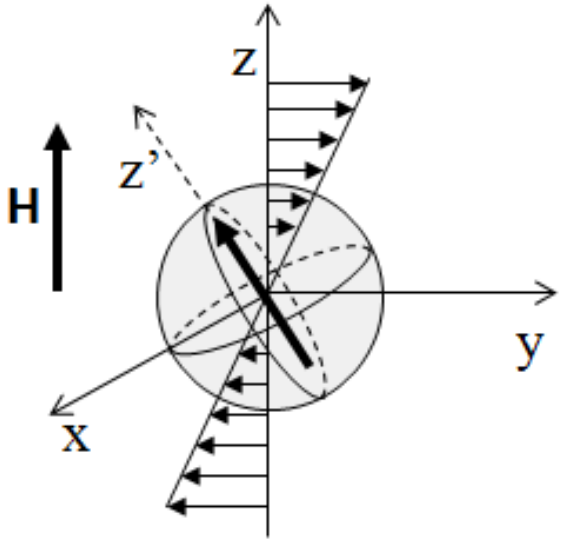

Figure 1.8 Particle model and coordinate axis

Here we consider that the magnetic dipole moment of the particle, μ', is directed along the z'-axis. In addition, the magnetic field, **H**, is assumed to be applied in the yz-plane and that the simple shear flow is along the y-axis.

The system under consideration is assumed to be of infinite extent; we will ignore the effect of boundaries and transients associated with momentum (both linear and angular) diffusion. As such, all spatial derivatives are zero, except for those of the translational velocity. If the shear rate is denoted by $\dot{\gamma}$, then the unperturbed flow velocity **v**, and the local angular velocity of the fluid $\boldsymbol{\omega}_f$, are given by

$$\mathbf{v} = \dot{\gamma}(t) z \mathbf{i}_y, \quad \frac{1}{2}\nabla \times \mathbf{v} = -\frac{1}{2}\dot{\gamma}(t)\mathbf{i}_x . \tag{1.26}$$

The translational and rotational motion of a particle is described by classical mechanics as

$$\mathbf{F}_h + \mathbf{F}_m + \mathbf{F}_b = M\frac{d\mathbf{v}}{dt} \tag{1.27}$$

$$\mathbf{T}_h + \mathbf{T}_m + \mathbf{T}_b = I\frac{d\omega}{dt} \tag{1.28}$$

where $\omega = \frac{d\Phi}{dt}$ is the angular velocity of the particle, Φ the rotation vector, I the moment of inertia, M the mass, and **F** and **T** are the forces and torques acting on the particle which are of three kinds; $\mathbf{F}_h, \mathbf{T}_h$ due to hydrodynamic effects, $\mathbf{F}_m, \mathbf{T}_m$ due to magnetic effects, and $\mathbf{F}_B, \mathbf{T}_B$ due to Brownian motion.

1.4.1 BROWNIAN DYNAMICS

Brownian dynamics simulations are based on the integration of the stochastic angular momentum equation in order to obtain the evolution with time of the particle orientation. Because of the small sizes and low masses of nanoparticles in a ferrofluid, moment of inertia of the particle is negligible. Therefore, the time scale I / ζ_r for the angular velocity correlation is short compared to the natural observation time for Brownian motion, and when the inertial term in the equation of motion can be neglected, hence (1.28) is simplified to,

$$\mathbf{F}_h^{'} + \mathbf{F}_m^{'} + \mathbf{F}_b^{'} = \mathbf{0} \tag{1.29}$$

$$\mathbf{T}_h^{'} + \mathbf{T}_m^{'} + \mathbf{T}_b^{'} = \mathbf{0} \tag{1.30}$$

The prime indicates a vector with respect to particle locked coordinates. We are only interested in the rotational motion; hence we only evaluate Eqn (1.30).

The torque due to hydrodynamic forces is given by

$$\mathbf{T}_h^{'} = -\eta_0 \left[K_r^{'} (\boldsymbol{\omega}^{'} - \boldsymbol{\omega}_f^{'}) \right]. \tag{1.31}$$

Here η_0 is the viscosity of the fluid carrier, $K_r^{'} = 8\pi r^3$ the hydrodynamic resistance coefficient, and ω' and $\omega_f^{'}$ are the angular velocity for the particle and the fluid, respectively. The magnetic torque is given by

$$\mathbf{T}_m^{'} = \mu_0 \left(\boldsymbol{\mu}^{'} \times \mathbf{H}^{'} \right). \tag{1.32}$$

Here μ_0 is the permeability of free space, $\mathbf{H' = A \cdot H}$ is the applied magnetic field and it is transformed to the body fixed axis using the transformation matrix **A.** The transformation matrix is an operator which acts on the components of a vector in a coordinate system, yielding the components of the vector in another coordinate system. Because only three coordinates are necessary to specify the orientation of a rigid body, the Euler angles have been the most common set of coordinates to form a proper orthogonal transformation matrix. However, the Euler angles are difficult to use in numerical solutions because the trigonometric functions involved could lead to a singular problem [64]. To avoid those singularities in the algorithm the transformation matrix is then expressed in terms of the Euler parameters, *e*0, *e*1, *e*2, and *e*3, as

$$\mathbf{A} = \begin{bmatrix} e_0^2 + e_1^2 - e_2^2 - e_3^2 & 2\left(e_1 e_2 + e_0 e_3\right) & 2\left(e_1 e_3 + e_0 e_2\right) \\ 2\left(e_1 e_2 - e_0 e_3\right) & e_0^2 - e_1^2 + e_2^2 - e_3^2 & 2\left(e_3 e_2 + e_0 e_1\right) \\ 2\left(e_1 e_3 + e_0 e_2\right) & 2\left(e_3 e_2 - e_0 e_1\right) & e_0^2 - e_1^2 - e_2^2 + e_3^2 \end{bmatrix} \tag{1.33}$$

in which the quaternions must satisfy the relation $e_0^2 + e_1^2 + e_2^2 + e_3^2 = 1$.

The Brownian torque is represented by a stochastic term

$$\mathbf{T}_{B,i} = \beta_i^r \cdot \mathbf{w}_i^r \,. \tag{1.34}$$

Using the fluctuation dissipation theorem [65] the matrix β_i^r satisfies:

$$\zeta_{ii}^{rr} = \left(k_B T\right)^{-1} \beta_i^r \cdot \left(\beta_i^r\right)^T . \tag{1.35}$$

The vector $\mathbf{w}^r$ is a random vector, which follows a Gaussian distribution with mean and covariance given by

$$\left\langle \mathbf{w}_i^r \right\rangle = 0, \quad \left\langle \mathbf{w}_i^r \mathbf{w}_i^r \right\rangle = 2\mathbf{D}_{ii}^{rr} \Delta t \,. \tag{1.36}$$

In order to reduce the number of variables in the angular momentum equation, time is non-

dimensionalized with respect to the rotational diffusion coefficient, $D_r = k_B T \left(\eta_0 K_r\right)^{-1}$, and the vector variables are non-dimensionalized with respect to their corresponding magnitudes,

$$\tilde{\boldsymbol{\mu}}' = \frac{\boldsymbol{\mu}'}{\mu}, \quad \tilde{\mathbf{H}}' = \frac{\mathbf{H}'}{H}, \quad \tilde{\boldsymbol{\omega}}' = \frac{\boldsymbol{\omega}'}{D_r}, \quad \tilde{\boldsymbol{\omega}}_f' = \frac{\boldsymbol{\omega}_f'}{\dot{\gamma}}. \tag{1.37}$$

Setting $d\tilde{\Phi}' = \tilde{\omega}' d\tilde{t}$ where $d\tilde{\Phi}'$ is the infinitesimal rotation vector, integrating from time $\tilde{t}$ to $\tilde{t} + \Delta\tilde{t}$ using a first-order forward Euler method and applying the fluctuation-dissipation theorem to the Brownian term, we obtain

$$\Delta\tilde{\boldsymbol{\Phi}}' = \alpha\left(\tilde{\boldsymbol{\mu}}' \times \tilde{\mathbf{H}}'\right)\Delta\tilde{t} - \mathrm{Pe}\,\tilde{\boldsymbol{\omega}}_f' \Delta\tilde{t} + \tilde{\mathbf{B}}' \cdot \tilde{\mathbf{w}}'. \tag{1.38}$$

The algorithm proceeds from a starting configuration by calculating the change in orientation at each time step by evaluating and using

$$\begin{bmatrix} \Delta e_0 \\ \Delta e_1 \\ \Delta e_2 \\ \Delta e_3 \end{bmatrix} = \begin{bmatrix} e_0 & -e_1 & -e_2 & -e_3 \\ e_1 & e_0 & -e_3 & e_2 \\ e_2 & e_3 & e_0 & -e_1 \\ e_3 & -e_2 & e_1 & e_0 \end{bmatrix} \begin{bmatrix} 0 \\ \Delta\Phi_x' \\ \Delta\Phi_y' \\ \Delta\Phi_z' \end{bmatrix}, \tag{1.39}$$

to evaluate the change in quaternion parameters. After each time step the quaternion parameters of each particle are normalized.

1.5 MAGNETOVISCOSITY CALCULATION OF BROWNIAN DYNAMICS SIMULATIONS FOR A SEMI-DILUTE SUSPENSION

The viscous (or deviatoric) stress tensor $\boldsymbol{\tau}$ for a suspension of dipolar particles subjected to an external field is characterized by both a symmetric and an antisymmetric part

$$\boldsymbol{\tau} = \boldsymbol{\tau}^s + \boldsymbol{\tau}^a. \tag{1.40}$$

The antisymmetric component $\boldsymbol{\tau}^a$ arises from the angular slip velocity between the local angular velocity of the suspension and the average angular velocity of the particles [66]. This slip velocity

appears as a result of hindered rotation of the particles due to external couples, resulting in a greater rate of mechanical energy dissipation, and hence, a larger apparent viscosity.

The antisymmetric component of the viscous stress tensor due to the action of magnetic couples in a dilute suspension can be obtained from

$$\boldsymbol{\tau}^{a} = -\frac{n}{2}\left\langle \boldsymbol{\varepsilon}\cdot\mathbf{T}_{m}\right\rangle, \tag{1.41}$$

in which n is the number density of particles, $\boldsymbol{\varepsilon}$ is the alternating unit tensor, and $\mathbf{T}_m$ is the magnetic torque referred to space fixed axes. The term in brackets on the right-hand side of Eqn (1.41) denotes an average over the ensemble of particles in the suspension. We are interested in the influence of the asymmetry of the particles on the magnetoviscosity of the suspension when it is under an external magnetic field. For the simple shear flow given in Eqn (1.26), the apparent viscosity of the suspension due to the antisymmetric part of the viscous stress tensor is given by $\eta_{zy}^{m} = \dfrac{\boldsymbol{\tau}_{zy}^{m}}{\dot{\gamma}}$, which is referred to as the magnetoviscosity of the suspension. For a dilute suspension, the intrinsic magnetoviscosity $\left[\eta_{zy}^{m}\right]$ is defined as

$$\left[\eta_{zy}^{m}\right] = \lim_{\phi\to 0}\frac{\eta_{zy}^{m}}{\phi\eta_{0}}. \tag{1.42}$$

Combining Eqn (1.41) and Eqn (1.42) the magnetoviscosity equation in dimensionless form is then

$$\left[\eta_{zy}^{m}\right] = -3\frac{\alpha}{Pe}\left\langle \boldsymbol{\varepsilon}\cdot\left(\tilde{\boldsymbol{\mu}}\times\tilde{\mathbf{H}}\right)\right\rangle_{zy}. \tag{1.43}$$

The equation shows $\left[\eta_{zy}^{m}\right]$ as function of the Langevin parameter, α, and Péclet number, Pe. Using the transformation matrix presented in Eqn (1.33), the magnetoviscosity equation is express in terms of the quaternion parameters. The equation is then

$$\left[\eta_{zy}^{m}\right] = -3\frac{\alpha}{\mathrm{Pe}}\left\langle 2(e_2e_3 - e_0e_1)\tilde{H}_z \right\rangle_{zy}. \tag{1.44}$$

Eqn (1.44) furnishes $\left[\eta_{zy}^{m}\right]$ as a function of the Langevin parameter, the dimensionless shear-rate expressed as a rotational Péclet number, and the average orientation of the particles.

1.6 OVERVIEW OF THE THESIS AND MOTIVATION

The main objective of this dissertation is to apply Brownian dynamics simulations to study the magnetic and rheological properties of a ferrofluid suspension composed of spherical particles in the dilute and semi dilute limit subjected to direct current (dc) and alternating current (ac) magnetic field and constant and oscillating shear flow. The simulations were performed under several conditions of magnetic field and shear flow. In addition, numerical and analytical solutions of the magnetization relaxation equations were obtained and compared with our simulation results to validate which equation describes the considered situation appropriately.

Chapter 2 presents a study of the intrinsic magnetoviscosity of a magnetic fluid composed of non-interacting spherical permanently magnetized particles and subjected to a magnetic field and shear flow using Brownian dynamics simulations. We compare the results with predictions of continuum level models for the validation of the various magnetization relaxation equations in describing the so-called magnetoviscosity. We also study the effect of the angle between the magnetic field and the vorticity on the magnetoviscosity. Finally, simulation results over a wide range of conditions are collapsed into master curves which provide insight into the scaling laws relating magnetoviscosity, magnetic field strength, and shear rate, introducing a new rotational Mason number. The work presented here was published in the journal Physical Review E in 2010.

Chapter 3 focuses on the study of the transient response of dilute ferrofluids to step

changes in the applied magnetic field and rate of shear deformation applying Brownian dynamics simulations of the rotational dynamics of magnetic nanoparticles. Additionally, a simple analysis based on the phenomenological magnetization equations is applied to demonstrate that these equations capture the observed phenomena. The work presented in this chapter was published in the Journal of Magnetism and Magnetic Materials in 2011.

Chapter 4 presents a dynamic magnetoviscosity of a ferrofluid subjected to a constant magnetic field and an oscillatory shear flow. Rheological properties were obtained and compared with the predictions obtained from the ferrohydrodynamic equations using the kinetic magnetization equation of Martsenyuk, Raikher, and Shliomis. The work presented was published in the Journal of Physical Review E in 2011.

Chapter 5 presents energy dissipation studies for non interacting particles subjected to an oscillating magnetic field. Dynamic susceptibility was obtained and compared with the predictions of the magnetization relaxation equation of Martsenyuk, Raikher, and Shliomis (MRSh). In addition, energy dissipation was obtained from simulations and compared with the Rosensweig theory and the predictions used the MRSh equation. Results are summarized in terms of a non-dimensional energy dissipation rate, which is a function of the applied field amplitude, parameterized by the Langevin parameter, and the product of field frequency and relaxation time.

Chapter 6 presents results for an algorithm that considers particle-particle magnetic interactions. Equilibrium and dynamic properties of semidilute suspensions subjected to dc and ac magnetic fields are shown.

Finally, the relevant contributions of the thesis are summarized in Chapter 7. Complementary data and copies of algorithms are included in the Appendix.

2

2 MAGNETOVISCOSITY IN DILUTE FERROFLUIDS FROM ROTATIONAL BROWNIAN DYNAMICS SIMULATIONS

Prior work on modeling the behavior of ferrofluids has focused on using phenomenological suspension scale continuum equations. A disadvantage of this approach is the controversy surrounding the equation describing the rate of change of the ferrofluid magnetization, the so-called magnetization relaxation equation. In this contribution the viscosity of dilute suspensions of spherical magnetic nanoparticles suspended in a Newtonian fluid and under applied shear and constant magnetic fields is studied through rotational Brownian dynamics simulations. Simulation results are compared with the predictions of suspension-scale models based on three magnetization relaxation equations. Excellent agreement is observed between simulation results and the predictions of an equation due to Martsenyuk, Raikher, and Shliomis. Good qualitative agreement is observed with predictions of other equations, although these models fail to accurately predict the magnitude and shear rate dependence of the magnetic field dependent effective viscosity. Finally, simulation results over a wide range of conditions are collapsed into master curves using a newly defined Mason number based on the balance of hydrodynamic and magnetic torques.

2.1 INTRODUCTION

The first experimental report of changes in viscosity due to a magnetic field was published by Rosensweig *et al.* in 1969 [46], who carried out experiments over a wide range of variables such as solvent viscosity, ferric induction, particle diameter, temperature, applied field, shear rate, and number concentration. They observed viscosity increments in ferrofluids under shear and magnetic fields. The viscosity of the fluid in a magnetic field was also estimated by dimensional analysis and verified experimentally. Subsequently McTague [47] described the magnetoviscosity of a highly dilute colloidal suspension of cobalt particles in a Hagen-Poiseuille flow.

Suspension-scale models to describe the effect of magnetic fields on the viscosity of ferrofluids have been developed by Shliomis [49, 51], Martsenyuk *et al.* [48], Felderhof [67], and others [68, 69]. These models often differ in the assumptions made for the so-called magnetization relaxation equation [48, 49, 51, 67, 69, 70], underscoring the controversy found in the macroscopic description of ferrofluid flow, even in the infinitely dilute limit. The most commonly used magnetization equation was developed by Shliomis in 1972 [49]. Shliomis's analysis stems from the use of a macroscopic, *ad hoc* phenomenological magnetization equation obtained as a modification of the Debye relaxation equation and given by

$$\frac{d\mathbf{M}}{dt} = \boldsymbol{\Omega} \times \mathbf{M} - \frac{1}{\tau_B}\left(\mathbf{M} - \mathbf{M}_0\right) - \frac{1}{6\eta\phi}\mathbf{M} \times \left(\mathbf{M} \times \mathbf{H}\right). \tag{2.1}$$

Here **M** stands for the ferrofluid magnetization under the magnetic field **H** and the flow vorticity $\boldsymbol{\Omega} = \frac{1}{2}\nabla \times \mathbf{v}$. In Eqn (2) $\tau_B = {}^{3\eta V}\!/_{k_B T}$ stands for the characteristic Brownian relaxation time of rotational particle diffusion, since the particles are assumed to possess particle-locked magnetic dipoles. At equilibrium in a stationary field, $\mathbf{M}_0$ is described well by the Langevin function

$$\mathbf{M_0} = nmL(\alpha)\frac{\mathbf{H}}{H};\ \alpha = \frac{mH}{k_B T};\ L(\alpha) = \coth\alpha - \alpha^{-1} \tag{2.2}$$

where *m* is the magnetic dipole moment of a single particle, *n* is the number density of the particles, and α is the Langevin parameter. Considering rotational motion of the particles relative to the carrier liquid and Eqn (2.2), Shliomis derived an equation for the rotational viscosity in planar Poiseuille or Couette flow under the influence of a constant uniform magnetic field. The result is

$$\eta_r = \frac{1}{4}\tau_\perp M_0 H \tag{2.3}$$

where $\tau_\perp = \dfrac{2\tau_B}{2+\alpha L(\alpha)}$ is the relaxation time of the transverse (to the field) component of the magnetization. According to Shliomis [49], in the limit of low shear rate and short magnetization relaxation time, $\Omega\tau_B << 1$, the rotational viscosity is given by

$$\eta_r(\alpha) = \frac{3}{2}\phi\eta_0\frac{\alpha - \tanh\alpha}{\alpha + \tanh\alpha}\sin^2\beta, \tag{2.4}$$

where β is the angle between field and vorticity.

Shortly thereafter, Martsenyuk and collaborators [48] proposed another magnetization equation (MRSh) derived microscopically from the Fokker-Planck equation. They employed for this purpose an effective-field method which results in closure of the first moment of magnetization. The MRSh magnetization equation is then

$$\frac{d\mathbf{M}}{dt} = \mathbf{\Omega}\times\mathbf{M} - \frac{\mathbf{H}\left[\mathbf{H}\cdot(\mathbf{M}-\mathbf{M}_0)\right]}{\tau_\parallel H^2} - \frac{\mathbf{H}\times(\mathbf{M}\times\mathbf{H})}{\tau_\perp H^2} \tag{2.5}$$

where $\tau_\parallel = \dfrac{d\ln L(\alpha)}{d\ln\alpha}$ and $\tau_\perp = \dfrac{2L(\alpha)}{\alpha - L(\alpha)}\tau$ are the parallel and transverse relaxation times. Using Shliomis's definition for the rotational viscosity, Eqn (2.3), Martsenyuk *et al.* [48] obtained for the

rotational viscosity

$$\eta_r(\alpha) = \frac{3}{2}\eta\phi\frac{\alpha L^2(\alpha)}{\alpha - L(\alpha)}. \tag{2.6}$$

Tsebers [62] compared the Sh'72 and MRSh equations using numerical simulations of the Brownian motion of ferromagnetic particles to study the field dependence of the magnetization relaxation time. These simulations indicated that the MRSh equation provides an excellent description of the dynamics of fluid magnetization in the absence of shear. Although this work was an important step in evaluating these equations, further work is needed to understand the effect of shear and compare predictions for the magnetoviscosity for both equations.

Several years later Shliomis [51] proposed yet another magnetization equation derived from irreversible thermodynamics and employed it in the calculation of the rotational viscosity in a magnetic field. This third magnetization equation is

$$\frac{d\mathbf{H}_e}{dt} = \boldsymbol{\Omega}\times\mathbf{H}_e - \frac{1}{\tau}(\mathbf{H}_e - \mathbf{H}) - \frac{1}{6\eta\phi}\mathbf{H}_e\times(\mathbf{M}\times\mathbf{H}). \tag{2.7}$$

In Eqn (2.7) the effective field $\mathbf{H}_e$ is that corresponding to the nonequilibrium magnetization, obtained from the inverse Langevin function. For low field strength, Eqn (2.7) predicts the same dependence, described by Eqn (2.4), of rotational viscosity on the magnetic field strength as Eqn (2.1).

It will be seen in the simulations discussed below that the shear rate $\dot{\gamma}$, parameterized through the rotational Péclet number $Pe_r = \dot{\gamma}/D_r$ where D_r is the rotational diffusivity of the magnetic particles, has a significant effect on the magnetoviscosity. Hence, it is important to know the predictions of the above mentioned relaxation equations for the shear rate dependence of the magnetoviscosity. In order to obtain the shear rate dependence of the rotational viscosity predicted by the various magnetization equations it is convenient to pass from the fields **H** and $\mathbf{H}_e$

to their nondimensional values of α and ε. According to Shliomis [51], both Eqn (2.1) and Eqn (2.7) admit a steady solution in which the effective field tracks the true field with lag angle γ. The dependence of the effective field, ε and γ, and true field, α, upon Ωτ for Eqn (2.1) is given by

$$\sqrt{\alpha^2-\varepsilon^2}=\frac{2\Omega\tau\alpha\varepsilon}{2\alpha+\varepsilon^2 L(\varepsilon)};\quad \cos\gamma=\frac{\varepsilon}{\alpha} \tag{2.8}$$

Taking in consideration Eqn (2.3) and Eqn (2.8), the rotational viscosity is then

$$\eta_r=\frac{3}{2}\eta\phi\frac{\varepsilon^2 L(\alpha)}{2\alpha+\varepsilon^2 L(\varepsilon)}. \tag{2.9}$$

Similarly for the MRSh equation, Eqn (2.5), the effective field ε and field α are related by

$$\sqrt{\alpha^2-\varepsilon^2}=\frac{2\Omega\tau\varepsilon L(\varepsilon)}{\varepsilon-L(\varepsilon)};\quad \cos\gamma=\frac{\varepsilon}{\alpha}. \tag{2.10}$$

which results in the following expression for the rotational viscosity

$$\eta_r=\frac{3}{2}\eta\phi\frac{\varepsilon L^2(\varepsilon)}{\varepsilon-L(\varepsilon)}. \tag{2.11}$$

Finally, for the third relaxation equation, Eqn (2.7), the effective field ε and field α are related by

$$\sqrt{\alpha^2-\varepsilon^2}=\frac{2\Omega\tau\varepsilon}{2+\varepsilon L(\varepsilon)};\quad \cos\gamma=\frac{\varepsilon}{\alpha} \tag{2.12}$$

which results in

$$\eta_r=\frac{3}{2}\eta\phi\frac{\varepsilon L(\varepsilon)}{2+\varepsilon L(\varepsilon)}. \tag{2.13}$$

Several researchers [22, 71-74] have experimentally investigated the rheological properties of ferrofluids using rotational rheometers. Most of these studies compared experimental results with theoretical models of the magnetic viscosity [22, 24, 75, 76]. For example, Patel *et al*. [77] compared the viscosity of a magnetic fluid obtained experimentally with the MRSh and Felderhof [67] magnetoviscosity expressions. However, in contrast with most analyses, in Patel *et al.*'s work

the magnetic field was applied perpendicular to the axis of the capillary viscometer; hence the direction of the field was not uniformly perpendicular to the vorticity of the flow. In analyzing their data, Patel *et al.* assumed the magnetoviscosity depends on the angle β between the vorticity and magnetic field according to Eqn (2.4), that is, with a correction factor of $\sin^2\beta$, and used this correction factor to compare the predictions of Sh'72 [49], MRSh [48], and Felderhof [67] to their measurements using a capillary tube. Note that although the $\sin^2\beta$ dependence in Eqn (2.4) for the Sh'72 magnetization relaxation equation was derived analytically, this result is only applicable for small fields and shear rates, and the predicted $\sin^2\beta$ is not necessarily applicable for the other equations tested by Patel *et al.* Whether this assumed dependence is correct is subject to further inquiry and is discussed below.

Because ferrofluids are opaque, measurement of bulk flow profiles is challenging [12, 78]. On the other hand, there are no methods to measure the average rate of spin of the particles (the so-called spin velocity). In addition, it is not always possible to orient the direction of the applied field uniformly in a direction that is perpendicular or parallel to the vorticity of the flow. Also, most ferrofluids used in experiments contain high particle concentrations, resulting in particle-particle magnetic interactions such as chaining, the effects of which are not captured by the preceding theories. Finally, because most ferrofluids consist of nanoparticles suspended in low viscosity carrier fluids the shear rates typically obtained in experiments are not sufficient to explore the full shear rate dependence predicted by theory. The preceding experimental limitations make direct particle-scale simulations an attractive tool to improve understanding of the macroscopic behavior of dilute ferrofluids, exploring the applicability and limitations of suspension scale governing and constitutive equations, and developing new applications.

The rheological properties of ferrofluids have been studied by numerical simulations such

as in the work of Morimoto *et al.* [29], who studied the so-called negative viscosity effect predicted theoretically by Shliomis and Morozov [27]. Morimoto studied this effect in a 2D magnetic fluid composed of disc-like particles subjected to shear flow and alternating magnetic fields. They found the rotational viscosity is high when the frequency of the magnetic field is low and it becomes negative in an intermediate frequency range. Satoh studied the influence of the magnetic field strength, shear rate, and rotational Brownian motion on transport coefficients such as viscosity and diffusivity in dilute suspensions of rodlike [79] and spherocylinder [80] particles. The results in both cases show that the orientation distribution is dependent on the relative ratio of magnetic field and shear rate. Sánchez and Rinaldi [59] used rotational Brownian dynamics simulations to study the rheological properties of ellipsoidal particles in magnetic and shear flow fields. They found that ellipsoidal particles show a significant effect of aspect ratio on the intrinsic magnetoviscosity of the suspension. In addition, they also found that it is possible to fit the data for ellipsoids to a master curve by defining an effective Péclet number $Pe_{r,eff} = Pe_r(D_{r,\max} / D_{r,eff})$, where $D_{r,eff}$ is obtained from averaging the rotational diffusion tensor, $\boldsymbol{D}_r^{'}$, around the magnetic axis of the particle. More recently, Sánchez and Rinaldi [81] used Brownian dynamics simulations to study the effect of alternating and rotating magnetic fields on the viscosity of magnetic nanoparticle suspensions. These simulations demonstrated that the so-called negative viscosity effect is more pronounced under the application of rotating magnetic fields when the field co-rotates with the vorticity of the flow.

The purpose of this chapter is to offer additional insight into ferrohydrodynamics and the validity of the various magnetization relaxation equations in describing the so-called magnetoviscosity. In the present work we study the intrinsic magnetoviscosity of a magnetic fluid composed of non-interacting spherical permanently magnetized particles and subjected to a magnetic field and shear

flow by Brownian dynamics simulations and compare the results with predictions of continuum level models. We also study the effect of the angle between the magnetic field and the vorticity on the magnetoviscosity. Finally, simulation results over a wide range of conditions are collapsed into master curves which provide insight into the scaling laws relating magnetoviscosity, magnetic field strength, and shear rate, introducing a new rotational Mason number.

2.2 ROTATIONAL BROWNIAN DYNAMICS SIMULATIONS

2.2.1 ALGORITHM FORMULATION

The algorithm follows the process explained in Chapter 1, Section 1.5. It proceeds from a starting configuration by calculating the change in orientation at each time step. After each time step the quaternion parameters of each particle are normalized. All runs were performed starting from a random configuration, using 10^5 non-interacting particles, a time step of $\Delta\tilde{t} = 0.01$, Langevin parameters of $0.1 < \alpha < 100.0$, and dimensionless shear rates of $0.1 < Pe_r < 100.0$. Angles between the magnetic field and vorticity varied between $0 < \beta < \pi/2$.

2.3 RESULTS

2.3.1 COMPARISON WITH CONTINUUM LEVEL MODELS

Figure 2.1 shows the intrinsic magnetoviscosity of a suspension of spherical particles as a function of the Langevin parameter α and for different values of the rotational Péclet number [82]. At high values of α the intrinsic magnetoviscosity approaches a saturation value, indicating that the magnetic dipole moments of the particles are aligned with the magnetic field due to the

preponderance of the magnetic torque over the Brownian and hydrodynamic torques. Moreover, the simulations do not predict a hysteresis of the magnetoviscosity at high shear and high field as calculated by Shliomis [49] and He *et al.* [25] using the ferrohydrodynamics equations and the Sh'72 magnetization relaxation equation.

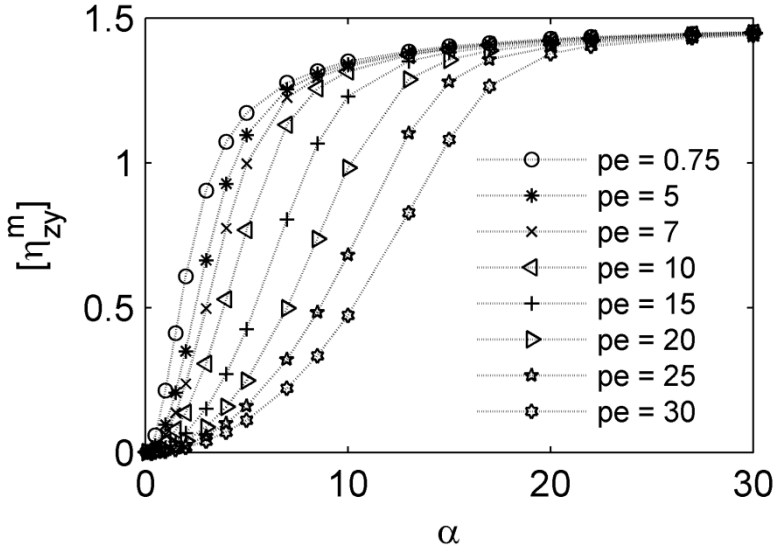

Figure 2.1 Intrinsic magnetoviscosity of an infinitely dilute suspension of spherical particles with embedded dipoles, as a function of the dimensionless magnetic field magnitude for different values of the dimensionless shear rate.

Now we proceed to compare the predictions for the magnetoviscosity of the various magnetization relaxation equations to the results of our simulations. In the case of $Pe_r << 4$, corresponding to $\Omega\tau << 1$ in Shliomis and MRSh's analyses $\left(\Omega\tau = \frac{Pe_r}{4}\right)$, Eqn (2.4), obtained from the Sh'72 and Sh'01 equations, agrees with results obtained from our simulations at low and high α but deviates from our results at intermediate values of α, as shown in **Figure 2.2**. On the other hand, Eqn (2.6), obtained using the MRSh magnetization equation, is in excellent agreement with our results over the whole range of α, which indicates that the introduction of the concept of an effective field is a good approximation to the behavior of dilute ferrofluids.

When the ferrofluid is subjected to a sufficiently large shear rate, $\Omega\tau \geq 1$, the flow induces demagnetization since the magnetic particles tend to be rotated out of alignment with the magnetic field. Formally, this effect results in decreasing the parameter ε determined by Eqn (2.8), Eqn (2.10), and Eqn (2.12). Results for different values of $\Omega\tau$ for the Sh'72 equation, Eqn (2.9), the MRSh equation, Eqn (2.11), and the Sh'01 equation, Eqn (2.13), are also shown in **Figure 2.2**, compared with our simulation results. As seen from the Figure, the higher the shear rate the larger the discrepancy between viscosity values predicted by the Sh'72 and Sh'01 equations and our results. On the other hand, the MRSh equation is in excellent agreement with our results under all conditions tested.

One might argue that for the commonly-used low viscosity ferrofluids it is difficult to achieve shear rates sufficient to see the effects of **Figure 2.2**, however this is not always the case. High viscosity ferrofluids can be prepared for which the shear rate range typically accessible in rheometers should be sufficient to see these effects. More importantly and practically, ferrofluids are applied in fluid bearings such as in hard drive shafts. In such applications very high shear rates can be experienced by the ferrofluid. For example, in the work of Miwa et al. [83] ferrofluids are subjected to nominal shear rates as high as 10^8 s^{-1}. For a typical ferrofluid with 10 nm diameter nanoparticles and a base fluid viscosity of 10 cP this would correspond to a rotational Péclet number greater than 1000. Finally, the important point of the result of Figure 2.2 is the demonstration that of the three magnetization relaxation equations being evaluated here it is only the MRSh equation which yields results in quantitative agreement with direct simulations of the rotational dynamics of non-interacting Brownian magnetic nanoparticles over a wide range of values of the shear rate and magnetic field strength. The Sh'72 and Sh'01 only yield results in qualitative agreement with the direct simulations. We note further that although the Sh'01

equation seems to be in better agreement with our simulations than the Sh'72 equation, the Sh'01 magnetization relaxation equation fails to correctly predict the relaxation dynamics of a ferrofluid from an applied equilibrium magnetic field, as shown in **Appendix A**.

Figure 2.3 shows the intrinsic magnetoviscosity of the suspension as a function of the magnetic field for different values of the angle β between the magnetic field and vorticity. Clearly, the factor $\sin^2\beta$ in Eqn (2.4) is not uniformly valid. This indicates, for example, that in the work of Patel *et al.* [77] the assumed relationship between the angle β and the magnetoviscosity is incorrect, except for very low or very high magnetic fields and shear rates. The fact that the often assumed $\sin^2\beta$ dependence of the magnetoviscosity on the angle β is incorrect has important implications for experiments aimed at determining the magnetic field dependent rheology of ferrofluids, as it indicates that experiments must be carried under conditions such that the vorticity and magnetic field are perpendicular throughout the sample. This constraint is particularly important if accurate determinations are desired under moderate magnetic fields and shear rates.

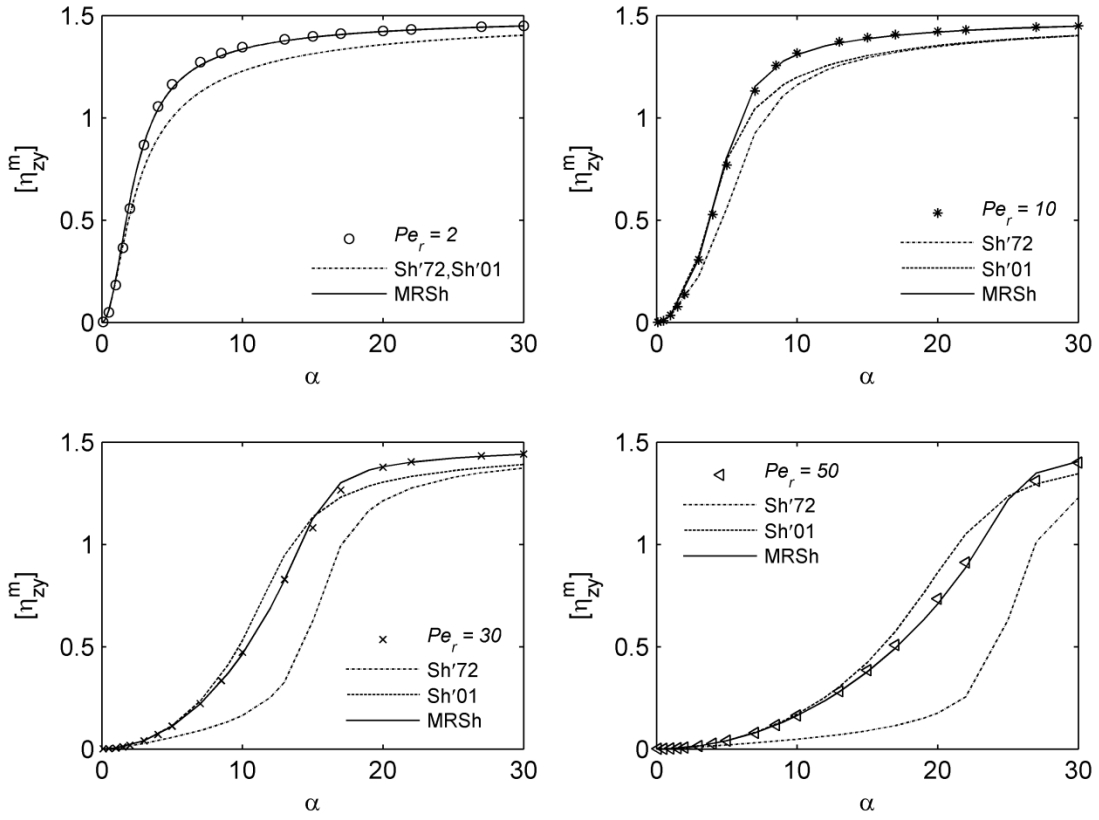

Figure 2.2 Intrinsic magnetoviscosity as a function of the dimensionless magnetic field magnitude for different values of the dimensionless shear rate, compared with the predictions of the Sh'72, Sh'01 and MRSh magnetization relaxation equations.

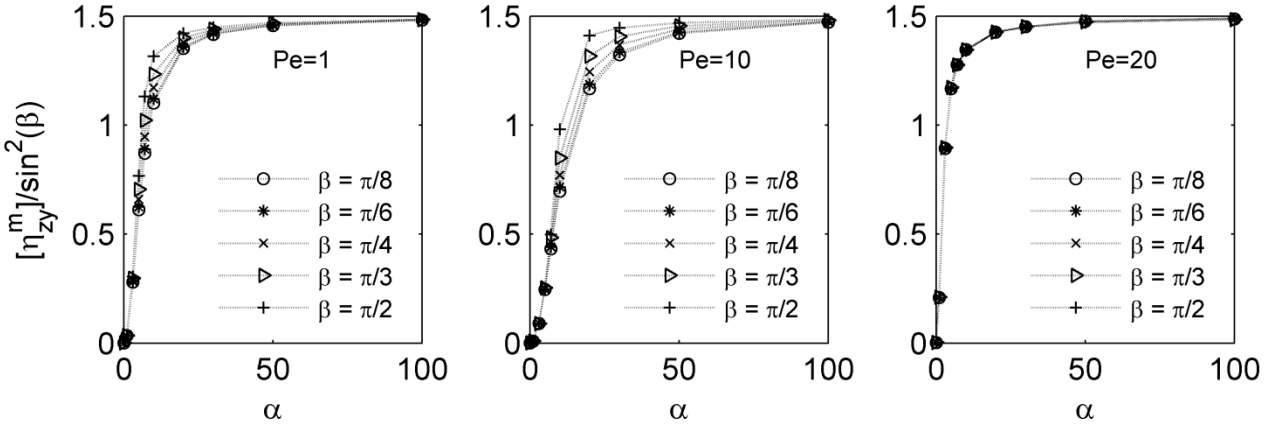

Figure 2.3 Intrinsic magnetoviscosity normalized with respect to $\sin^2\beta$ as a function of the dimensionless magnetic field magnitude for different values of the dimensionless shear rate and of the angle between the magnetic field and vorticity.

2.3.2 SCALING OF THE MAGNETOVISCOSITY USING A TORQUE-BASED MASON NUMBER

As it has been seen above, our direct simulations of the rotational dynamics of magnetic nanoparticles in shear and magnetic fields demonstrate that the continuum equations including the MRSh magnetization relaxation equation adequately describe the shear rate and magnetic field dependence of the magnetoviscosity of dilute ferrofluids. Another approach to the interpretation of the shear and magnetic field dependence of the viscosity of ferrofluids is the use of characteristic dimensionless parameters that capture the basic physics of the phenomena. In the closely related field of magnetorheological fluids recent work has demonstrated that magnetorheological measurements over a wide range of conditions can be collapsed into master curves though the introduction of an appropriately defined Mason number [84]. This approach has also been adopted with respect to inverse ferrofluids [85] and magnetite based ferrofluids [21, 72]. In all these cases the working hypothesis is that the shear and magnetic field dependence of the viscosity of the suspension arises due to chain formation, with the magnetic field promoting chain formation and the shear field tending to destroy these chains. In these cases the particles are magnetizable; that is, their magnetic dipole moments are aligned with the local magnetic field and rotate freely within the particle. Chains form because of dipole-dipole interactions pulling particles together such that their dipoles align end-to-end. On the other hand, the shear field exerts a hydrodynamic force tending to pull the particles apart. On the basis of this balance of forces the Mason number is defined as

$$Mn \equiv \frac{F_{\dot{\gamma}}}{F_H}, \tag{2.14}$$

where $F_{\dot{\gamma}}$ is the hydrodynamic force due to the shear and F_H is the magnetic force between dipoles. Using this definition of the Mason number the following expression is obtained [86-88]

$$Mn = \frac{\eta_0 \dot{\gamma}}{2\mu_0 \mu \beta^2 H_0^2}, \tag{2.15}$$

where $\beta = (\mu - \mu_0)/(\mu_0 + 2\mu) \approx 1$ is the magnetic contrast factor.

Although the Mason number defined according to Eqn (2.14) and Eqn (2.15) has been appropriate for magnetorheological fluids and semi-dilute to concentrated ferrofluids composed of magnetic nanoparticles, it should be clear that it cannot be suitable to describe the magnetic field and shear dependence of the viscosity of infinitely dilute ferrofluids consisting of suspensions of nanoparticles with permanent magnetic dipoles (i.e., Brownian ferrofluids), for which Eqn (2.4) and Eqn (2.6) apply. This is because in the infinitely dilute limit chains cannot form. However, as will be shown below, the magnetic field and shear dependence of the viscosity of these fluids can be adequately described using a Mason number defined as the ratio of hydrodynamic and magnetic torques on the particles.

For the following it will make more sense to recast the results shown in **Figure 2.1** as intrinsic magnetoviscosity as a function of dimensionless shear rate Pe_r. This is shown in **Figure 2.4**, wherein it is seen that the intrinsic magnetoviscosity for low Pe_r has a plateau value which is a function of the magnetic field strength, parameterized by α. With increasing Pe_r the intrinsic magnetoviscosity is seen to decrease, that is the fluid shear thins. It is seen that the critical Pe_r for shear thinning is a function of α, however the curves for each α have similar shape, suggesting that an appropriate scale may exist that collapses the data. Here we show how this can be done using a Mason number defined as the ratio of magnetic to hydrodynamic torques on the particles.

Figure 2.5 illustrates the orientation distribution of the magnetic dipoles for a series of simulations at a constant value of the parameter α. The value of $\alpha = 30$ was chosen as this

produces a shaper distribution around an average orientation. It is seen that as Pe_r increases from 0.1 to 60 the average orientation of the particles increases from an angle of almost 0 to close to 90 with respect to the direction of the magnetic field. This range of values of Pe_r correspond to the plateau region of the intrinsic magnetoviscosity for $\alpha = 30$, shown in **Figure 2.4**, and to the situation in which the dipoles do not, on average, rotate due to the balance of hydrodynamic and magnetic torques. On the other hand for $Pe_r > 60$ the particles begin to rotate as the hydrodynamic torque exceeds the magnetic torque. These ranges of values of the Péclet number correspond to the shear thinning region of the intrinsic magnetoviscosity for $\alpha = 30$, shown in **Figure 2.4**. These observations suggest that an angle of 90° between the average particle orientation and the magnetic field corresponds to the critical condition for which shear thinning occurs in the fluid.

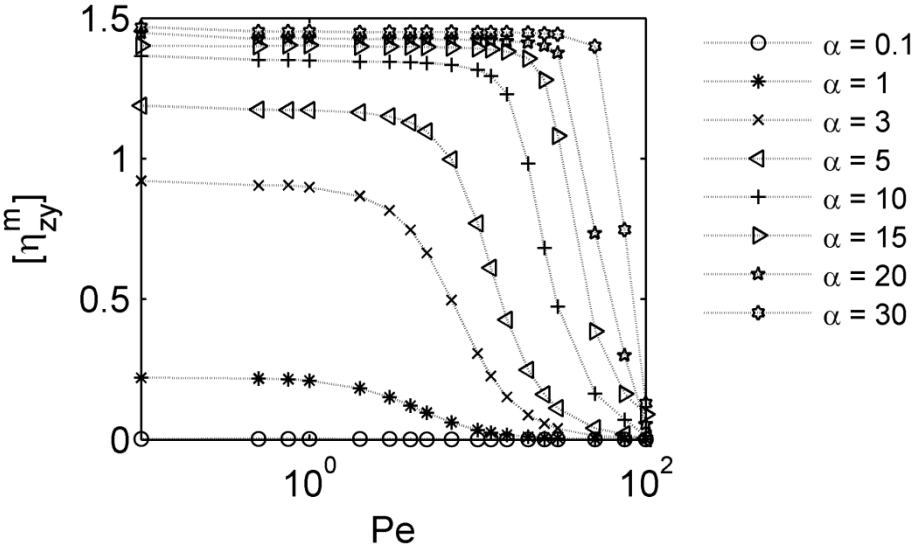

Figure 2.4 Intrinsic magnetoviscosity of a suspension of spherical particles as a function of rotational Péclet number for different values of the Langevin parameter

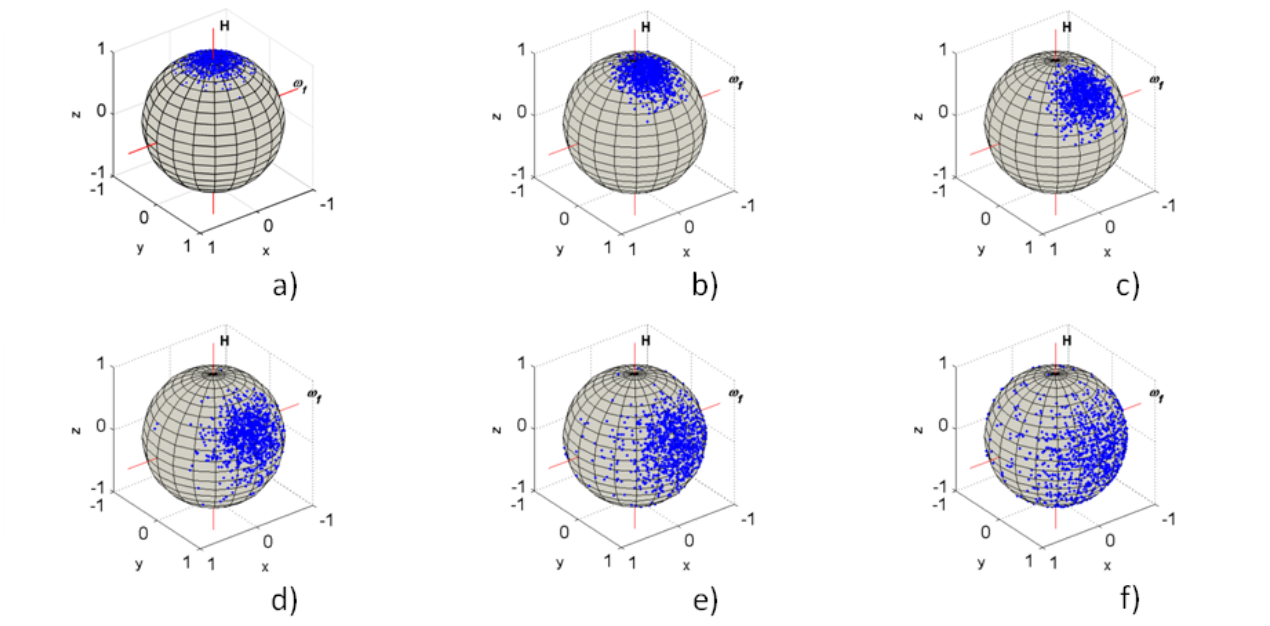

Figure 2.5 Orientation distributions of the magnetic dipole moments of the magnetic particles of a) Pe_r = 1.0 b) Pe_r = 20.0 c) Pe_r = 40.0 d) Pe_r = 50.0 e) Pe_r = 60 f) Pe_r = 75 and α = 30.0. Each dot corresponds to a particle with its magnetic dipole moment aligned with the corresponding point in the unit sphere. The directions of the magnetic field H and vorticity of the flow ω_f are shown.

As discussed above, the magnetic field and shear dependence of the viscosity of magnetorheological and chain-forming ferrofluids can be described using the so-called Mason number. Here we obtain a new Mason number based on the balance of hydrodynamic and magnetic torques on the particles. We proceed by recognizing that the source of the magnetoviscosity in an infinitely dilute suspension of Brownian nanoparticles is the hindered rotation arising from the tendency to align the particle's dipoles with the applied magnetic field. Such hindered rotation results in increased energy dissipation in the fluid surrounding the particles, and hence in an increased suspension-scale viscosity. The magnetic torque hindering the particle's rotation is opposed by the hydrodynamic torque exerted by the fluid on the particles. A shear-dependent decrease in the magnetoviscosity of the ferrofluid (shear thinning) is observed

when the hydrodynamic torque exceeds the maximum magnetic torque on the particles, and hence the particles begin to rotate with the surrounding fluid. We define a torque-based Mason number, Mn_T, for this case as

$$Mn_T \equiv \frac{T_{\dot{\gamma}}}{T_H}, \tag{2.16}$$

where $T_{\dot{\gamma}}$ is the hydrodynamic torque exerted by the surrounding fluid on the particle, given by

$$T_{\dot{\gamma}} = 8\pi r^3 \eta_0 \frac{\dot{\gamma}}{2}, \tag{2.17}$$

and T_H is the maximum magnetic torque, corresponding to the condition when the particle's dipole is perpendicular to the applied magnetic field, given by

$$T_H = \mu_0 \mu H . \tag{2.18}$$

Substituting Eqn (2.17) and Eqn (2.18) in Eqn (2.16) yields

$$Mn_T = \frac{8\pi r^3 \eta_0 \dot{\gamma}}{2\mu_0 \mu H} = \frac{Pe_r}{2\alpha}. \tag{2.19}$$

Comparing Eqn (2.15) and Eqn (2.19) it is interesting that both depend on the relative magnitudes of the shear rate $\dot{\gamma}$ and magnetic field *H*. Both Mason numbers are linear in the shear rate, however, the force-based Mason number in Eqn (2.15) is proportional to the inverse square of the magnetic field whereas the torque-based Mason number in Eqn (2.19) is proportional to the inverse of the magnetic field.

The results for the magnetoviscosity for all of our simulations in which the magnetic field and vorticity are perpendicular are plotted as a function of the torque-based Mason number in **Figure 2.6**. For comparison purposes the predictions of the MRSh equation are shown as solid lines for selected values of Pe_r. It is evident from this Figure that for each value of the

dimensionless shear rate, Pe_r, the intrinsic magnetoviscosity is initially constant and equal to 3/2 and then decreases as a power law for high values of Mn_T, wherein $\left[\eta_{zy}^m\right] = AMn_T^{-2}$, with *A* being a Pe_r dependent proportionality factor. Note that for large values of Pe_r the results collapse into a single master curve, that is, *A* eventually asymptotes to a constant value.

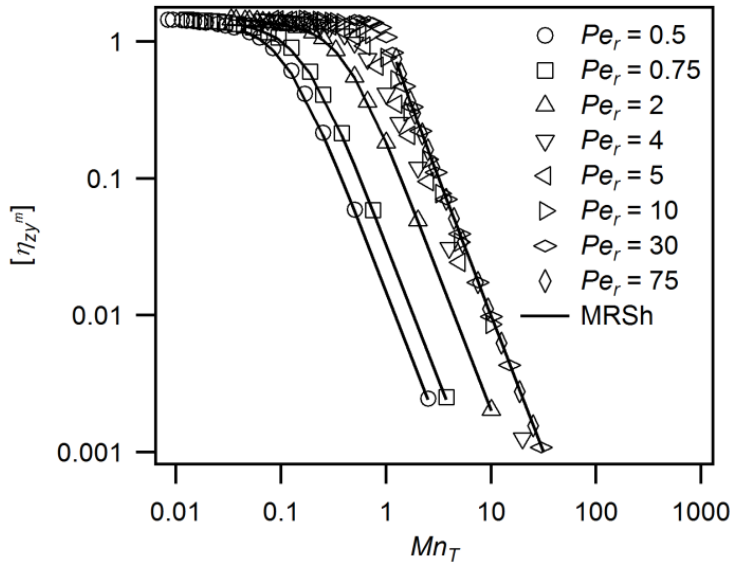

Figure 2.6 Intrinsic magnetoviscosity as a function of the torque-based Mason number for various values of the dimensionless shear rate Pe_r. The solid lines correspond to the predictions of the MRSh equation for Pe_r =0.25, 0.75, 2, and 75, from left to right.

A critical Mason number $Mn_{T,crit}$ can be defined to characterize the transition between approximately constant intrinsic magnetoviscosity and shear thinning following power law behavior. This is done by extrapolating the power law region to intercept the line corresponding to $\left[\eta_{zy}^m\right] = \frac{3}{2}$, resulting in the relationship

$$\frac{3}{2} \equiv AMn_{T,crit}^{-2}. \tag{2.20}$$

Note that this definition of $Mn_{T,crit}$ implies

$$\left[\eta_{zy}^{m}\right] = \frac{3}{2}\left[\frac{Mn_{T,crit}}{Mn_T}\right]^2, \tag{2.21}$$

in the shear thinning region, which allows us to determine the values of $Mn_{T,crit}$.

Figure 2.7 illustrates the Pe_r dependence of the critical Mason number $Mn_{T,crit}$. There it is seen that the critical Mason number initially increases linearly with Pe_r but eventually saturates to a value of 0.85. Interestingly, the calculated values of $Mn_{T,crit}$ follow a curve reminiscent of the Langevin function, with

$$Mn_{T,crit} \approx 0.85 L\left(Pe_r\right) = 0.85\left[\coth Pe_r - \frac{1}{Pe_r}\right] \tag{2.22}$$

Combining Eqn (2.21) with Eqn (2.22) yields the as-of-yet *ad hoc* expression

$$\left[\eta_{zy}^{m}\right] \approx 2.1\left(\frac{L\left(Pe_r\right)}{Mn_T}\right)^2 \tag{2.23}$$

for the shear thinning region.

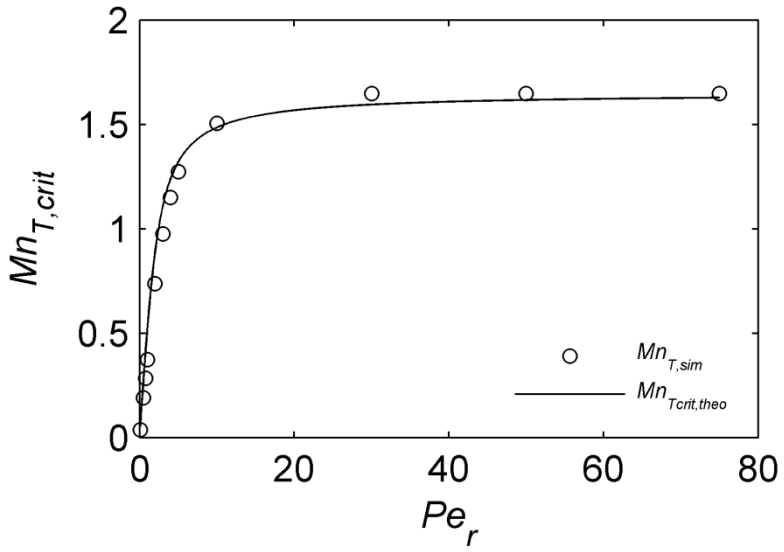

Figure 2.7 Critical Mason number $Mn_{T,crit}$ as a function of the applied dimensionless shear rate Pe_r. The solid line correspond to the Langevin function with argument Pe_r , from Eqn (2.22).

Figure 2.8 shows how Eqn (2.23) can be used to reduce all of the simulation results into a single master curve describing the magnetic field and shear rate dependence of the magnetoviscosity of dilute ferrofluids, by plotting the intrinsic magnetoviscosity as a function of $Mn_T / L(Pe_r)$. By combining the observation that for low Mn_T the magnetoviscosity is given by $\left[\eta_{zy}^m\right] = \frac{3}{2}$, whereas for large values of Mn_T it is given by Eqn (2.23) results in the following correlation for the magnetoviscosity over the complete range of Mn_T and for all values of Pe_r in the simulations

$$\left[\eta_{zy}^m\right] = \frac{3/2}{1+1.4\left[\frac{Mn_T}{L(Pe_r)}\right]^2}. \tag{2.24}$$

The predictions of Eqn (2.24) are shown as a solid line in **Figure 2.8**, showing excellent agreement with all of the simulation results.

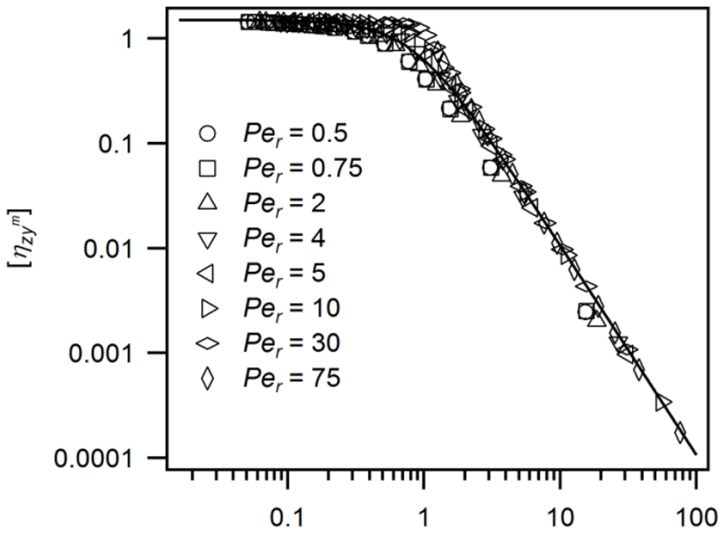

Figure 2.8 Intrinsic magnetoviscosity from all simulations reduced to a single master curve using the dimensionless parameter $1+1.4\left[\frac{Mn_T}{L(Pe_r)}\right]$ as y-axis. The solid line corresponds to Eqn (2.24).

2.4 CONCLUSIONS

The rheology of dilute suspensions of spherical magnetic nanoparticles suspended in a Newtonian fluid and under applied shear and constant magnetic fields was studied through rotational Brownian dynamics simulations. For suspensions of spherical particles, excellent agreement was observed between predictions of the Martsenyuk, Raikher, and Shliomis (MRSh) relaxation equation and our direct simulations. The intrinsic magnetoviscosity calculated from Shliomis' 1972 equation deviates from the results of our simulations for intermediate values of the Langevin parameter. The use of an approximate phenomenological equation (Sh'72) for the change in magnetization results in the discrepancies observed. Similarly, the equation obtained from irreversible thermodynamics, Sh'01, presents good qualitative agreement with our results, but not quantitative agreement. Furthermore, we note that this equation incorrectly predicts the field dependence of the relaxation from equilibrium magnetization of a collection of magnetic dipoles (see **Appendix A**) hence this equation cannot provide an accurate representation of the behavior of dilute ferrofluids. Our simulations also show that the assumed $\sin^2\beta$ dependence of the magnetoviscosity on the angle β between the vorticity and the magnetic field is only valid for low fields and high shear rates. Finally, it was shown that the magnetoviscosity of dilute ferrofluids can be described using a newly defined rotational Mason number given by $Mn_T = \frac{\tau\dot{\gamma}}{\alpha} = \frac{Pe_r}{2\alpha}$, which collapses the simulation results into a single master curve. According to this analysis, there is a critical ratio of Pe_r and α for which the suspension becomes shear thinning. This critical ratio is initially a linear function of Pe_r and then saturates for high values of Pe_r. Furthermore, in the shear thinning region the magnetoviscosity is seen to possess power law dependence on Mn_T with an exponent of -2. Combining these observations yields a

correlation for the calculated magnetoviscosity in the complete simulated Mn_T and Pe_r range with the single dimensionless parameter $Mn_T / L(Pe_r)$, where $L(Pe_r) = \coth Pe_r - 1/Pe_r$.

3

3 TRANSIENT MAGNETOVISCOSITY OF DILUTE FERROFLUIDS

The magnetic field induced change in the viscosity of a ferrofluid, commonly known as the magnetoviscous effect and parameterized through the magnetoviscosity, is one of the most interesting and practically relevant aspects of ferrofluid phenomena. Although the steady state behavior of ferrofluids under conditions of applied constant magnetic fields has received considerable attention, comparatively little attention has been given to the transient response of the magnetoviscosity to changes in the applied magnetic field or rate of shear deformation. Such transient response can provide further insight into the dynamics of ferrofluids and find practical application in the design of devices which take advantage of the magnetoviscous effect and which inevitably must deal with changes in the applied magnetic field and deformation. In this contribution Brownian dynamics simulations and a simple model based on the ferrohydrodynamics equations are applied to explore the dependence of the transient magnetoviscosity for two cases: (I) a ferrofluid in a constant shear flow wherein the magnetic field is suddenly turned on, and (II) a ferrofluid in a constant magnetic field wherein the shear flow is suddenly started. Both simulations and analysis show that the transient approach to a steady state magnetoviscosity can be either monotonic or oscillatory depending on the relative magnitudes of the applied magnetic field and shear rate.

3.1 INTRODUCTION

Under the effect of an applied constant magnetic field, the magnetic particles in a ferrofluid respond by aligning their dipoles in the direction of the applied field. The resulting hindered rotation of the suspended particles leads to an increase in the rate of energy dissipation of the flowing suspension and hence an increase in the effective viscosity of the suspension. This is the most basic form of the so-called magnetoviscous effect, which in addition to the mechanism explained above can result due to formation of chains which further deform the fluid streamlines and lead to increased energy dissipation. The increase in viscosity of a ferrofluid under such conditions is typically parameterized through the so-called magnetoviscosity. This phenomenon was first observed experimentally by McTague [47] and subsequently theoretically described by Shliomis[48-51]. Since then it has been the subject of a wide range of studies and technological applications of ferrofluids, as described in the book by Odenbach [53].

Despite the long history of fundamental and applied research on the magnetoviscous effect, there have been no studies which describe the transient response of a ferrofluid as it achieves the steady state magnetoviscosity. This is the case, even as it should be realized that such transient behavior can provide important insight into the dynamics of ferrofluids and practically relevant information in the design of devices which take advantage of the magnetoviscous effect. In this chapter we apply Brownian dynamics simulations of the rotational dynamics of magnetic nanoparticles to study the transient response of dilute ferrofluids to step changes in the applied magnetic field and rate of shear deformation. Additionally, a simple analysis based on the ferrohydrodynamics equations is applied to demonstrate that these equations capture the observed phenomena. For simplicity, the linear limit of magnetization (i.e., low applied magnetic fields) is considered here. The practically relevant non-linear magnetization regime will be considered in a

future contribution. In addition we discuss simulations and compared with our mathematical model based on the ferrohydrodynamics equations.

3.2 SIMULATION ALGORITHM AND PARAMETERS

The algorithm proceeds from a starting configuration by calculating the change in orientation at each time step. After each time step the quaternion parameters of each particle are normalized. All runs were performed starting from a random configuration, using 10^5 noninteracting particles, a time step of $\tilde{t}$ = 0.01, Langevin parameters of α = 1, 5, 10, and dimensionless shear rates of Pe = 1, 5, 10. The intrinsic magnetoviscosity $\left[\eta_{zy}^{m}\right]$ for a dilute suspension was evaluated as in [89].

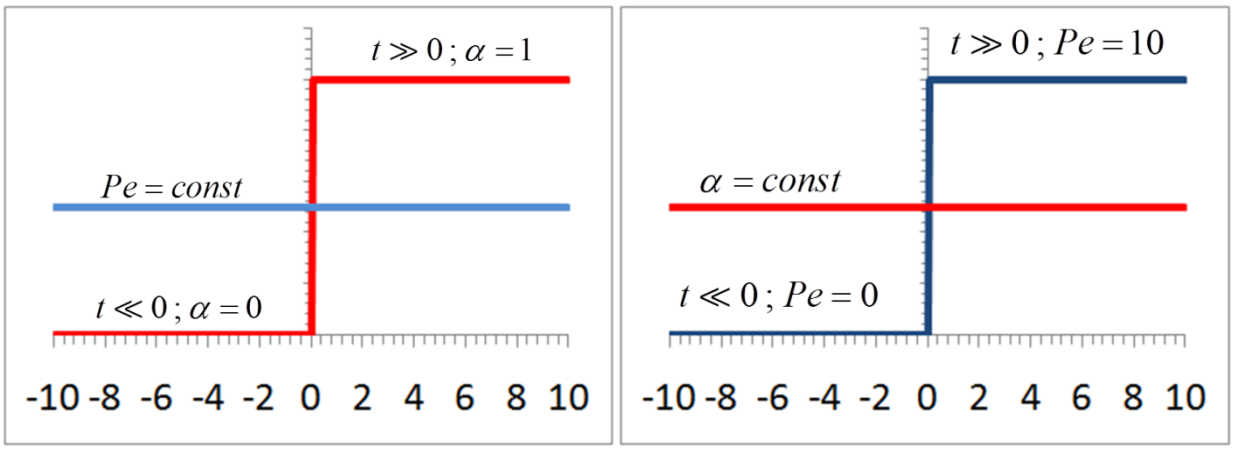

Figure 3.1 Schematic sketch of the two processes develops. a) Constant shear flow is applied to the system and the magnetic field is suddenly turned on. b) Constant magnetic field applied to the system and the shear flow is suddenly started

3.3 RESULTS

3.3.1 COMPUTATIONAL SIMULATIONS

Figure 3.2 shows calculated magnetoviscosity transients for the case in which the ferrofluid is subjected to a constant dimensionless shear rate of Pe = 1.0, 5.0, and 10.0 and the magnetic field is switched at t = 0 from α = 0 to α = 1.0. At constant shear rate in the absence of a magnetic field the particles can freely rotate relative to the fluid, hence the magnetoviscosity is zero for t < 0. It is interesting to note that depending on the value of the applied non-dimensional shear rate the magnetoviscosity is seen to monotonically approach the steady state value (for Pe = 1.0) or is seen to overshoot and then oscillate towards the steady state value (for Pe = 5.0 and 10.0).

Figure 3.3 show the results for the case where a constant magnetic field α = 1.0, 5.0, and 10.0 is applied and the ferrofluid is subjected to a step change in shear rate at t = 0, from Pe = 0 to Pe = 10. It is seen that depending on the conditions, the magnetoviscosity first overshoots and then oscillates towards the steady state value. However, here it is seen that increasing values of the applied field damp these oscillations, until for high enough fields (e.g., α = 10) the magnetoviscosity approaches the steady state value monotonically.

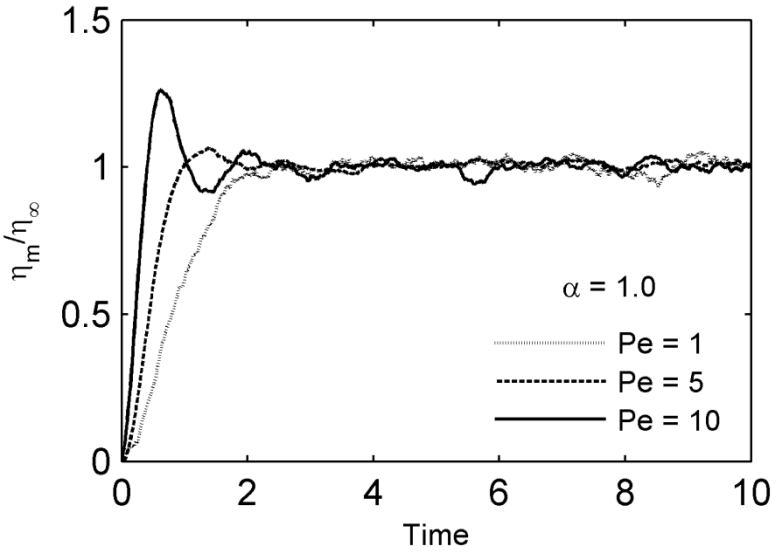

Figure 3.2 Transient magnetoviscosity transients for the case in which the ferrofluid is subjected to a constant dimensionless shear rate of *Pe* = 1.0, 5.0, and 10.0 and the magnetic field is switched at *t* = 0 from α = 0 to α = 1.0

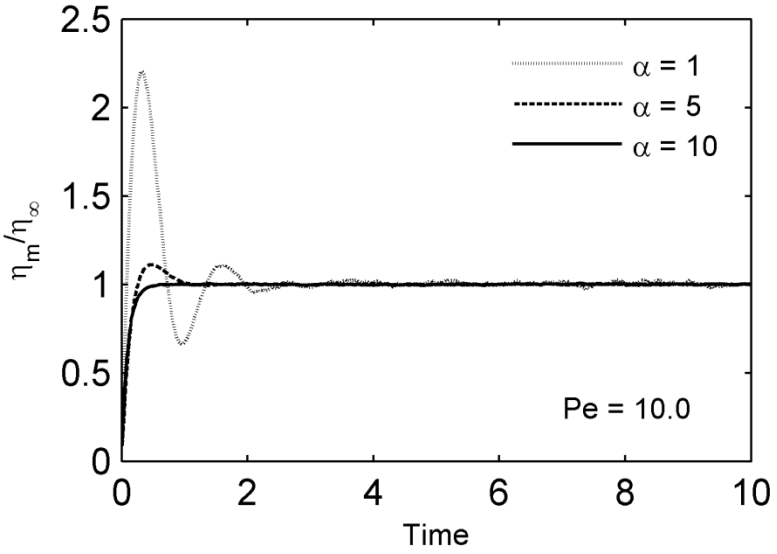

Figure 3.3 Transient magnetoviscosity for the case where a constant magnetic field α = 1.0, 5.0, and 10.0 is applied and the ferrofluid is subjected to a step change in shear rate at *t* = 0, from *Pe* = 0 to *Pe* = 10

3.3.2 MATHEMATICAL ANALYSIS BASED ON THE FERROHYDRODYNAMIC EQUATIONS

In this section we derive a simple model for the situations of start-up of an applied magnetic field on a ferrofluid in a simple shear flow and start-up of simple shear flow on a ferrofluid subjected to a constant magnetic field. For simplicity the analysis is limited to small magnitudes of the magnetic field, in order to linearize the governing equations. For ferrofluids consisting of particles with rigidly-locked magnetic dipoles, so-called thermally blocked particles, in the infinitely dilute limit the commonly accepted governing equations are

$$\nabla\cdot\mathbf{v}=0\,, \tag{3.1}$$

$$\rho\frac{D\mathbf{v}}{Dt}=\mu_0\mathbf{M}\cdot\nabla\mathbf{H}-\nabla p+2\zeta\nabla\times\omega+\eta_e\nabla^2\mathbf{v}\,, \tag{3.2}$$

$$\rho I\frac{D\omega}{Dt}=\mu_0\mathbf{M}\times\mathbf{H}+2\zeta\nabla\times\mathbf{v}-4\zeta\omega\,, \tag{3.3}$$

$$\frac{\partial\mathbf{M}}{\partial t}+\mathbf{v}\cdot\nabla\mathbf{M}=\omega\times\mathbf{M}-\frac{1}{\tau}\left(\mathbf{M}-\mathbf{M}_{eq}\right). \tag{3.4}$$

Here **v** is the mass average velocity, ρ is the fluid density, **M** is the suspension magnetization, **H** is the magnetic field, p is the fluid pressure, ζ is the so-called vortex viscosity, ω is the ferrofluid spin velocity, $\eta_e=\eta+\zeta$ is an effective viscosity with η the shear viscosity of the ferrofluid, I is the specific moment-of-inertia density, $\tau=D_r^{-1}/2=3\eta_0V/k_BT$ is the characteristic Brownian relaxation time of the ferrofluid, and $\mathbf{M}_{eq}$ is the equilibrium magnetization the ferrofluid would achieve in the absence of the disturbances of flow. Note that we are using the magnetization relaxation equation due to Shliomis [49] for simplicity. The analysis can be extended to other magnetization relaxation equations, however the one used here should be able to capture the qualitative aspects of the behavior of the ferrofluid. In addition to

the governing equations in Eqn (3.1) - (3.4), Maxwell's equations in the magnetoquasistatic limit are obeyed; however, these are trivially satisfied by the imposed magnetic field and flow.

The system under consideration will be assumed to be of infinite extent, that is, we will ignore the effect of boundaries and transients associated with momentum (both linear and angular) diffusion. As such, all spatial derivatives are zero, except for those of the translational velocity, which satisfies the condition of simple shear flow

$$\mathbf{v} = \dot{\gamma}(t)\, z\mathbf{i}_y, \quad \frac{1}{2}\nabla\times\mathbf{v} = -\frac{1}{2}\dot{\gamma}(t)\mathbf{i}_x\,. \tag{3.5}$$

Under these considerations the governing equations reduce to

$$\rho\frac{\partial\mathbf{v}}{\partial t} = 0\,, \tag{3.6}$$

$$\rho I\frac{\partial\omega}{\partial t} = \mu_0\mathbf{M}\times\mathbf{H} - 2\xi\dot{\gamma}(t)\mathbf{i}_x - 4\xi\omega\,, \tag{3.7}$$

$$\frac{\partial\mathbf{M}}{\partial t} = \omega\times\mathbf{M} - \frac{1}{\tau}\left(\mathbf{M}-\mathbf{M}_{eq}\right). \tag{3.8}$$

Now, typically for ferrofluids the moment-of-inertia density is negligible, hence we assume $\rho I \sim 0$. In the following, we will limit attention to the case of a unidirectional applied magnetic field, $\mathbf{H} = H_z(t)\mathbf{i}_z$. In this case the simple shear flow will result in a magnetization which lies in the *yz* plane, hence we have $\mathbf{M} = M_y(t)\mathbf{i}_y + M_z(t)\mathbf{i}_z$, with the spin velocity in the orthogonal direction *x*, hence $\omega = \omega_x(t)\mathbf{i}_x$. Finally, as stated previously, we will limit attention to the case of small applied field magnitudes; hence the equilibrium magnetization is given by the linear relation $\mathbf{M}_{eq} = \chi_i\mathbf{H}$. These relations are substituted in Eqn (3.6) - (3.8) to obtain

$$0 = \mu_0\mathbf{M}\times\mathbf{H} - 2\varsigma\dot{\gamma}\mathbf{i}_x - 4\varsigma\omega_x\mathbf{i}_x\,, \tag{3.9}$$

$$\frac{\partial \mathbf{M}}{\partial t} = \omega_x \mathbf{i}_x \times \mathbf{M} - \frac{1}{\tau}\left(\mathbf{M} - \chi_i \mathbf{H}\right), \tag{3.10}$$

or, in component form

$$0 = \mu_0 M_y H_z - 2\varsigma\dot{\gamma} - 4\varsigma\omega_x, \tag{3.11}$$

$$\frac{\partial M_y}{\partial t} = -\omega_x M_z - \frac{1}{\tau} M_y, \tag{3.12}$$

$$\frac{\partial M_z}{\partial t} = \omega_x M_y - \frac{1}{\tau} M_z + \frac{\chi_i}{\tau} H_z. \tag{3.13}$$

In order to simplify the analysis and allow comparisons with the results of simulations we introduce the dimensionless quantities

$$\begin{aligned} &t = {t}/{2\tau}, \quad \omega = {\omega_x}/{\dot{\gamma}}, \quad f = {M_y}/{\chi_i H_0}, \quad g = {M_z}/{\chi_i H_0}, \\ &h = {H_z}/{H_0}, \quad k(t) = {\dot{\gamma}(t)}/{\dot{\gamma}}, \quad Mn = \frac{\zeta\dot{\gamma}}{\mu_0 \chi_i H_0^2}, \quad Pe = 2\dot{\gamma}\tau, \end{aligned} \tag{3.14}$$

to obtain

$$0 = Mn^{-1} f(t)h(t) - 2k(t) - 4\omega(t), \tag{3.15}$$

$$\frac{\partial f}{\partial t} = -Pe\omega(t)g(t) - 2f(t), \tag{3.16}$$

$$\frac{\partial g}{\partial t} = Pe\omega(t) f(t) - 2g(t) + 2h(t). \tag{3.17}$$

Equation (3.15) can be solved for $\omega(t)$

$$\omega(t) = \frac{1}{4} Mn^{-1} f(t) h(t) - \frac{1}{2} k(t), \tag{3.18}$$

and the result substituted in (3.16) and (3.17) to obtain

$$\frac{\partial f}{\partial t} = -PeMn^{-1} \frac{1}{4} f(t)h(t)g(t) + \frac{1}{2} Pek(t)g(t) - 2f(t), \tag{3.19}$$

$$\frac{\partial g}{\partial t} = PeMn^{-1}\frac{1}{4}f^2(t)h(t) - \frac{1}{2}Pek(t)f(t) - 2g(t) + 2h(t), \tag{3.20}$$

However, we take note that $\zeta = \frac{3}{2}\phi\eta_0$ with ϕ the volumetric fraction of particles in the ferrofluid, and that $\chi_i = \frac{\mu_0\phi M_d^2 V}{3k_B T}$, hence the product $PeMn^{-1}$ is shown to be proportional to the Langevin parameter

$$Mn^{-1}Pe = 2\mu_0\chi_i H_0^2\tau/\zeta = 4/3\,\alpha^2. \tag{3.21}$$

Thus Eqn (3.19) and Eqn (3.20) reduce to

$$\frac{\partial f}{\partial t} = -\frac{1}{3}\alpha^2 f(t)h(t)g(t) + \frac{1}{2}Pek(t)g(t) - 2f(t), \tag{3.22}$$

$$\frac{\partial g}{\partial t} = \frac{1}{3}\alpha^2 f^2(t)h(t) - \frac{1}{2}Pek(t)f(t) - 2g(t) + 2h(t). \tag{3.23}$$

Now, in considering the regime of linear magnetization we have tacitly assumed that $\alpha << 1$ and neglected terms of order higher than α, hence, without incurring in any inconsistency of our assumptions we may neglect the terms proportional to α^2 to obtain

$$\frac{\partial f}{\partial t} = \frac{1}{2}Pek(t)g(t) - 2f(t) \tag{3.24}$$

$$\frac{\partial g}{\partial t} = -\frac{1}{2}Pek(t)f(t) - 2g(t) + 2h(t) \tag{3.25}$$

In what follows we will be interested in evaluating the intrinsic magnetic viscosity, applicable for an infinitely dilute ferrofluid. This is the quantity obtained from the simulations discussed above, and on the basis of the continuum ferrohydrodynamic governing equations is obtained from

$$\eta_m = \frac{\tau_{zy}^a}{\dot{\gamma}\phi\eta} = -\frac{\zeta}{\dot{\gamma}\phi\eta}\left[\nabla \times \mathbf{v} - 2\omega\right]_x = \frac{3}{2}\left[1 + \frac{1}{2}Mn^{-1} f(t) h(t) - k(t)\right]. \tag{3.26}$$

Also, for comparison purposes we reduce Shliomis's expression for the magnetoviscosity [49] to the following expression for the intrinsic magnetoviscosity

$$\eta_{m,Sh} = \frac{3}{2}\frac{\alpha - \tanh\alpha}{\alpha + \tanh\alpha}. \tag{3.27}$$

With the simplified Eqn (3.24), (3.25), and (3.26) we now proceed to consider the two cases described in the introduction.

3.3.3 CASE 1: THERE IS SIMPLE SHEAR FLOW IN THE ABSENCE OF MAGNETIC FIELD AND THE MAGNETIC FIELD IS THEN SUDDENLY TURNED ON

This case corresponds to the parameters ($k(t) = 1$, $h(t > 0) = 1$, $f(0) = 0$, $g(0) = 0$). In this case we have

$$\eta_m = \frac{3}{4}Mn^{-1} f(t), \tag{3.28}$$

and

$$\frac{\partial f}{\partial t} = \frac{1}{2}Peg(t) - 2f(t), \tag{3.29}$$

$$\frac{\partial g}{\partial t} = -\frac{1}{2}Pef(t) - 2g(t) + 2. \tag{3.30}$$

This is a system of inhomogeneous linear differential equations with constant coefficients. It can be integrated to obtain

$$f(t) = \frac{\left[4Pe - 4Pe\,e^{-2t}\cos\left(\frac{Pet}{2}\right) - 16e^{-2t}\sin\left(\frac{Pet}{2}\right)\right]}{16 + Pe^2} \tag{3.31}$$

$$g(t)=\frac{\left[16-16e^{-2t}\cos\left(\frac{Pet}{2}\right)+4Pe\,e^{-2t}\sin\left(\frac{Pet}{2}\right)\right]}{16+Pe^2}. \tag{3.32}$$

Then the intrinsic magnetoviscosity for this case would be

$$\eta_m=4\alpha^2\frac{\left[1-e^{-2t}\cos\left(\frac{Pet}{2}\right)-4Pe^{-1}e^{-2t}\sin\left(\frac{Pet}{2}\right)\right]}{16+Pe^2}. \tag{3.33}$$

For small Péclet number this expression reduces to

$$\eta_m=\alpha^2\frac{1-4Pe^{-1}e^{-2t}\sin\left(\frac{Pet}{2}\right)}{4}, \tag{3.34}$$

which would look like a monotonic approach towards a steady state value. For comparison, Shliomis's expression for small values of α reduces to

$$\eta_{m,Sh}=\frac{1}{4}\alpha^2+O\left(\alpha^2\right), \tag{3.35}$$

hence our steady state solution agrees with Shliomis's expression in the long-time small α and *Pe* limit.

For large Péclet Eqn (3.33) reduces to

$$\eta_m=4\alpha^2\frac{1-e^{-2t}\cos\left(Pet\right)}{Pe^2}, \tag{3.36}$$

which would correspond to an exponential approach to steady state with superimposed oscillations. These results are illustrated in **Figure 3.4**.

3.3.4 CASE II: THERE IS A CONSTANT INITIAL MAGNETIC FIELD AND ZERO SHEAR AND THEN THE SHEAR IS SUDDENLY STARTED

This case corresponds to the parameters: $k(t>0)=1$, $h(t)=1$, $f(0)=0$, $g(0)=0$. The

solution for this case is very similar to Case I and as such we only show the final result for the magnetoviscosity

$$\eta_m = \alpha^2 \frac{\left[4 - 4e^{-2t}\cos\left(\frac{Pet}{2}\right) + 4\,Pe\,e^{-2t}\sin\left(\frac{Pet}{2}\right)\right]}{16 + Pe^2}. \tag{3.37}$$

As in Case I, depending on the relative magnitudes of α and *Pe* this solution predicts either a monotonic or oscillatory approach of the magnetoviscosity to a steady state value, as illustrated in **Figure 3.5**.

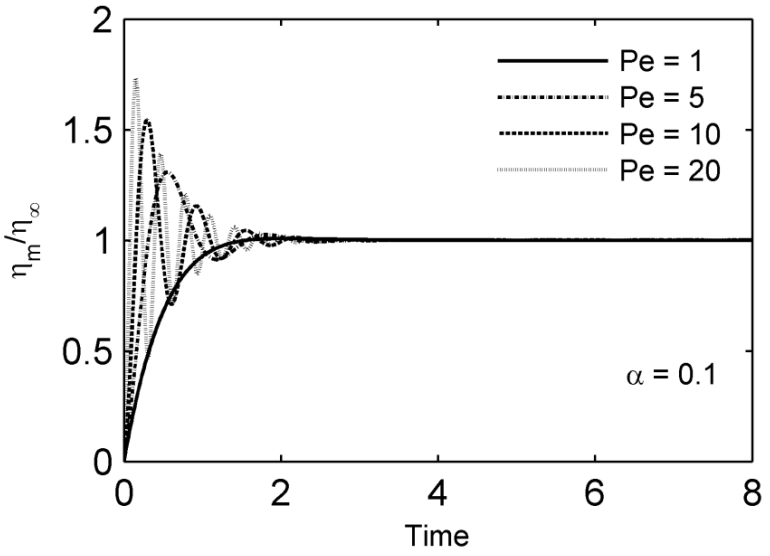

Figure 3.4 Mathematical analysis for the case in which the ferrofluid is subjected to a constant dimensionless shear rate and the magnetic field is turned on.

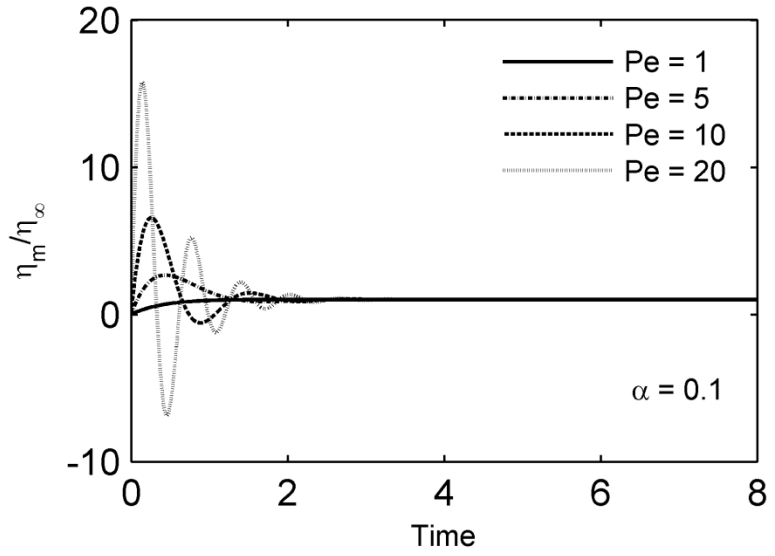

Figure 3.5 Mathematical analysis for the case in which the ferrofluid is subjected to a constant magnetic field and the dimensionless shear rate is suddenly on.

3.4 CONCLUSIONS

Although the magnetoviscous effect in ferrofluids has received considerable attention, the associated problem of the transient approach to the steady state remains largely unexplored, even as it should provide interesting insight into the dynamics of ferrofluids and should be relevant in application development. We have applied the Brownian dynamics simulation method to study the transient behavior in the magnetoviscosity of a dilute ferrofluid in response to step changes in shear rate and magnetic field. For comparison purposes, a simple mathematical analysis based on the ferrohydrodynamics equations in the linear magnetization limit was also derived. In both cases it was observed that the approach of the magnetoviscosity to the steady state value can be either monotonic or oscillatory depending on the particular values of magnetic field amplitude and shear rate. Such observations are relevant in the operation of devices which take advantage of the magnetoviscous effect, as oscillatory response can lead to instability in device performance.

4

4 OSCILLATORY SHEAR RESPONSE OF DILUTE FERROFLUIDS: PREDICTIONS FROM ROTATIONAL BROWNIAN DYNAMICS SIMULATIONS AND FERROHYDRODYNAMICS MODELING

The response of ferrofluids to constant shear and magnetic fields has received a lot of attention, but the response of ferrofluids to oscillatory shear remains largely unexplored. In the present work we used rotational Brownian dynamics to study the dynamic properties of ferrofluids with thermally blocked nanoparticles under oscillatory shear and constant magnetic fields. Comparisons between simulations and modeling using the ferrohydrodynamics equations were also made. Simulation results show that for small rotational Péclet number the in-phase and out-of-phase components of the complex viscosity depend on the magnitude of the magnetic field and frequency of the shear, following a Maxwell-like model with field dependent viscosity and characteristic time equal to the field-dependent transverse magnetic relaxation time of the nanoparticles. Comparison between simulations and the numerical solution of the ferrohydrodynamic equations shows that the oscillatory rotational magnetoviscosity for an oscillating shear field obtained using the kinetic magnetization relaxation equation quantitatively agrees with simulations for a wide range of Péclet number and Langevin parameter, but has quantitative deviations from the simulations at high values of the Langevin parameter. These predictions indicate an apparent elastic character to the rheology of these suspensions, even though we are considering the infinitely dilute limit in which there are negligible particle-particle interactions and as such chains do not form. Additionally, an asymptotic analytical solution of the ferrohydrodynamics equations, valid for $Pe << 2$, was used to demonstrate that the Cox-Merz rule

applies for dilute ferrofluids under conditions of small shear rates. At higher shear rates the Cox-Merz rule ceases to apply.

4.1 INTRODUCTION

The magnetorheology of ferrofluids has been an active area of experimental [26, 46, 47, 90-92] and theoretical [21, 48, 49, 93-95] research for decades. The focus of most work has been the steady state response of dilute and semi-dilute ferrofluids to imposed constant shear and magnetic fields [24-26, 47, 50, 59, 67, 81, 96, 97]. There has also been some work on response of ferrofluids to oscillating [15, 26-28, 81, 98, 99] and rotating [12, 30, 32, 81, 88, 100, 101] magnetic fields, however here again a steady flow has been considered. Recently, the dynamics of the transient magnetoviscous effect has received attention [16, 102] with emphasis on response of ferrofluids to step changes in the applied magnetic or shear fields.

Surprisingly, the response of ferrofluids to oscillating shear fields seems to have received little attention, even though oscillatory shear experiments are common rheological tools to study complex fluids[103-105]. In these measurements both stress and strain vary cyclically with time, with sinusoidal variation being the most commonly used. The cycle time, or frequency of oscillation, defines the time scale of the test. Thus, by observing material response as a function of frequency, mechanical properties can be probed at different time scales. Klingenberg [106, 107] used molecular dynamics to study the oscillatory shear response of electrorheological suspensions composed of dielectric spheres in a Newtonian fluid between parallel-plate electrodes. The response obtained was described by frequency dependent moduli determined by a competition between hydrodynamic and electrostatic interactions that dominate chain formation, deformation, and breakage. Similar response was predicted for magnetorheological fluids (MR),

concentrated suspensions of micron-sized magnetizable particles, and expressed as a relation between magnetic and hydrodynamic forces using the so-called Mason number [86]. Kanai and Amari [108] studied flocculated suspensions of micron-sized ferric oxide particles in mineral oil. They found strain-thickening behavior one decade larger than in the non-magnetic base oil, which they attributed to particle-particle interactions. Li *et al*. [109] studied the dynamic behavior of magnetorheological (MR) fluids under oscillatory shear. Linear viscoelastic behavior was observed in these fluids only at very small strain amplitudes, and the response could be captured using a Pipkin diagram describing the rheological behavior as a function of strain amplitude and frequency. Claracq *et al.*[105] used micron-sized colloidal magnetic particles coated with latex to study the viscoelastic behavior of MR fluids subjected to small deformations. They related the magnetic force to the elastic modulus using a Mason number and compared their results with those obtained by Klingenberg [106, 107] using simulations. They found that the application of a magnetic field causes aggregation of the particles into chains in the magnetic field direction and that these were destroyed when high shear rates perpendicular to the magnetic field were applied. de Gans *et al.* [110] investigated a MR fluid consisting of colloidal silica spheres suspended in an organic ferrofluid, a so-called inverse ferrofluid. They found that the storage modulus, G', was an order of magnitude larger than the loss modulus, G'', at all magnetic fields studied. In addition, a model considering a collection of non-interacting spherical particles was derived for the high frequency limit of the storage modulus. Ramos *et al*. [111] also used a silica-based inverse ferrofluid to study the magnetorheology behavior under small amplitude oscillatory shear in the presence of an external magnetic field. Their results were compared with those of de Gans *et. al* [85, 110] and chain models and excellent agreement was obtained.

For many systems the steady state viscosity is difficult to measure at high shear rate. Data

obtained from oscillatory experiments are usually more reliable and the Cox-Merz rule has been used to predict the viscosity at a steady shear rate, $\eta(\dot{\gamma})$, from oscillatory measurements. Although only partial justification for the Cox-Merz rule has been provided [112] the Cox-Merz rule has been found to hold for many polymer melts, and concentrated and semi-dilute solutions [103]. Recently, Chae and collaborators [113] demonstrated that the Cox-Merz rule was inapplicable to concentrated dispersions of asymmetric magnetic particles. However, they studied a magnetic dispersion of particles with average length of 350 nm which tends to form aggregates and clusters which are difficult to destroy even at high shear rates. Thus the applicability of the so-called Cox-Merz rule to ferrofluids remains an open question.

As the reviewed literature indicates, oscillatory shear experiments have resulted in important insight into the dynamics of magnetorheological fluids and flocculated suspensions for which the viscoelastic moduli seem to depend primarily on the dynamics and mechanics of chain formation, deformation, and breakage. Surprisingly, oscillatory shear experiments have received little application in the study of ferrofluids, even though chain formation, deformation, and breakage are also important processes that determine the magnetorheological properties of ferrofluids [53]. Recently, Pinho *et al*. [114] reported a series of oscillatory shear measurements with commercial ferrofluids in applied magnetic fields. They only reported viscous damping of the force on an oscillating plate in contact with ferrofluid subjected to a constant magnetic field. The viscous damping and associated viscosity increased with magnetic field and monotonically decreased with oscillation frequency, which was limited to 10-50 Hz. Under the conditions of this study the ferrofluid apparently did not display an elastic contribution in the response to the oscillatory shear. Furthermore, the authors did not provide detailed physical or magnetic characterization of the fluid, making interpretation of their results difficult, and did not attempt to

model the observed behavior. Still their contribution is significant as it appears to be the first application of oscillatory techniques to the study of ferrofluids.

In this contribution we study the dynamic magnetoviscosity of a ferrofluid, composed of non-interacting spherical permanently magnetized particles, subjected to a constant magnetic field and an oscillatory shear flow described by

$$\dot{\gamma} = \frac{d\, v_y}{d\, z} = \dot{\gamma}_0 \sin\left(\Omega t\right). \tag{3.38}$$

To do so we apply rotational Brownian dynamics simulations in the inertialess limit and compare these to predictions obtained from the ferrohydrodynamic equations using the kinetic magnetization equation of Martsenyuk, Raikher, and Shliomis [48].

For this simulation the unperturbed flow velocity, $\mathbf{v}$, and the vorticity of the fluid $\boldsymbol{\omega}_f$ are given by

$$\mathbf{v} = \dot{\gamma}\left(t\right) z \mathbf{i}_y = \dot{\gamma}_0 \sin\left(\Omega t\right) z \mathbf{i}_y \;\; ; \boldsymbol{\omega}_f = -\tfrac{1}{2}\dot{\gamma}\left(t\right)\mathbf{i}_x = -\tfrac{1}{2}\dot{\gamma}_0 \sin\left(\Omega t\right)\mathbf{i}_x . \tag{3.39}$$

Applying the same process as in Section 1.5 and using Eqn (3.39) we obtain

$$\Delta\tilde{\boldsymbol{\Phi}}' = \alpha\left(\tilde{\boldsymbol{\mu}}' \times \tilde{\mathbf{H}}'\right)\Delta\tilde{t} - \mathrm{Pe}\sin(\tilde{\Omega}\Delta\tilde{t})\tilde{\boldsymbol{\omega}}_f'\Delta\tilde{t} + \tilde{\mathbf{w}}' . \tag{3.40}$$

The algorithm proceeds from a starting configuration by calculating the change in orientation at each time step. After each time step the quaternion parameters of each particle are normalized. All runs were performed starting from a random configuration, using 10^5 noninteracting particles. The system is stabilized at constant magnetic field and zero shear until it reaches equilibrium, typically after $\tilde{t} = 10$. At this point the oscillatory shear is turned on. A time step of $\tilde{t}$ = 0.0005 was used in order to observe the fastest processes in the system in a frequency range of $0.01 < \tilde{\Omega} < 100.0$. Langevin parameters of α = 0.1, 1.0, and 10.0, and dimensionless shear rates of Pe = 1.0, 5.0, and 10.0 were used.

Because an oscillating shear is applied one would expect a time-periodic magnetoviscosity. When α and Pe are small (i.e., not far from equilibrium) one would expect the response for a sinusoidal shear such as Eqn (3.38) to be equally sinusoidal but with a phase lag. On the other hand, for large values of α and Pe one would expect deviations from sinusoidal response but still time-periodic behavior. To parameterize the dynamic magnetoviscosity we introduce the nth-order in-phase $\eta_n^{'}$ and out-of-phase $\eta_n^{''}$ viscosities using a Fourier series representation of the time dependent pseudo-steady intrinsic magnetoviscosity

$$\left[\eta_{zy}^{m}\right] = \sum_{n=1}^{\infty} \eta_{m,n}^{'} \sin\left(n\Omega t\right) + \sum_{n=1}^{\infty} \eta_{m,n}^{''} \cos\left(n\Omega t\right). \tag{3.41}$$

The n-th order in-phase and out-phase dynamic viscosities can be obtained from

$$\eta_{m,n}^{'} = \frac{1}{\pi}\int_{-\pi}^{\pi} \tilde{\eta}\left(t\right)\sin\left(n\Omega t\right)d\left(\Omega t\right) \quad , \quad \eta_{m,n}^{''} = \frac{1}{\pi}\int_{-\pi}^{\pi} \tilde{\eta}\left(t\right)\cos\left(n\Omega t\right)d\left(\Omega t\right) \quad . \tag{3.42}$$

For low values of α and Pe we expect purely sinusoidal behavior and as such $\eta_n^{'} = 0, \eta_n^{''} = 0$ for $n > 1.0$. However, for large α and Pe we expect deviations from sinusoidal behavior, captured by $\eta_{m,n}^{'} \neq 0$ and $\eta_{m,n}^{''} \neq 0$ with $n > 1.0$. Although Eqn (3.42) defines $\eta_{m,n}^{'}$ and $\eta_{m,n}^{''}$ for any order of n we will focus only on $n = 1$ when analyzing the simulation results, as these are the quantities typically measured in oscillatory shear experiments. In that case we write $\eta_m^{'}$ and $\eta_m^{''}$ for the components of the dynamic magnetoviscosity.

4.2 CONTINUUM MODELING

For ferrofluids consisting of particles with rigidly-locked magnetic dipoles suspended in an incompressible fluid in the infinitely dilute limit, the commonly accepted governing

ferrohydrodynamics equations are [1]

$$\nabla \cdot \mathbf{v}=0\,, \tag{3.43}$$

$$\rho \frac{D\mathbf{v}}{Dt}=\mu_0 \mathbf{M}\cdot\nabla\mathbf{H}-\nabla p+2\zeta\,\nabla\times\boldsymbol{\omega}+\eta_e\nabla^2\mathbf{v}\,, \tag{3.44}$$

$$0=\mu_0\mathbf{M}\times\mathbf{H}+2\zeta\nabla\times\mathbf{v}-4\zeta\omega\,. \tag{3.45}$$

Here **v** is the mass average velocity, ρ is the fluid density, **M** is the suspension magnetization, **H** is the magnetic field, p is the fluid pressure, ζ is the so-called vortex viscosity, $\boldsymbol{\omega}$ is the ferrofluid spin velocity, and $\eta_e=\eta+\zeta$ is an effective viscosity with η the shear viscosity of the ferrofluid. Note that in Eqn (3.44) we have left out the term corresponding to the couple stress and the controversial spin viscosity [12, 30, 78, 100, 115, 116]. This is justified as we are here considering the limit of infinite dilution for which there are no particle-particle magnetic or hydrodynamic interactions and hence no mechanism for transport of internal angular momentum. We have also left out the term corresponding to the moment of inertia density of the nanoparticles, which is a good assumption owing to the small particle size typical of ferrofluids.

Martsenyuk, Raikher, and Shliomis [48] proposed a magnetization relaxation equation, denoted here as the MRSh equation, derived microscopically from the Fokker-Planck equation. This equation has been found to describe well the magnetic field and shear rate dependence of the magnetoviscosity of dilute ferrofluids [96]. The equation is derived using an effective-field method which results in closure of the first moment of magnetization, yielding

$$\frac{d\mathbf{M}}{dt}=\boldsymbol{\Omega}\times\mathbf{M}-\frac{\mathbf{H}\left[\mathbf{H}\cdot\left(\mathbf{M}-\mathbf{M}_{eq}\right)\right]}{\tau_{\parallel}H^2}-\frac{\mathbf{H}\times\left(\mathbf{M}\times\mathbf{H}\right)}{\tau_{\perp}H^2}\,. \tag{3.46}$$

Here **M** stands for the ferrofluid magnetization due to the magnetic field **H** and the flow vorticity $\boldsymbol{\Omega}=\frac{1}{2}\nabla\times\mathbf{v}$. At equilibrium in a stationary field $\mathbf{M}_{eq}$ is described by the Langevin function

$L(\alpha)$,

$$\mathbf{M}_{eq} = nmL(\alpha)\frac{\mathbf{H}}{H} = M_s\left(\coth\alpha - \alpha^{-1}\right)\mathbf{i}_z;\ \alpha = \frac{mH}{k_BT};\ L(\alpha) = \coth\alpha - \alpha^{-1}, \tag{3.47}$$

where *m* is the magnetic dipole moment of an individual particle, *n* is the number density of the particles, and α is the Langevin parameter.

The parallel $\tau_{\|}$ and transverse $\tau_{\perp}$ relaxation times of Eqn (3.46) are given by

$$\tau_{\|} = \frac{d\ln L(\alpha)}{d\ln\alpha}, \quad \tau_{\perp} = \frac{2L(\alpha)}{\alpha - L(\alpha)}\tau, \tag{3.48}$$

with

$$\tau = \frac{3\eta V}{k_BT}, \tag{3.49}$$

being the characteristic Brownian relaxation time of rotational particle diffusion.

The system under consideration will be assumed to be of infinite extent; that is, we will ignore the effect of boundaries and transients associated with momentum diffusion. As such, all spatial derivatives are zero, except for those of the translational velocity which satisfies the condition of simple shear flow in Eqn (3.39). In the following, we will limit attention to the case of a unidirectional applied magnetic field, $\mathbf{H} = H_0\mathbf{i}_z$ and the oscillating simple shear flow of Eqn (3.39). Maxwell's equations in the magnetoquasistatic limit are obeyed; however, these are trivially satisfied by the imposed magnetic field and flow. In this case the simple shear flow will result in a magnetization which lies in the *yz* plane, hence we have $\mathbf{M} = M_y(t)\mathbf{i}_y + M_z(t)\mathbf{i}_z$. Therefore, in component form Eqn (3.46) becomes

$$\frac{\partial M_y}{\partial t} = \frac{1}{2}\dot{\gamma}(t)M_z(t) - \frac{M_y}{\tau_{\perp}};\ \frac{\partial M_z}{\partial t} = -\frac{1}{2}\dot{\gamma}(t)M_y(t) - \frac{\left[M_z(t) - M_sL(\alpha)\right]}{\tau_{\|}}. \tag{3.50}$$

In order to facilitate the analysis and comparisons with the results of Brownian dynamics simulations we introduce the dimensionless quantities

$$\begin{gathered}\tilde{t} = t/2\tau,\ \tilde{\tau}_{\perp} = \frac{\tau_{\perp}}{2\tau},\ \tilde{\tau}_{\parallel} = \frac{\tau_{\parallel}}{2\tau},\ \mathrm{Pe} = 2\dot{\gamma}_0\tau,\ \varepsilon = \frac{Pe}{2} \\ f(\tilde{t}) = M_y/M_s L(\alpha),\ g(\tilde{t}) = M_z/M_s L(\alpha),\ \mathrm{Mn} = \frac{\zeta\dot{\gamma}}{\mu_0 M_s L(\alpha) H_0}\end{gathered}, \tag{3.51}$$

where Mn is a form of the Mason number, the ratio between the viscous and magnetic stresses [87, 117]. Substituting Eqn (3.51) in Eqn (3.50) we obtain

$$\frac{\partial f}{\partial t} = \varepsilon \sin(\tilde{\Omega}\tilde{t}) g(\tilde{t}) - \frac{1}{\tilde{\tau}_{\perp}} f(\tilde{t});\ \frac{\partial g}{\partial t} = -\varepsilon \sin(\tilde{\Omega}\tilde{t}) f(\tilde{t}) - \frac{1}{\tilde{\tau}_{\parallel}}\left[g(\tilde{t}) - 1\right] \tag{3.52}$$

with the initial conditions $f(t=0) = 0$ and $g(t=0) = 1$. In general, Eqn (3.52) has to be solved numerically. However, first we obtain an asymptotic analytical solution in order to gain physical insight.

4.2.1 REGULAR PERTURBATION SOLUTION

To solve Eqn (3.52) analytically we apply a regular perturbation expansion in the small parameter $\varepsilon = Pe/2 < 1$, with the form

$$f(t) = \sum_{n=0}^{\infty} \varepsilon^n f_n(t);\ g(t) = \sum_{n=0}^{\infty} \varepsilon^n g_n(t). \tag{3.53}$$

Eqn (3.53) is introduced into Eqn (3.52) and each term expanded to obtain an equation in power series of ε. The n^{th} order problem corresponds to the terms multiplied by ε^n. Each of these problems can be solved in turn and the solutions added to obtain a power series approximation to the actual solution.

The zeroth order problem is given by

$$\frac{\partial f_0}{\partial t} = -\frac{1}{\tilde{\tau}_\perp} f_0(\tilde{t})\,,\; f_0(0) = 0\,;\; \frac{\partial g_0}{\partial t} = -\frac{1}{\tilde{\tau}_\parallel}\left[g_0(\tilde{t}) - 1\right],\; g_0(0) = 1\,, \tag{3.54}$$

with the solution

$$f_0(\tilde{t}) = 0\,;\; g_0(\tilde{t}) = 1, \tag{3.55}$$

corresponding to equilibrium. The transient approach to this pseudosteady equilibrium state could be obtained, but is not relevant as we seek to understand the pseudosteady response at long times.

The first order problem is given by

$$\frac{\partial f_1}{\partial \tilde{t}} = \sin(\tilde{\Omega}\tilde{t}) g_o(\tilde{t}) - \frac{1}{\tilde{\tau}_\perp} f_1(\tilde{t}),\; f_1(0) = 0\,;\; \frac{\partial g_1}{\partial \tilde{t}} = -\frac{1}{\tilde{\tau}_\parallel} g_1(\tilde{t})\,,\; g_1(0) = 0. \tag{3.56}$$

This system of equations is solved to obtain

$$f_1(\tilde{t}) = \tilde{\tau}_\perp \frac{\sin(\tilde{\Omega}\tilde{t}) - \tilde{\Omega}\tilde{\tau}_\perp \cos(\tilde{\Omega}\tilde{t})}{\left(1 + \tilde{\tau}_\perp^2 \tilde{\Omega}^2\right)}\,;\; g_1(\tilde{t}) = 0\,. \tag{3.57}$$

The second order problem is given by

$$\frac{\partial f_2}{\partial \tilde{t}} = -\frac{1}{\tilde{\tau}_\perp} f_2(\tilde{t})\,;\; \frac{\partial g_2}{\partial \tilde{t}} = -\sin\left(\tilde{\Omega}\tilde{t}\right) f_1(\tilde{t}) - \frac{1}{\tilde{\tau}_\parallel} g_2(\tilde{t}) \tag{3.58}$$

which results in

$$\begin{aligned} &f_2(\tilde{t}) = 0\,; \\ &g_2(\tilde{t}) = \frac{\tilde{\tau}_\parallel \tilde{\tau}_\perp \left[-1 - 4\tilde{\tau}_\parallel{}^2 \tilde{\Omega}^2 + (1 - 2\tilde{\tau}_\parallel \tilde{\tau}_\perp \tilde{\Omega}^2)\cos\left(2\tilde{\Omega}\tilde{t}\right) + (2\tilde{\tau}_\parallel + \tilde{\tau}_\perp)\tilde{\Omega}\sin\left(2\tilde{\Omega}\tilde{t}\right)\right]}{8(1 + 4\ \tilde{\tau}_\parallel{}^2\ \tilde{\Omega}^2)(1 + \tilde{\tau}_\perp{}^2\ \tilde{\Omega}^2)}\,. \end{aligned} \tag{3.59}$$

Similarly for the third order problem we have

$$\frac{\partial f_3}{\partial \tilde{t}} = \sin(\tilde{\Omega}\tilde{t}) g_2(\tilde{t}) - \frac{1}{\tilde{\tau}_\perp} f_3(\tilde{t})\,;\; \frac{\partial g_3}{\partial \tilde{t}} = -\frac{1}{\tilde{\tau}_\parallel} g_3(\tilde{t})\,. \tag{3.60}$$

This is solved to obtain

$$f_3(\tilde{t}) = -C_1\tilde{\tau}_\perp^2\tilde{\Omega}\cos\left(\tilde{t}\tilde{\Omega}\right) + C_2\,\tilde{\tau}_\perp\sin\left(\tilde{t}\tilde{\Omega}\right) - C_3\,\tilde{\tau}_\perp^2\tilde{\tau}_\parallel\tilde{\Omega}\cos\left(3\tilde{t}\tilde{\Omega}\right) + C_4\tilde{\tau}_\perp^2\tilde{\tau}_\parallel\sin\left(3\tilde{t}\tilde{\Omega}\right);$$
$$g_3(\tilde{t}) = 0\,. \tag{3.61}$$

where

$$C_1 = \frac{2 + \tilde{\tau}_\parallel\tilde{\tau}_\perp + 4\tau_\parallel^3\tilde{\tau}_\perp\tilde{\Omega}^2 + 2\tilde{\tau}_\perp{}^2\tilde{\Omega}^2 + \tilde{\tau}_\parallel^2\left\{1 + \tilde{\Omega}^2\left[8 + \tilde{\tau}_\perp^2\left(8\tilde{\Omega}^2 - 1\right)\right]\right\}}{2(1 + 4\tilde{\tau}_\parallel{}^2\tilde{\Omega}^2)(1 + \tilde{\tau}_\perp{}^2\tilde{\Omega}^2)^2}, \tag{3.62}$$

$$C_2 = \frac{4 + 8\tau_\parallel^3\tilde{\tau}_\perp\tilde{\Omega}^2 + 4\tilde{\tau}_\perp{}^2\tilde{\Omega}^2 + \tilde{\tau}_\parallel\tilde{\tau}_\perp\left(3 - \tilde{\tau}_\perp{}^2\tilde{\Omega}^2\right) + 4\tilde{\tau}_\parallel{}^2\tilde{\Omega}^2\left[4 + \tilde{\tau}_\perp{}^2\left(4\tilde{\Omega}^2 - 1\right)\right]}{4(1 + 4\tilde{\tau}_\parallel{}^2\tilde{\Omega}^2)(1 + \tilde{\tau}_\perp{}^2\tilde{\Omega}^2)^2}, \tag{3.63}$$

$$C_3 = \frac{-2\tilde{\tau}_\perp + \tilde{\tau}_\parallel\left(3\tilde{\tau}_\perp{}^2\tilde{\Omega}^2 - 1\right)}{2(1 + 4\tilde{\tau}_\parallel{}^2\tilde{\Omega}^2)(1 + \tilde{\tau}_\perp{}^2\tilde{\Omega}^2)^2\left(1 + 9\tilde{\tau}_\perp{}^2\tilde{\Omega}^2\right)}, \tag{3.64}$$

$$C_4 = \frac{-1 + \tilde{\tau}_\perp\tilde{\Omega}^2\left(8\tilde{\tau}_\parallel + 3\tilde{\tau}_\perp\right)}{4(1 + 4\tilde{\tau}_\parallel{}^2\tilde{\Omega}^2)(1 + \tilde{\tau}_\perp{}^2\tilde{\Omega}^2)^2\left(1 + 9\tilde{\tau}_\perp{}^2\tilde{\Omega}^2\right)}. \tag{3.65}$$

From the solutions to the zeroth to third order problems we may infer that $f_n = 0$ if n is odd and $g_n = 0$ if n is even. Then according to Eqn (3.53) we have

$$f(\tilde{t}) = \tilde{\tau}_\perp\frac{\cos(\tilde{\Omega}\tilde{t}) + \tilde{\Omega}\,\tilde{\tau}_\perp\sin(\tilde{\Omega}\tilde{t})}{2\left(1 + \tilde{\tau}_\perp^2\tilde{\Omega}^2\right)}\varepsilon + \left[-C_1\tilde{\tau}_\perp^2\tilde{\Omega}\cos\left(\tilde{t}\tilde{\Omega}\right) + C_2\,\tilde{\tau}_\perp\sin\left(\tilde{t}\tilde{\Omega}\right) - C_3\,\tilde{\tau}_\perp^2\tilde{\tau}_\parallel\tilde{\Omega}\cos\left(3\tilde{t}\tilde{\Omega}\right) + C_4\tilde{\tau}_\perp^2\tilde{\tau}_\parallel\sin\left(3\tilde{t}\tilde{\Omega}\right)\right]\varepsilon^3 + O\left(\varepsilon^5\right). \tag{3.66}$$

We are interested in evaluating the intrinsic magnetoviscosity, defined as in [59] and which is given by

$$\tilde{\eta}_m = \frac{\eta_m}{\eta_0} = \frac{3}{4}\mathrm{Mn}^{-1}f(\tilde{t})\,. \tag{3.67}$$

Substituting (3.66) in (3.67) the intrinsic magnetoviscosity can be expressed as

$$\tilde{\eta}_m = \frac{3}{4}\varepsilon \mathrm{Mn}^{-1}\left\{\begin{array}{l} \dfrac{\cos(\tilde{\Omega}\tilde{t}) + \tilde{\Omega}\tilde{\tau}_\perp \sin(\tilde{\Omega}\tilde{t})}{2\left(1+\tilde{\tau}_\perp^2\tilde{\Omega}^2\right)}\tilde{\tau}_\perp + \\ \left[\begin{array}{l} -C_1\tilde{\tau}_\perp^2\tilde{\Omega}\cos\left(\tilde{t}\tilde{\Omega}\right) + C_2\tilde{\tau}_\perp \sin\left(\tilde{t}\tilde{\Omega}\right) \\ -C_3\tilde{\tau}_\perp^2\tilde{\tau}_\parallel\tilde{\Omega}\cos\left(3\tilde{t}\tilde{\Omega}\right) + C_4\tilde{\tau}_\perp^2\tilde{\tau}_\parallel \sin\left(3\tilde{t}\tilde{\Omega}\right) \end{array}\right]\varepsilon^2 \\ +O\left(\varepsilon^4\right) \end{array}\right\}. \tag{3.68}$$

Next we recognize that in the infinitely dilute limit

$$\mathrm{Mn}^{-1}\varepsilon = \frac{\mathrm{Mn}^{-1}\,\mathrm{Pe}}{2} = 2\alpha L(\alpha). \tag{3.69}$$

Substituting Eqn s. (3.47), (3.49), and (3.69) in (3.68) and keeping only the first term in the regular perturbation solution, we obtain

$$\tilde{\eta}_m = \frac{3}{2}\frac{\alpha L^2(\alpha)}{\alpha - L(\alpha)}\frac{\sin\left(\tilde{\Omega}\tilde{t}\right) - \tilde{\Omega}\tilde{\tau}_\perp\cos\left(\tilde{\Omega}\tilde{t}\right)}{\left(1+\tilde{\Omega}^2\tilde{\tau}_\perp^2\right)} + O(\varepsilon^2). \tag{3.70}$$

Applying Eqn (3.41) we obtain the following forms for the nondimensional in-phase $\tilde{\eta}^{'}$ and out-phase $\tilde{\eta}^{''}$ dynamic magnetoviscosity

$$\tilde{\eta}_m^{'} = \left[\frac{3}{2}\frac{\alpha L^2(\alpha)}{\alpha - L(\alpha)}\right]\frac{1}{1+\tilde{\Omega}^2\tilde{\tau}_\perp^2} \quad , \quad \tilde{\eta}_m^{''} = \left[\frac{3}{2}\frac{\alpha L^2(\alpha)}{\alpha - L(\alpha)}\right]\frac{\tilde{\Omega}^2\tilde{\tau}_\perp^2}{1+\tilde{\Omega}^2\tilde{\tau}_\perp^2} \quad . \tag{3.71}$$

In obtaining Eqn (3.71) from Eqn (3.68) we have chosen to keep, for simplicity, only the leading order term$\left[O\left(\varepsilon\right)\right]$. In this case the response is seen to be purely sinusoidal. However, we note that inspection of Eqn (3.68) demonstrates that deviations from purely sinusoidal behavior are predicted as Pe increases. These deviations are seen as additional harmonic contributions [terms with $\cos\left(3\tilde{\Omega}\tilde{t}\right)$ and $\sin\left(3\tilde{\Omega}\tilde{t}\right)$ in Eqn (3.68)] which would correspond to higher order $\left(n>1\right)$ in-phase $\tilde{\eta}_{m,n}^{'}$ and out-of-phase $\tilde{\eta}_{m,n}^{''}$ magnetoviscosities.

These expressions in Eqn (3.71) for the in-phase and out-phase components of the magnetoviscosity are similar to the model for the dynamic viscosity of a Maxwell fluid, but with field dependent relaxation time given by Eqn (3.48) and field dependent viscosity equal to $\eta_m = \frac{3}{2}\frac{\alpha L^2(\alpha)}{\alpha - L(\alpha)}\eta\phi$. The Maxwell model describes the viscoelastic behavior of a material using simple mechanical elements such a spring and a dashpot. This model is acceptable as a first approximation to relaxation behavior. If we use the same model to interpret our results, it is clear that the magnetic torque corresponds to the spring while the rotational fluid drag corresponds to the dashpot, and the characteristic time is equal to the field-dependent transverse relaxation time of the nanoparticles.

4.2.2 NUMERICAL SOLUTION

The numerical solution of Eqn (3.52) was obtained using the ODE45 function in MATLAB. This function implements a Runge-Kutta method with a variable time step for efficient computation. The algorithm solves the equations and yields the time-dependent magnetoviscosity. The dynamic in-phase and out-of-phase magnetoviscosities were obtained through numeric implementation of Eqn (3.42) using the trapezoidal rule. This was found to give satisfactory values owing to the small time step size used for numerical output $\left(\Delta\tilde{t} = 0.001\right)$.

4.3 COMPARISON OF SIMULATIONS AND CONTINUUM MODELING

The dynamic magnetoviscosity as a function of shear oscillation frequency for different Langevin Parameters and for Pe = 1.0 is shown in **Figure 4.1**. First, it is noticeable that the dynamic magnetoviscosity increases with increasing magnetic field. Also, as the magnetic field

increases there is a displacement of the crossover frequency for the in-phase and out-of-phase dynamic viscosities to higher frequencies, indicating a decrease of the ferrofluid relaxation time with increasing magnetic field. At frequencies below the crossover η' dominates, indicating viscous behavior, but at higher frequencies η'' dominates indicating an elastic character to the magnetoviscosity. A comparison with the analytical solution of MRSh is also shown for $\varepsilon = 0.5$. The solution agrees with the simulation results for all Langevin parameters, but deviations are seen at higher frequencies for $\alpha = 0.1$. For Pe < 1 we do not see a significant effect of Pe on the simulated dynamic viscosity, consistent with Eqn (3.71).

Another approach for the interpretation of the shear and magnetic field dependence of the dynamic viscosity of ferrofluids is the use of characteristic dimensionless parameters that capture the basic physics of the phenomena. As shown in **Figure 4.2**, using the transverse relaxation time, Eqn (3.48), it is possible to define a new scaled frequency $\tilde{\Omega}_{\perp} = 2\Omega\tau_{\perp}$ with which all the simulation results for Pe < 1 collapse into a single curve.

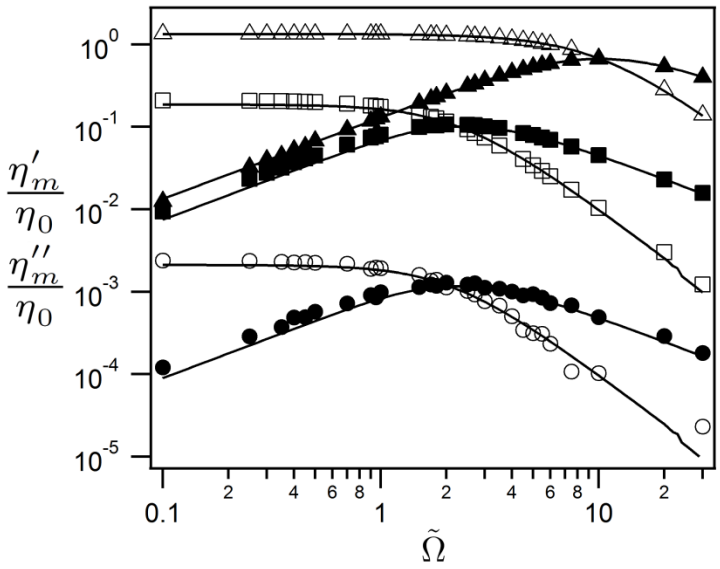

Figure 4.1 In-phase and out-phase magnetoviscosity for different Langevin parameters and Pe = 1. For the in-phase dynamic magnetoviscosity: open circles (○) α = 0.1, open squares (□) α = 1.0, and open triangles (△) α = 10.0. For the out-of-phase dynamic magnetoviscosity, closed circles (●) α = 0.1, closed squares (■) α = 1.0, and closed triangles (▲) α = 10.0. The straight line (—) corresponds to Eqn (3.71).

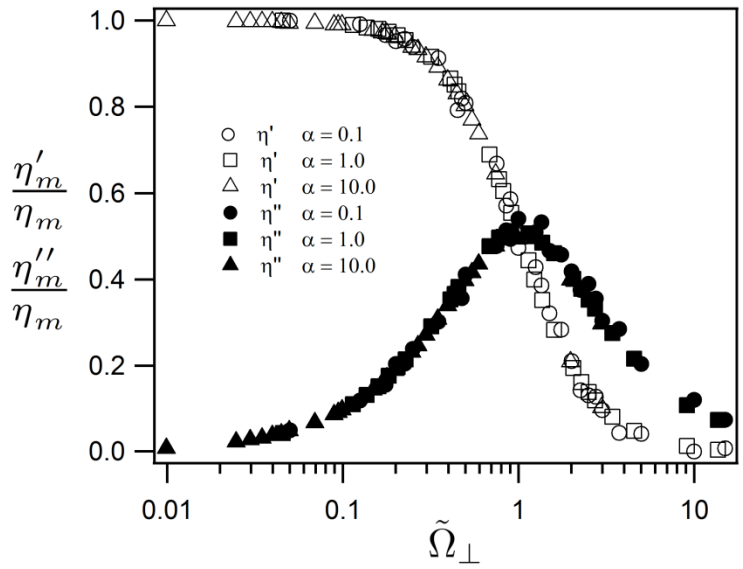

Figure 4.2 Normalized in-phase, $\frac{\eta_m^{'}}{\eta_m}$, and out-phase, $\frac{\eta_m^{''}}{\eta_m}$, dynamic magnetoviscosity for Pe = 1 reduced to a master curve using the dimensionless effective frequency, $\tilde{\Omega}_\perp$.

The oscillatory rheological behavior of the ferrofluid at high shear is shown in **Figure 4.3** for Pe = 5 and **Figure 4.4** for Pe = 10. For both Péclet values it is found that the crossover point shifts to higher frequencies as the magnetic field increases, indicating a decrease of the characteristic time of the ferrofluid response to the oscillatory shear. However, if we interpret the frequency of the peak in $\tilde{\eta}_m^{'}$ as an inverse relaxation time we find that the field dependence of this relaxation time is no longer given by Eqn (3.48) for $\tau_{\perp}$. For Pe = 10.0 (**Figure 4.4**), before the $\tilde{\eta}_m^{'}$ and $\tilde{\eta}_m^{''}$ crossover, there is a clear peak in the $\tilde{\eta}_m^{'}$ curve and $\tilde{\eta}_m^{''}$ becomes higher in magnitude than $\tilde{\eta}_m^{'}$, indicative of a viscous-elastic transition with respect to frequency. A comparison with the numerical solution for Eqn (3.52) is also shown. It is appreciable that the magnetoviscosity obtained by numerical solution of the governing equations using the MRSh equation quantitatively agrees with simulations for both Péclet numbers and different Langevin parameters. It also predicts the viscous-elastic transition shown for Pe = 10. However, as the Langevin parameter increases there is a quantitative deviation of the numerical solution compared with the simulation results in the $\tilde{\eta}_m^{'}$ curve, indicating that the MRSh magnetization relaxation equation is no longer able to quantitatively predict dilute ferrofluid behavior in an oscillating shear flow.

Breakdown of agreement between simulations and predictions using the MRSh equation is further evident when comparing the time dependence of the magnetoviscosity predicted using the two approaches, as shown in Figures 4.5 to 4.8. **Figure 4.5** illustrates oscillatory but not sinusoidal response to the sinusoidal shear flow for Pe = 5.0 and α =1.0. It also shows that sinusoidal response in the magnetoviscosity is recovered at higher applied fields $(\alpha = 10.0)$. In **Figure 4.5** and **Figure 4.6** the agreement between simulations and numerical solution using the

MRSh equation is such that the two curves superimpose. This is also true in **Figure 4.7** for Pe = 10.0 and α =1, where again it is seen that the magnetoviscosity response is not sinusoidal under these conditions. Sinusoidal response is again recovered for higher applied fields, as shown in **Figure 4.8** for Pe=10 and α =10, however this Figure also shows deviation between the predictions of simulations and numerical solution. Interestingly, Figures 4.5 and 4.7 correspond to Mn > 1 whereas Figures 4.6 and 4.8 correspond to Mn < 1. As noted before the Mason number represents the ratio of viscous to magnetic stresses, hence these observations indicate that when the viscous stresses dominate the magnetic stresses deviations may occur from purely sinusoidal magnetoviscous response of a dilute ferrofluid to a sinusoidal oscillating shear flow.

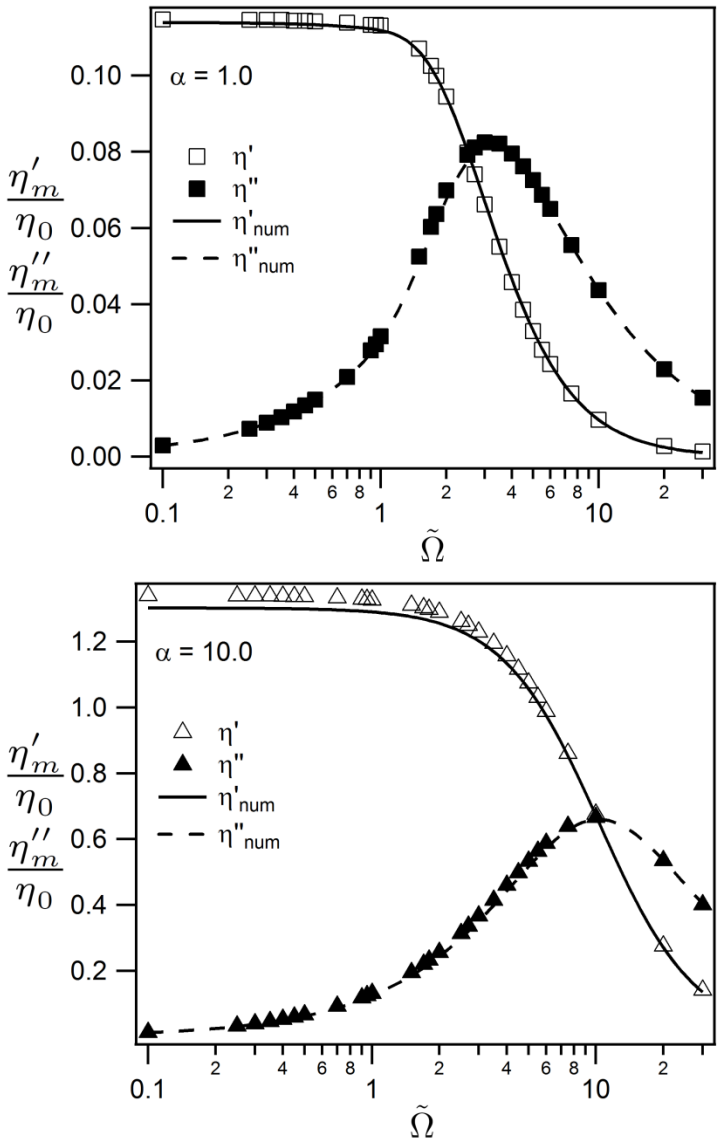

Figure 4.3 In-phase and out-of-phase magnetoviscosity at Pe = 5 for different Langevin parameters for simulation and numerical results

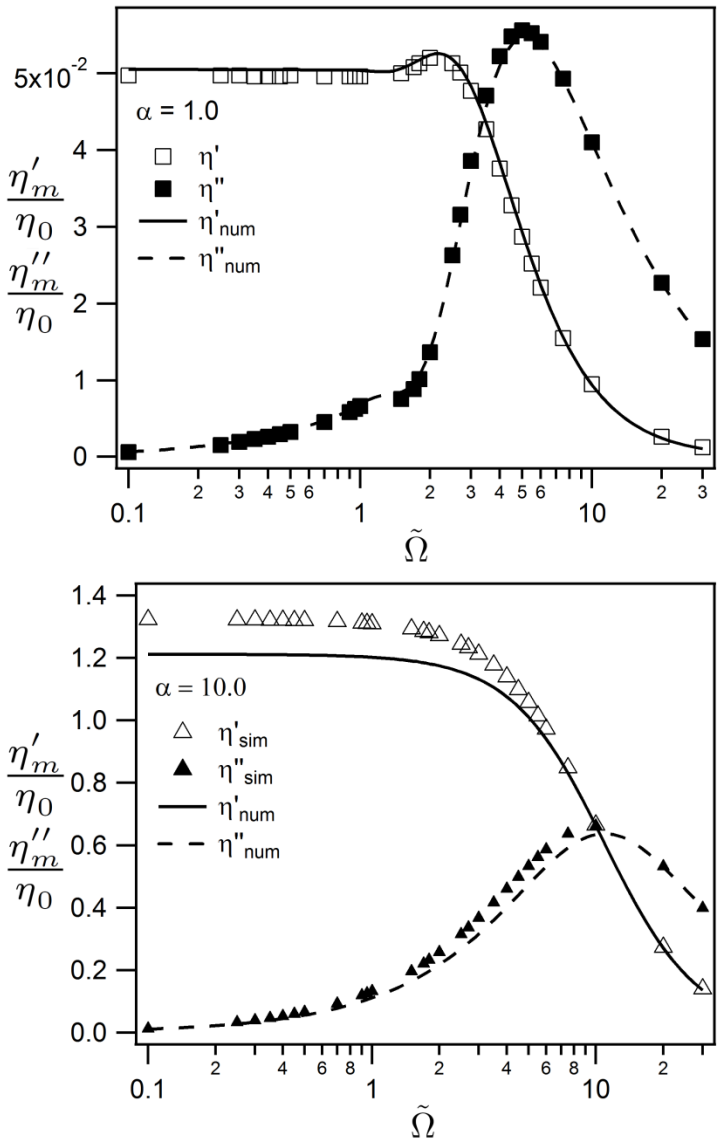

Figure 4.4 In-phase and out-of-phase magnetoviscosity for Pe = 10 at different Langevin parameters for simulation and numerical results

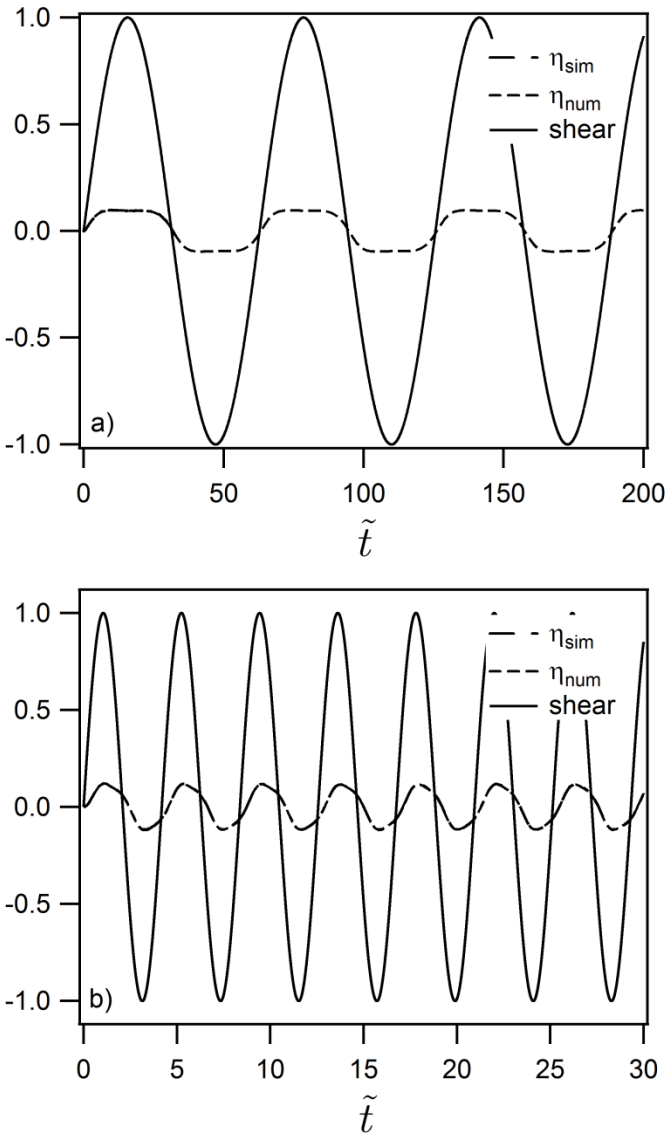

Figure 4.5 Magnetoviscosity as a function of time for Pe = 5 and α = 1.0 and for a) $\tilde{\Omega}$ = 0.1 and b) $\tilde{\Omega}$ = 1.5.

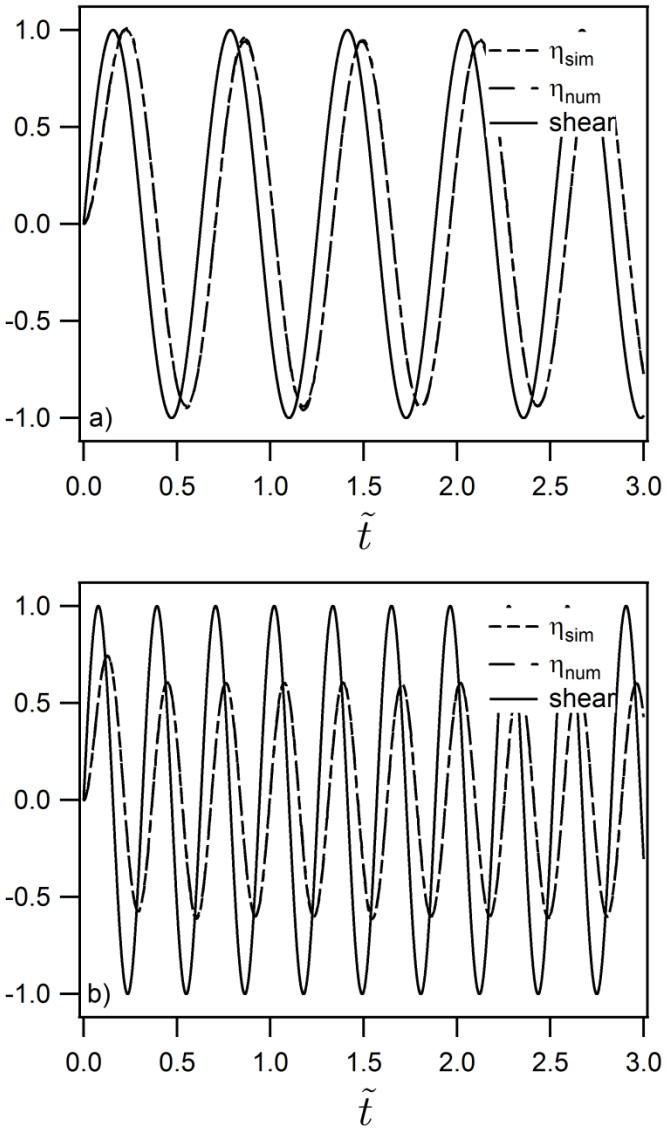

Figure 4.6 Magnetoviscosity as a function of time for Pe = 5 and α = 10.0 and for a) $\tilde{\Omega}$ = 10.0 and b) $\tilde{\Omega}$ = 20.0.

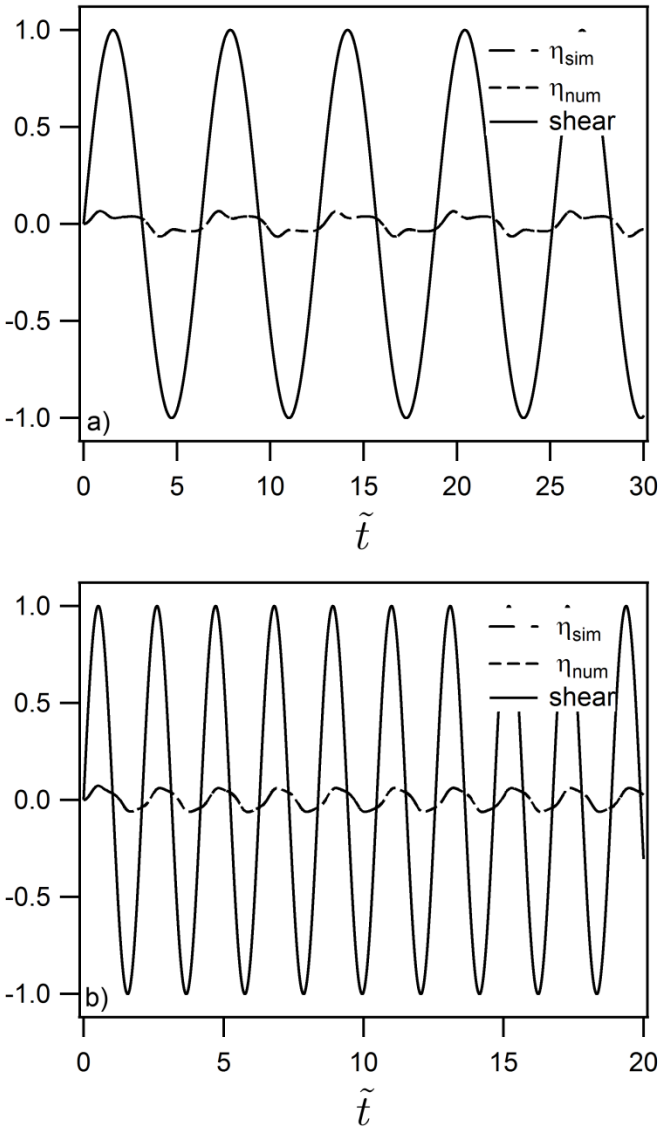

Figure 4.7 Magnetoviscosity as a function of time for Pe = 10 and α = 1.0 and for a) $\tilde{\Omega}$ = 1.0, b) $\tilde{\Omega}$ = 3.0.

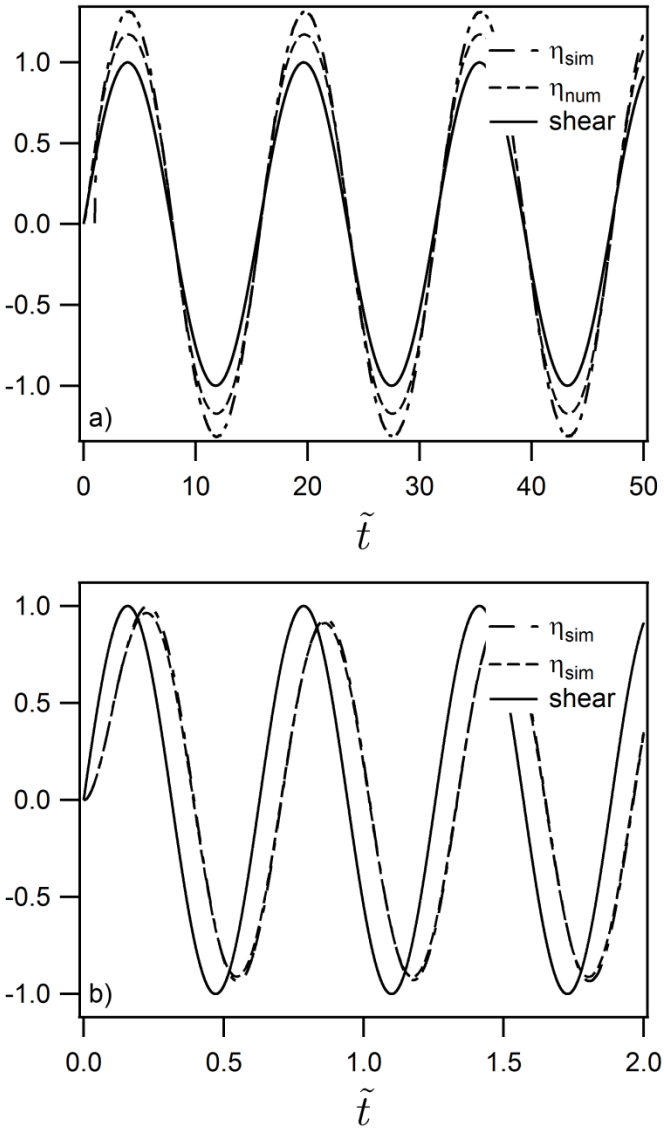

Figure 4.8 Magnetoviscosity as function of time for Pe = 10 and α = 10.0 and for a) $\tilde{\Omega}$ = 0.4 and b) $\tilde{\Omega}$ = 20.0

4.4 CONSIDERATION OF THE COX-MERZ RULE FOR DILUTE FERROFLUID

The Cox-Merz rule [118] states that $\eta(\dot{\gamma}) = \eta^*(\Omega)$ when $\Omega = \dot{\gamma}$, where $\eta(\dot{\gamma})$ is the viscosity at a steady shear rate, and $\eta^*(\Omega)$ is the dynamic viscosity at oscillating frequency Ω. The dynamic viscosity is obtained from the in-phase and out-of-phase viscosities using

$$\eta_m^* = \left[\left(\eta_m^{'} \right)^2 + \left(\eta_m^{"} \right)^2 \right]^{\frac{1}{2}}. \tag{3.72}$$

Note that using the MRSh equation the steady state magnetoviscosity in a constant magnetic field and shear flow is precisely given by [48]

$$\eta_m = \frac{3}{2} \frac{\alpha L^2(\alpha)}{\alpha - L(\alpha)} \eta_0 \phi. \tag{3.73}$$

In our case, using Eqn (3.71) in Eqn (3.72) it can be easily shown that

$$\eta_m^* = \eta_m \left[\left(\frac{1}{1+\Omega^2 \tau_\perp^2} \right)^2 + \left(\frac{\Omega \tau_\perp}{1+\Omega^2 \tau_\perp^2} \right)^2 \right]^{\frac{1}{2}} = \eta_m, \tag{3.74}$$

demonstrating that the Cox-Merz rule applies for dilute ferrofluids under conditions for which Pe << 2.

However, under these conditions the magnetoviscosity is independent of shear rate, making the result rather trivial. Next we consider the applicability of the Cox-Merz rule for higher shear rates by comparing the simulation results of the present contribution to those of our previous work [61] for the steady shear magnetoviscosity. To do so we consider the case where the oscillatory shear flow is given by

$$\dot{\gamma} = \gamma_0 \Omega \sin(\Omega t). \tag{3.75}$$

Note that this is the same as Eqn (3.38) with $\dot{\gamma}_0 = \gamma_0 \Omega$, hence the rotational Péclet number is now $\mathrm{Pe} = \gamma_0 \tilde{\Omega}$ and the frequency is non-dimensionalized with respect to the rotational diffusion coefficient, D_r. The frequency varied from 0.1 to 100.0 and the Langevin parameters used were $\alpha = [0.1, 1.0, 3.0, 5.0, 10.0, 15.0, 20.0, 30.0]$. **Figure 9** shows the complex viscosity calculated from Eqn (3.73) as a function of frequency and the steady state viscosity (from [61]) as a function of shear rate. It is shown that in the limit of low shear rate and low frequency the

dynamic viscosity and the steady state viscosity are similar, indicating the Cox-Merz rule applies under these conditions. However, as the frequency increases the complex viscosity decreases faster than the steady state magnetoviscosity as a function of Pe. Thus, at higher shear rates the Cox-Merz rule ceases to apply.

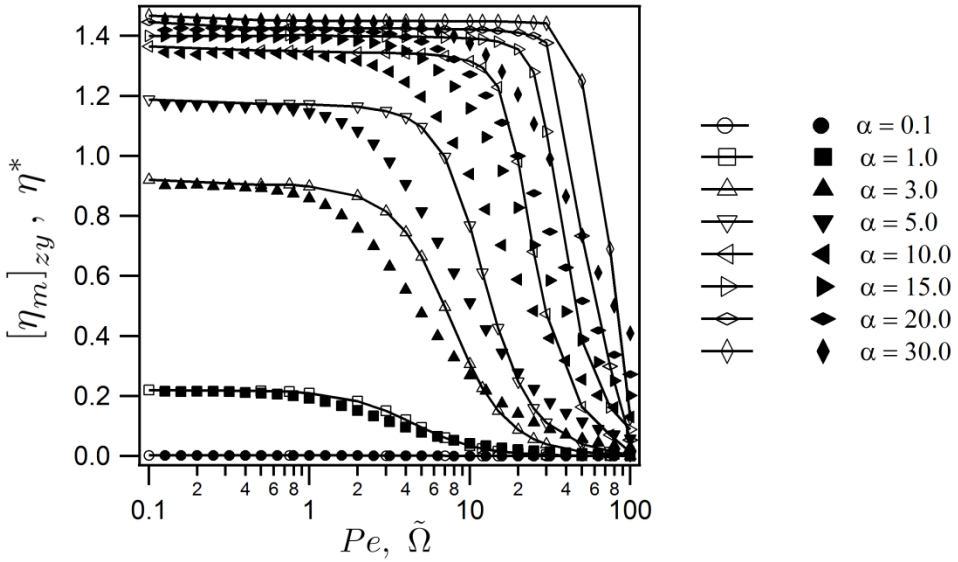

Figure 4.9 Steady shear magnetoviscosity and complex magnetoviscosity as a function of shear rate (Pe) and frequency $\left(\tilde{\Omega}\right)$, respectively. Open symbols are for the steady state magnetoviscosity while closed symbols are for the complex magnetoviscosity.

4.5 CONCLUSIONS

The dynamic properties of dilute ferrofluids under oscillatory shear and constant magnetic fields were studied using Brownian dynamic simulations and continuum modeling using the ferrohydrodynamics equations. Results show that the in-phase and out-of-phase components of the complex magnetoviscosity depend on both magnetic field strength and the frequency and magnitude of the sinusoidal oscillatory shear wave. Even though we are considering the infinitely dilute limit in which there are negligible particle-particle interactions (and therefore no particle chaining) the results indicate an apparent elastic character to the rheology of these suspensions. At

small rotational Péclet number a regular perturbation solution of the continuum equations shows that the response of the magnetoviscosity follows a Maxwell-like model with field dependent viscosity and characteristic time equal to the field-dependent transverse relaxation time. A numerical solution of the ferrohydrodynamics equations was also obtained. Comparison between the numerical solution and simulations shows that the magnetoviscosity obtained using the kinetic magnetization relaxation equation agrees with simulations for a wide range of Péclet number and Langevin parameter, but deviates from the simulations at high values of the Langevin parameter. The Cox-Merz rule for dilute ferrofluids was evaluated using an asymptotic analytical solution of the ferrohydrodynamics equations, valid for $Pe << 2$. It was demonstrated that the Cox-Merz rule applies for dilute ferrofluids under conditions of small shear rates but does not apply at higher shear rates.

5

5 NONLINEAR ENERGY DISSIPATION OF MAGNETIC NANOPARTICLES IN OSCILLATING MAGNETIC FIELDS

Heating effects in ferrofluids subjected to alternating magnetic fields are important for many emerging applications. Despite the many applications in which this heating effect is relevant, it appears that heating of colloidal magnetic fluid due to time varying magnetic field has not been significantly studied from a fundamental perspective. The heat dissipation rate was described by Rosensweig for a collection of non-interacting particles. However this analysis was limited to small applied magnetic field amplitude and frequency due to the use of the phenomenological magnetization relaxation equation derived by Shliomis. This implies that the expression derived by Rosensweig should only be applicable to values of the Langevin parameter less than unity and frequencies below the inverse relaxation time. In this contribution we approach this problem from an alternative phenomenological point of view by solving the phenomenological magnetization relaxation equation exactly for the case of arbitrary magnetic field amplitude and frequency and by solving the magnetization relaxation equation of Martsenyuk, Raikher, and Shliomis numerically. We also used Brownian dynamics simulations of non interacting magnetic nanoparticles subjected to an alternating magnetic field to estimate the rate of energy dissipation and compare the results of the phenomenological theories to the particle-scale simulations. The results are summarized in terms of a non-dimensional energy dissipation rate and show that Rosensweig's expression provides an upper bound on the energy dissipation rate achieved at high field frequency and amplitude.

5.1 INTRODUCTION

Suspensions of magnetic nanoparticles, the so-called ferrofluids, are attractive in a wide range of applications because of their ability to respond to a magnetic field. An important characteristic of this kind of complex fluid is that in the presence of an alternating magnetic field the suspension can generate heat [119-121]. This effect has been used in promising applications such as cancer treatment by magnetic hyperthermia [8, 122-130], which take advantage of the greater sensitivity of tumor tissue to heat than normal temperature. It is desirable to maximize the energy dissipation rate of the magnetic material in order to reduce the amount of material that need to be delivered to the intended tissue. In contrast to this application that takes advantage of heat dissipation of the magnetic particles, there are other applications [117, 131-134] where the temperature increase due to the presence of an alternating field is counter-productive as in the case of loudspeakers [3] in which a layer of ferrofluid is held in place by the permanent magnet in the loudspeaker, replacing the air gap between magnet and voice coil. In contrast with the wide range of emerging applications of ferrofluids, there are just a few theoretical and experimental [135-138] studies of the heat dissipation mechanism.

The heating power of magnetic nanoparticles is determined by several factors including particle type, the frequency of the alternating magnetic field, and the magnetic field intensity. Namely, the two mechanisms most responsible for magnetic relaxation in nanoparticles and subsequently of the heat dissipated by nanoparticles in ferrofluids, are the physical rotation of the individual particles in the fluid (Brownian relaxation) and the collective rotation of the atomic magnetic moments within each particle (Néel relaxation) [34]. For Brownian relaxation the rate of magnetization reorientation is determined by viscosity and particle size, and is determined by

$$\tau_B = \frac{3\eta V}{k_B T}, \tag{4.1}$$

were η is the fluid viscosity, V the volume of a single particle, k_B is the Boltzmann constant, and T the absolute temperature, whereas the Néel relaxation time is determined by

$$\tau_N = \tau_0 \exp\left(\frac{KV}{k_B T}\right), \tag{4.2}$$

where K denotes the magnetocrystalline anisotropy constant and τ_0 is a time constant. Both of these relaxation mechanisms are single particle effects and the shortest relaxation time dominates the process. In a ferrofluid the Brownian or Néel mechanisms both lead to an apparent superparamagnetic behavior, described by the same Langevin function

$$M_0 = M_s L(\alpha) \tag{4.3}$$

If the field, $\mathbf{H} = H_0 \mathbf{i}_z$, is suppressed, the magnetization relaxes to a new equilibrium state. However, in considering dynamic aspects of magnetic nanoparticle suspension, the rate of relaxation can become an important variable. In the case of an external oscillating magnetic field, $\mathbf{H} = H_0 \cos(\Omega t)\mathbf{i}_z$, the dipole moment of the particles follows the oscillations of the magnetic field with a phase-lag between the field and the particle. The magnetization expressed in terms of the complex susceptibility of the particles is

$$M(t) = H_0\left(\chi'\cos(\Omega t) + \chi''\sin(\Omega t)\right) \tag{4.4}$$

where

$$\tilde{\chi}' = \frac{1}{1+(\Omega\tau)^2}, \quad \tilde{\chi}'' = \frac{(\Omega\tau)}{1+(\Omega\tau)^2}. \tag{4.5}$$

Here χ' is the in-phase component and χ'' the out-of-phase component of the dynamic

susceptibility, χ, and $\tau = 1/\Omega_{max}$, where Ω_{max} is the frequency at which χ'' is a maximum. Experimental techniques for measuring the frequency dependent complex susceptibility have been used to determine the brownian relaxation time and hence the particle size of magnetic fluids composed of spherical particles [139-142]. However, most of the experimental studies on the role of Brownian and Néel mechanisms for determining the power dissipated as magnetic heating in ferrofluid have relied on immobilizing nanoparticle rotation by adding some materials to irreversibly solidify the sample [122, 130, 143]. Hence, Brownian contributions to AC losses are eliminated.

The principles underlining the heating of magnetic nanoparticles in a ferrofluid, was reviewed by Rosensweig [144], but it is limited to small applied magnetic field amplitude and frequency due to the use of the phenomenological magnetization relaxation equation, derived by Shliomis in 1972 [49], in the linear magnetization limit. These limitations led Raikher and Stepanov [145] to investigate the absorption of AC field energy in suspensions of magnetic dipoles using a formulation based on solution of the Fokker-Planck equation, predicting that the expression due to Rosensweig ceases to be valid for large values of the applied field frequency.

In this contribution, we approach this problem from an alternative phenomenological point of view by solving the phenomenological magnetization relaxation equation of Shliomis [49] exactly for the case of arbitrary magnetic field amplitude and frequency and by solving the magnetization relaxation equation of Martsenyuk, Raikher, and Shliomis (MRSh) [48] numerically, the latter has been found to accurately describe the magnetic field and shear rate dependence of the magnetoviscosity of dilute ferrofluids [61, 62, 146]. Brownian dynamics simulations of non interacting particles subjected to an oscillating magnetic field are compared with these solutions of the phenomenological models. The results are summarized in terms of a

non-dimensional energy dissipation rate, which is a function of the applied field amplitude, parameterized by the Langevin parameter, and the product of field frequency and relaxation time.

5.2 FORMULATION FOR THE ENERGY DISSIPATION RATE

5.2.1 ROSENSWEIG'S ANALYSIS

According to Rosensweig, for a constant volume adiabatic system in which the work done by the system is due to a magnetic forces, and considering the First law of thermodynamics, the change in internal energy is equal to the magnetic work

$$dU = \delta W . \tag{4.6}$$

In (4.6) the differential magnetic work is $dW = \mathbf{H} \times d\mathbf{B}$, **H** is the magnetic field and **B** is the magnetic induction. The average energy dissipation rate, $\left\langle \dot{Q}_c \right\rangle = \frac{\Omega}{2\pi} \Delta U$, for a cycle of a time periodic magnetic field is given by

$$\left\langle \dot{Q}_c \right\rangle = \frac{\Omega}{2\pi} \int_0^{\frac{2\pi}{\Omega}} \dot{Q} dt = \frac{\Omega}{2\pi} \int_0^{\frac{2\pi}{\Omega}} \mu_0 H \frac{dM}{dt} dt \tag{4.7}$$

However, it will be easier to consider this in terms of dimensionless variables, which we define as

$$\tilde{t} = \frac{t}{\tau} \;;\; \tilde{\Omega} = \Omega \tau \;;\; \tilde{H} = \frac{H}{H_0} \;;\; \tilde{M} = \frac{M}{M_s} \tag{4.8}$$

In that case, we obtain for the average energy dissipation rate

$$\left\langle \dot{Q}_c \right\rangle = \frac{\mu_0 H_0 M_s \Omega}{2\pi} \int_0^{\frac{2\pi}{\tilde{\Omega}}} \tilde{H} \frac{d\tilde{M}}{d\tilde{t}} d\tilde{t} \tag{4.9}$$

Finally, we define the dimensionless rate of energy dissipation as

$$\left\langle \tilde{\dot{Q}}_c \right\rangle = \frac{\left\langle \dot{Q}_c \right\rangle}{\mu_0 M_s H_0 \Omega / 2\pi} = \frac{2\pi}{\tilde{\Omega}} \frac{1}{\tilde{p}} \int_0^{\tilde{p}} \tilde{H} \frac{d\tilde{M}}{d\tilde{t}} d\tilde{t} = -\frac{2\pi}{\tilde{\Omega}} \frac{1}{\tilde{p}} \int_0^{\tilde{p}} \tilde{M} \frac{d\tilde{H}}{d\tilde{t}} d\tilde{t} \;\; ; \;\; \tilde{p} = \frac{2\pi}{\Omega\tau} \tag{4.10}$$

First, we consider a sinusoidal magnetic field H of amplitude H_0 small enough that the response of the suspension is linear. Under such conditions the magnetic field and magnetization are given by

$$\tilde{H} = \cos\tilde{\Omega}\tilde{t} \; ; \tilde{M} = \frac{H_0\chi'}{M_s}\cos\tilde{\Omega}\tilde{t} + \frac{H_0\chi''}{M_s}\sin\tilde{\Omega}\tilde{t} \, , \tag{4.11}$$

where the in-phase and out-of-phase components follow (4.5). Then the dimensionless rate of energy dissipation can be obtained from

$$\begin{aligned} \left\langle \tilde{\dot{Q}}_c \right\rangle &= -\frac{2\pi}{\tilde{\Omega}} \frac{1}{\tilde{p}} \int_0^{\tilde{p}} \tilde{M} \frac{d\tilde{H}}{d\tilde{t}} d\tilde{t} \\ &= \frac{2\pi}{\tilde{p}} \int_0^{\tilde{p}} \left[\frac{H_0\chi'}{M_s}\cos\tilde{\Omega}\tilde{t} + \frac{H_0\chi''}{M_s}\sin\tilde{\Omega}\tilde{t} \right] \sin\tilde{\Omega}\tilde{t} d\tilde{t} \\ &= \frac{\pi\chi'' H_0}{M_s} = \frac{\pi\chi_0 H_0}{M_s} \frac{\Omega\tau}{1+\Omega^2\tau^2} \end{aligned} \tag{4.12}$$

or, in dimensionless form

$$\left\langle \tilde{\dot{Q}}_c \right\rangle = \alpha \frac{\pi}{3} \left(\frac{\Omega\tau}{1+\Omega^2\tau^2} \right). \tag{4.13}$$

Recasting in dimensional form this is equivalent to

$$\left\langle \dot{Q}_c \right\rangle = \frac{\mu_0 \chi_0 H_0^2 \Omega^2 \tau}{2\left(1+\Omega^2\tau^2\right)} \tag{4.14}$$

which is the Rosensweig result [135]. Equation (4.14) predicts a linear relation between the dissipated power and the out-of-phase susceptibility of the ferrofluid and, a power of 2 dependence on magnetic field.

5.2.2 NONLINEAR ENERGY DISSIPATION RATE ACCORDING TO THE SHLIOMIS 1972 PHENOMENOLOGICAL MAGNETIZATION EQUATION

According to Shliomis, the time rate of change of the magnetization of a suspension of non interacting magnetic nanoparticles (a ferrofluid) obeys

$$\frac{dM}{dt} = \frac{1}{\tau}\left[M - M_s L(\alpha)\right] \; ; \; L(\alpha) = \coth\alpha - \frac{1}{\alpha} \; ; \; \alpha = \frac{\mu_0 M_d V H}{kT} \tag{4.15}$$

Here $L(\alpha)$ is the so-called Langevin function, and the argument α is the Langevin parameter. For small values of α the Langevin function reduces to the linear magnetization relaxation equation used to obtain the starting point equations in Rosensweig's analysis. Here we consider arbitrary values of α . In dimensionless form, and for an applied sinusoidal magnetic field, Shliomis's equation can be written as

$$\frac{d\tilde{M}}{d\tilde{t}} = \tilde{M} - \left[\coth\left(\alpha_0 \cos\tilde{\Omega}\tilde{t}\right) - \frac{1}{\alpha_0 \cos\tilde{\Omega}\tilde{t}}\right] , \tag{4.16}$$

where $\alpha_0 = \frac{\mu_0 M_d V H_0}{kT}$. Eqn (4.16) is a non-linear ordinary differential equation. However, because the magnetization response must be time-periodic in the pseudo-steady state, the magnetization can be represented through a Fourier series

$$\tilde{M} = \sum_{n=1}^{\infty} A_n \sin\left(n\tilde{\Omega}\tilde{t}\right) + \sum_{n=0}^{\infty} B_n \cos\left(n\tilde{\Omega}\tilde{t}\right) \tag{4.17}$$

For which the spectral coefficients A_n and B_n are given by

$$A_n = \frac{1}{\pi}\frac{n\tilde{\Omega}F_n(\alpha_0)}{1+n^2\tilde{\Omega}^2} \; ; \; B_n = \frac{1}{\pi}\frac{F_n(\alpha_0)}{1+n^2\tilde{\Omega}^2} \; , \tag{4.18}$$

where

$$F_n(\alpha)=\int_0^{\frac{2\pi}{\tilde{\Omega}}}\left[\coth\left(\alpha_0\cos\tilde{\Omega}\tilde{t}\right)-\frac{1}{\alpha_0\cos\tilde{\Omega}\tilde{t}}\right]\cos\left(\alpha_0\cos\tilde{\Omega}\tilde{t}\right)d\tilde{t}\ . \tag{4.19}$$

Now, for $n=1$, the dimensionless energy dissipation rate becomes

$$\begin{aligned}\left\langle\tilde{\dot{Q}}_c\right\rangle_{Sh'72}&=\frac{2\pi}{\tilde{p}}\int_0^{\tilde{p}}\tilde{M}\sin\tilde{\Omega}\tilde{t}d\tilde{t}\\&=\frac{2\pi}{\tilde{p}}\int_0^{\tilde{p}}\left[\sum_{n=1}^{\infty}A_n\sin\left(n\tilde{\Omega}\tilde{t}\right)+\sum_{n=0}^{\infty}B_n\cos\left(n\tilde{\Omega}\tilde{t}\right)\right]\sin\tilde{\Omega}\tilde{t}d\tilde{t}\end{aligned} \tag{4.20}$$

Hence the average rate of energy dissipation for the phenomenological magnetization equation of Sh'72 is

$$\left\langle\tilde{\dot{Q}}_c\right\rangle_{Sh'72}=\frac{\tilde{\Omega}}{1+\tilde{\Omega}^2}F_1(\alpha)\,. \tag{4.21}$$

5.2.3 NONLINEAR ENERGY DISSIPATION RATE ACCORDING TO THE MRSH MAGNETIZATION RELAXATION EQUATION

A more exact (and albeit more complicated) equation to describe the time rate of change of the magnetization of a suspension of magnetic nanoparticles was derived by Martsenyuk, Raikher, and Shliomis [48]

$$\frac{d\mathbf{M}}{dt}=\boldsymbol{\Omega}\times\mathbf{M}-\frac{\mathbf{H}\left[\mathbf{H}\cdot\left(\mathbf{M}-\mathbf{M}_0\right)\right]}{\tau_{\|}H^2}-\frac{\mathbf{H}\times\left(\mathbf{M}\times\mathbf{H}\right)}{\tau_{\perp}H^2} \tag{4.22}$$

where

$$\tau_{\|}=\frac{d\ln\left(L(\alpha)\right)}{d\ln\alpha}\tau_B\quad,\quad\tau_{\perp}=\frac{2L(\alpha)}{\alpha-L(\alpha)}\,. \tag{4.23}$$

are the parallel and transverse relaxation times. For the simple case of co-linear magnetization and magnetic field, this equation can be shown to reduce to the set of equations (in dimensionless form)

$$\frac{d\tilde{M}}{d\tilde{t}} = -\left[1 - \frac{\alpha_0 \cos\tilde{\Omega}\tilde{t}}{\alpha_e}\right]\tilde{M} \;;\; \tilde{M} = L(\alpha_e) \;;\; \alpha_e = \frac{\mu_0 M_d V H_e}{kT} \tag{4.24}$$

The physical significance of *He* is that it is the magnetic field which would be in equilibrium with the local magnetization at any given instant. This non-linear set of equations can be solved numerically and the corresponding dimensionless average rate of energy dissipation can be calculated from

$$\left\langle \tilde{\dot{Q}}_c \right\rangle_{MRSh} = \frac{2\pi}{\tilde{p}} \int_0^{\tilde{p}} \tilde{M} \sin\tilde{\Omega}\tilde{t} d\tilde{t} \,. \tag{4.25}$$

which indicates that the dimensionless average rate of energy dissipation is directly the first order out-of-phase susceptibility multiplied by a constant factor.

Eqn (4.21) and (4.25) were solved numerically using the ODE45 function in MATLAB which implements a Runge-Kutta method with a variable time step for efficient computation. The algorithm solves the equations and yields the time-dependent magnetization. The dynamic in-phase and out-of-phase susceptibilities were obtained through numeric implementation of Eqn (4.5) using the trapezoidal rule.

5.3 BROWNIAN DYNAMICS SIMULATIONS OF A DILUTE SUSPENSION OF MAGNETIZED PARTICLES SUBJECTED TO AC MAGNETIC FIELD

Brownian dynamics simulations are based on the integration of the stochastic angular momentum equation in a way to obtain the orientation of each particle in the inertialess limit

$$\mathbf{T}_h + \mathbf{T}_m + \mathbf{T}_b = \mathbf{0} \tag{4.26}$$

where the three torques acting on the particle are: $\mathbf{T}_h$ due to hydrodynamic effects, $\mathbf{T}_m$ due to magnetic effects, and $\mathbf{T}_B$ due to Brownian motion. The torque due to hydrodynamic effects is

given by

$$\mathbf{T}_h = -\eta_0 K_r \boldsymbol{\omega}. \tag{4.27}$$

In (4.27) η_0 is the viscosity of the fluid carrier, $K_r = 8\pi r^3$ the hydrodynamic rotational resistance coefficient, and $\boldsymbol{\omega}$ is the angular velocity of the particle. The magnetic torque is given by

$$\mathbf{T}_m = \mu_0 \left(\mathbf{m} \times \mathbf{H}\right), \tag{4.28}$$

where μ_0 is the permeability of free space, $\mathbf{m} = m\boldsymbol{\mu}$, and the magnetic field is $\mathbf{H} = H_0 \cos\left(\Omega t\right)\mathbf{i}_z$. In order to reduce the number of variables in the angular momentum equation, time was non-dimensionalized with respect to the rotational diffusion coefficient $D_r = k_B T \left(\eta_0 K_r\right)^{-1}$, and the vector variables were non-dimensionalized with respect to their corresponding magnitudes. Substituting Eqn (4.27), (4.28) into Eqn (4.26) and setting $d\tilde{\Phi} = \tilde{\omega} d\tilde{t}$ where $d\tilde{\Phi}$ is the infinitesimal rotation vector, integrating from time $\tilde{t}$ to $\tilde{t} + \Delta\tilde{t}$ using a first-order forward Euler method, and applying the fluctuation-dissipation theorem to the Brownian term, the resulting equation is

$$\Delta\tilde{\boldsymbol{\Phi}} = \alpha\left(\left(\tilde{\boldsymbol{\mu}} \times \tilde{\mathbf{H}}\right) \times \tilde{\boldsymbol{\mu}}\right)\Delta\tilde{t} + \tilde{\mathbf{w}} \times \tilde{\boldsymbol{\mu}}. \tag{4.29}$$

The vector $\tilde{\mathbf{w}}$ is a random vector which follows a Gaussian distribution with mean and covariance given by

$$\left\langle \tilde{\mathbf{w}}_i \right\rangle = 0, \quad \left\langle \tilde{\mathbf{w}}_i \tilde{\mathbf{w}}_i \right\rangle = \mathbf{I}\,\Delta\tilde{t}. \tag{4.30}$$

The algorithm proceeds from a starting configuration, using 10^5 non-interacting particles, by calculating the change in orientation at each time step. All runs were performed with a time step of $\Delta\tilde{t} =$ 0.01, Langevin parameters of $0.1 < \alpha < 100$ and magnetic field frequencies of

$0.1 < \Omega < 100.$

Because an oscillating magnetic field is applied one would expect a time-periodic magnetization. When α is small we would expect the response for a sinusoidal magnetic field to be equally sinusoidal but with a phase lag. On the other hand, for large values of α one would expect deviations from sinusoidal response but still time-periodic behavior. To describe the dynamic magnetization we introduce the n[th]-order in-phase $\chi_n^{'}$ and out-of-phase $\chi_n^{''}$ susceptibility using a Fourier series representation of the time dependent pseudo-steady magnetization

$$\tilde{m}_z = \frac{1}{3}\alpha \sum_{n=1}^{\infty} \chi_n^{'} \cos(n\Omega t) + \sum_{n=1}^{\infty} \chi_n^{''} \sin(n\Omega t). \qquad (4.31)$$

Here $n = 1$ denotes the fundamental susceptibility. Then the in-phase and out-of-phase susceptibility can be obtained from

$$\chi_n^{'} = \frac{3}{\pi\alpha} \int_0^{2\pi} \tilde{m}_z(\tilde{t}) \cos(n\tilde{\Omega}\tilde{t}) d(\tilde{\Omega}\tilde{t}) \quad , \quad \chi_n^{''} = \frac{3}{\pi\alpha} \int_0^{2\pi} \tilde{m}_z(\tilde{t}) \sin(n\tilde{\Omega}\tilde{t}) d(\tilde{\Omega}\tilde{t}) \quad . \qquad (4.32)$$

As mentioned above, the energy dissipation rate has been describe according to the thermodynamic analysis and the corresponding dimensionless average rate of energy dissipation can be calculated from (4.10) using simulations results of (4.29) and expressing magnetization as (4.31).

5.4 RESULTS

Figure 5.1 shows in-phase and out-of-phase components of the complex susceptibility as a function of the dimensionless frequency. As the magnetic field increases the in-phase susceptibility curve flattens and the out-of-phase susceptibility curve becomes wider. In addition,

the peak moves to higher frequencies. Moreover, the crossover of the curves occurs at higher frequencies indicating a shift in the effective relaxation time, which is illustrated in **Figure 5.2** and **Figure 5.3**.

As shown in **Figure 5.2**, as the magnetic field increases faster effective relaxation times are observed. Physically, there exists a phase-lag between the magnetization and the magnetic field. At low frequency the magnetic field has a characteristic time longer than the effective time of the particles hence the magnetization is able to follow the oscillating behavior in phase with the magnetic field. As the frequency increases the characteristic time of the magnetic field is lower than the effective time of the particles and the magnetization is no longer in phase with the oscillating behavior of the magnetic field. This effect is observed in the Brownian dynamics simulations and in the numerical solution of the MRSh magnetization equation. MRSh results show in agreement with our simulation except for highest Langevin parameters (i.e. $\alpha > 100$) where it failed to predict the ferrofluids behavior as shown in **Figure 5.3** even though effective relaxation times from simulations and the numerical solution are in agreement but differ from the perpendicular relaxation time predicted by MRSh as shown in **Figure 5.4**.

We now investigate the influence of frequency and magnetic field on the energy dissipation due to non-interacting particles relaxing by the Brownian mechanism. As theory shows, the energy dissipation from a nanoparticle depends upon its magnetic susceptibility which in turn depends on the magnetic field frequency and amplitude. As shown in **Figure 5.5**, simulations indicate higher energy dissipation rates for higher frequencies and lower magnetic fields. A comparison of average energy dissipation obtained from Rosensweig's analysis, our solution of the Shliomis 72 magnetization equation and MRSh magnetization equations, and Brownian dynamics simulations are shown in **Figure 5.6**. Rosensweig's analysis predicts a linear

dependence of energy dissipation with Langevin parameter. Solutions of the Sh72 and MRSh magnetization relaxation equations results agree with Rosensweig's analysis in the limit of low magnetic field intensity and frequency. However, at intermediate frequencies and high fields the energy dissipation deviates from the prediction of Rosensweig's analysis. Explicitly, it is seen that the energy dissipation rate predicted by solution of the Sh'72 and MRSh equations is lower than predicted by Eqn (4.13). Interestingly, the MRSh equation predicts agreement again with the results of Rosensweig for very high applied field frequency. Predictions from Brownian dynamics simulations similarly agree with the Rosensweig result for low field amplitudes, agree with the MRSh results for intermediate field amplitudes, and predict an even lower rate of energy dissipation for the highest applied magnetic field amplitudes.

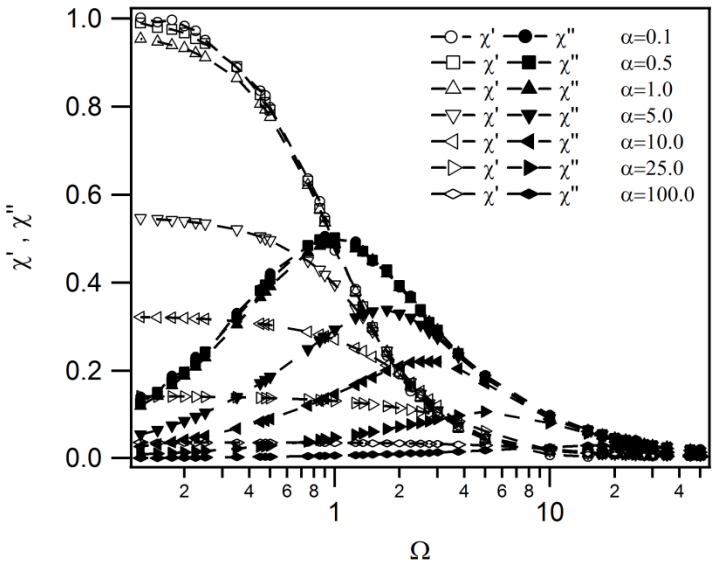

Figure 5.1 Real and imaginary components of the dimensionless complex susceptibility as a function of dimensionless frequency.

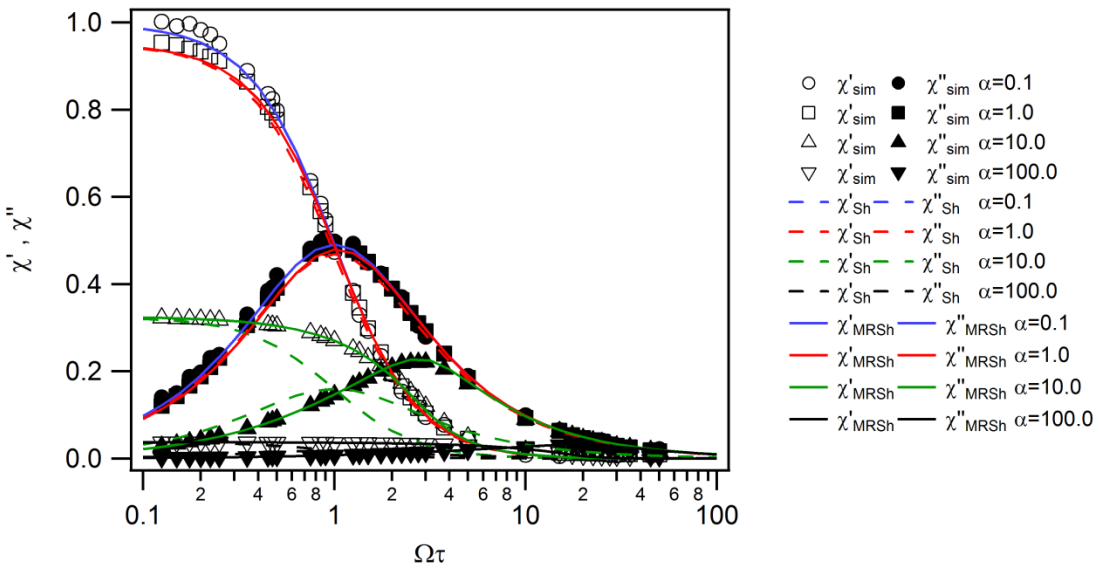

Figure 5.2 Real and imaginary components of the dimensionless complex susceptibility as a function of dimensionless frequency obtained from simulations compared with susceptibility obtained from the MRSh magnetization equation

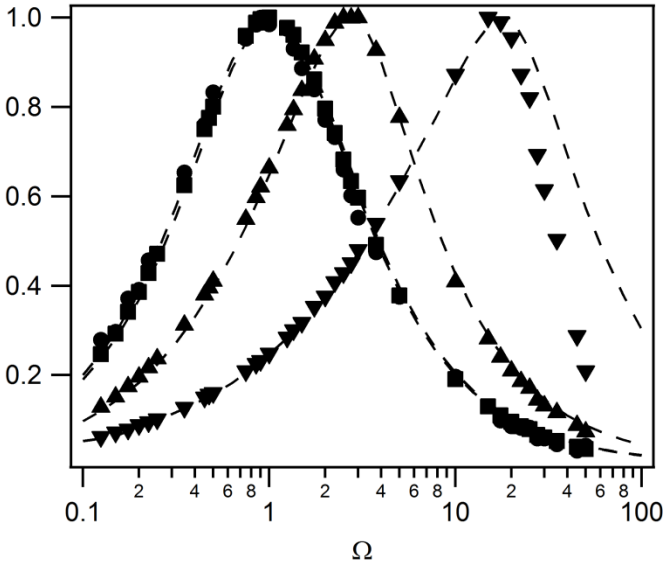

Figure 5.3 Dimensionless out-of-phase susceptibility as a function of dimensionless frequency. Circles (●) α = 0.1, squares (■) α = 1.0, upward triangles (▲) α = 10.0, and downward triangles (▼) α = 100.0. The straight line (—) corresponds to out-of-phase susceptibility obtained from the MRSh magnetization equation for the different values of the Langevin parameters.

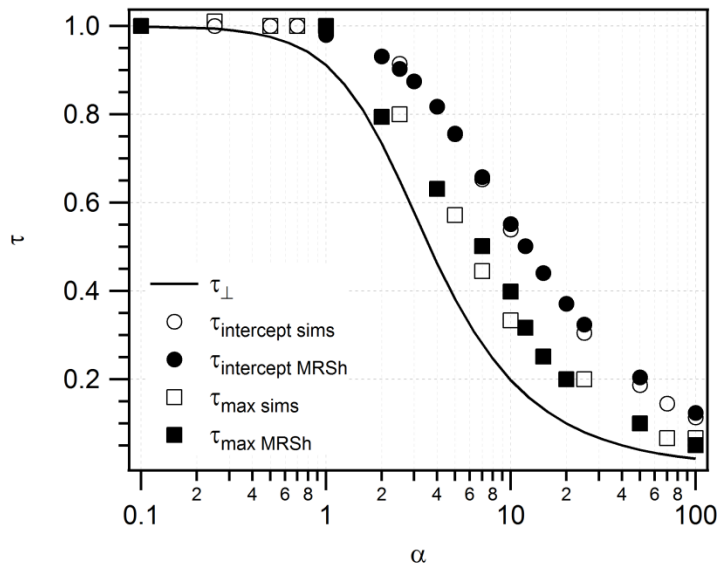

Figure 5.4 Relaxation time comparison between perpendicular relaxation predicted by MRSh, simulations and numerical solution

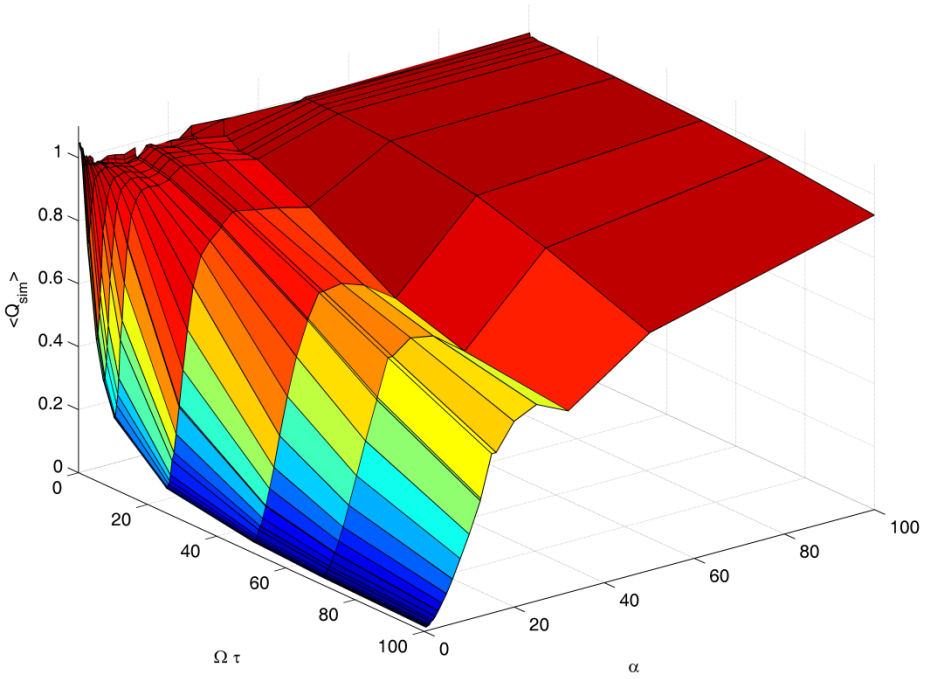

Figure 5.5 Energy dissipation rates obtained from Brownian dynamic simulations as a function of dimensionless frequency and Langevin parameter

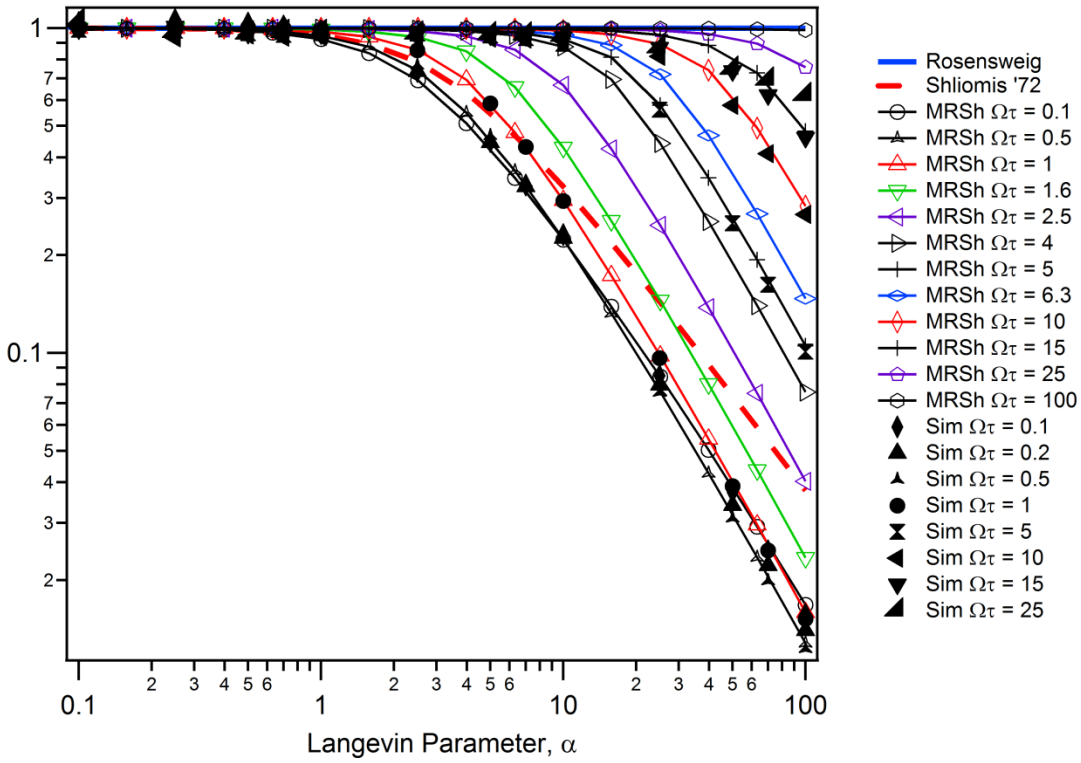

Figure 5.6 Non dimensional energy dissipation rate as a function of the Langevin parameter

5.5 CONCLUSIONS

Dynamic magnetization behavior was studied by Brownian dynamics simulations. Results show that as the magnetic field intensity increases, the crossover of the susceptibility curves moves to higher frequencies indicating a decrease in the effective relaxation time. Because energy dissipation from ferrofluids depends upon their complex magnetic susceptibility, which in turn is related to the ferrofluid relaxation time, we also obtain energy dissipation rate from the simulations and by obtaining a numerical solution of the Shliomis'72 and MRSh phenomenological magnetization equations. We showed that Rosensweig's original analysis is strictly limited to low magnetic field amplitude and frequency, owing to the limitations imposed by the use of Shliomis's magnetization relaxation equation and a linear form of the equilibrium

magnetization. However, using the more exact equation due to MRSh and use of Brownian dynamics simulations; we demonstrate that Rosensweig's expression surprisingly provides an upper bound on the energy dissipation rate achieved at high field frequency and amplitude. The results of our analysis should allow for rigorous testing of the underlying models using experiments and should permit more accurate estimation of energy dissipation rates in ferrofluids under typical application conditions of moderate magnetic fields. Although account of particle size polydispersity is not given here, this can be obtained through ensemble averaging using an appropriate size distribution model. Consideration of the effect of particle-particle interactions is left to a future contribution.

6

6 BROWNIAN DYNAMICS SIMULATIONS OF MAGNETICALLY INTERACTING MAGNETIZED PARTICLES IN D.C. AND A.C. MAGNETIC FIELDS

Brownian motion of magnetized interacting spherical particles suspended in Newtonian fluid, under applied d.c. and a.c. magnetic field was studied using Brownian dynamics simulations, including the effect of magnetic dipole-dipole interactions. The algorithm describing the change in the suspension magnetization was obtained from the stochastic angular momentum equation with the reaction field method for the long range dipolar interactions. We investigate magnetization curves, complex susceptibility in various concentrations and particle dipole moment ranges. Simulation results are in agreement with the Langevin function for equilibrium magnetization. Dynamic susceptibilities were obtained from the response to oscillating magnetic fields at different frequencies. Deviations from Debye's model were observed even for low dipolar interaction strength.

6.1 INTRODUCTION

Considerable interest has been given in the past decades to the dynamic magnetization of ferrofluids in the presence of applied magnetic fields and the corresponding complex magnetic susceptibility. This increased interest in a better understanding of the behavior of these materials is related to their renewed technological importance, with various applications such as drug targeting, and cancer treatment by magnetic hyperthermia [4, 147]. For this reason, magnetic properties of ferrofluids have been extensively studied for its dependence with particle size, composition, frequency, and magnitude of the applied magnetic field.

Experiments [53, 148] demonstrate that magnetodipolar particle-particle interactions significantly affect both the equilibrium and dynamical properties of ferrofluids. However, there is no clear and definitive answer to several key points. Theoretical models of dynamical properties of dilute ferrofluids with vanishing interparticle interactions have been proposed [48-51, 97]. These models lead to accurate results for highly dilute ferrofluids but cannot explain properties and behavior of ferrofluids where the particle interactions are significant. At present there is no general theory to predict, quantitatively, the properties of ferrofluids under typical experimental conditions. Normally, researchers consider different dynamical phenomena in ferrofluids separately, creating a combination of models that serve as a basis of constructing theories of real magnetic fluids [107, 149-154]. To seek further understanding of the interaction effects in particle systems, computer simulations [21, 94, 152, 153, 155, 156] become an important tool, whose main advantage is the easy way by which it is possible to vary parameters such as the relative strength of interactions.

In this contribution ac-susceptibility and magnetic relaxation measurements have been used to probe the concentration effects in the dynamic properties of ferrofluids using Brownian

dynamics simulations with the reaction field method used to calculate the long range dipolar interactions. It is considered that the magnetic moment of the particles is fixed with respect to the particle itself. The effects of the interactions are scrutinized by studying the change in the magnetic relaxation going from a non-interacting system to a system significant with particle interactions.

6.2 ALGORITHM FORMULATION

In section 1.4 we discussed how a magnetic field exerts a torque on the magnetic particles in the ferrofluid, influencing their free rotation in the shear flow. The theory used to describe the related phenomena explicitly excludes any interaction, resulting basically in a single particle model. In reality, the motion of each particle in a ferrofluid suspension is affected by interactions with the molecules of the solvent and with other magnetic particles, the flow of the solvent, and the action of the external magnetic field, resulting in interesting rheological and magnetic properties. Hence, the theory used in Chapter 2, 3 and 4, to describe the related phenomena is no longer applicable and both Eqn (1.29) and (1.30) have to be considered.

Ferrofluids are rather complicated systems colloids, because there exist several different interactions between the ferrofluid particles: (i) short-range repulsive interaction due to the presence of the coating layer on (ideally) each ferrofluid particle; (ii) long-range magnetodipolar interaction between magnetic moments of ferrofluid particles; and (iii) long-range hydrodynamic interactions arising because each moving particle induce a perturbation flow in the surrounding fluid and this flow acts on all other particles. In this work we do not consider hydrodynamic interactions.

The short range steric particle repulsion is the simplest interaction from the simulation

point of view, because the calculation of any short-range force for the whole system requires only $\sim N$ operations where N is the particle number, due to the possibility to introduce a final cut-off radius, R_{cut} , for such an interaction. The two most commonly used forms are the Lennard-Jones potential and the Yukawa exponential form. The Lennard-Jones potential was suggested a long time ago simply to accelerate the computation of the short-range potential. The Yukawa potential can in principle be derived from the interaction potential of an electric double layer and the Debye-Huckel theory of strong electrolytes, but neither of these justifications if valid at least for an organic solvent based ferrofluids with magnetic particles are coated by a neutral polymer shell. Because the actual form of U_{rep} is unknown, we choose to model interactions between particles i and j by the Lennard Jones potential [157]. The potential is given by

$$U_{ij}^{LJ}(r_{ij}) = 4\varepsilon\left[\left(\frac{\sigma}{r_{ij}}\right)^{12} - B\left(\frac{\sigma}{r_{ij}}\right)^{6}\right]. \tag{5.1}$$

Here r_{ij} is the distance between the center of the particles i and j, and D is a constant parameter that represents attraction effects between particles. The Lennard-Jones potential is purely repulsive for $B = 0$.

Magnetodipolar interaction, in contrast to steric repulsion, is a long-range interaction. This means that the cut-off of this interaction is not allowed. The problem of the evaluation of the long-range dipolar field is especially difficult for a ferrofluid because it represents a disordered particle system. The most widely used and accepted method in this context is the Ewald summation technique [56, 158] where the lattice sums over Coulomb or dipolar interactions are split into a real space part involving only particles within the central simulation cell, and a Fourier part involving a sum over reciprocal lattice vectors. The convergence of these parts is then

controlled by a few parameters such as the parameter κ determining the range of the real-space potentials, and the number of reciprocal lattice vectors, $a_{\max}$, taken into account in the evaluation of the Fourier part. Since these parameters are not independent of each other, the challenge in any practical application of Ewald sums consist of finding optimal values such that each partial sum converges towards a pre-described accuracy while at the same time the computational effort is minimized. The disadvantage of this method is the unrealistic way an instantaneous dipolar fluctuation of charge in the simulation box is duplicated in the infinite replica system.

In the case of dipole-dipole interaction, another method is the reaction field method. In this method, the field on a dipole in the simulation consists of two parts: the first is a short range contribution from molecules situated within a cutoff sphere or cavity, $\mathfrak{R}$, and the second arises from molecules outside the cavity which are considered to form a dielectric continuum, ε_s, producing a reaction field within the cavity (see Figure 6.1). The size of the reaction field acting on molecule i is proportional to the moment of the cavity surrounding i,

$$\varsigma_i = \frac{2(\varepsilon_s - 1)}{2\varepsilon_s + 1} \frac{1}{r_c^3} \sum_{j \in \mathfrak{R}} \boldsymbol{\mu}_j \tag{5.2}$$

where the summation extends over the molecules in the cavity, including i, and r_c is the radius of the cavity. The contribution to the energy from the reaction field is $-\frac{1}{2}\boldsymbol{\mu}_i \cdot \varsigma_i$. The torque on molecule i from the reaction field is $\boldsymbol{\mu}_i \times \varsigma_i$.

We consider the magnetic effects for particles that interact with each other are of two types: those due to the external magnetic field, given by Eqn (1.32), and those due to interaction between particles. The magnetic forces due to particle interactions can be calculated from the dipole-dipole interaction energy

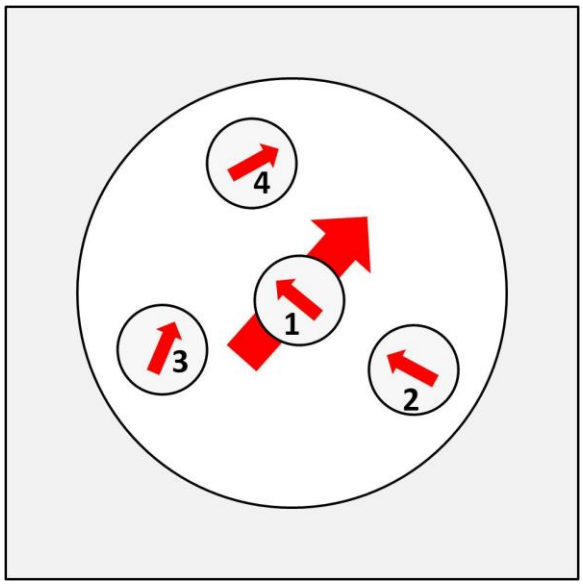

Figure 6.1 A cavity and reaction field. Molecules 2, 3, and 4 interact directly with molecule 1. The continuum polarized by the molecules in the cavity produces a reaction field at 1.

$$U_{dipole,ij} = \frac{\mu_0}{4\pi}\left[\frac{\mu_i\mu_j}{r_{ij}^3} - \frac{3\left(\mu_i r_{ij}\right)\left(\mu_j r_{ij}\right)}{r_{ij}^5}\right]. \tag{5.3}$$

The force on particle i is then derived from $\mathbf{F}_{m,i} = -\nabla_i U_{dipole,i}$, where $U_{dipole,i} = \sum_j U_{dipole,j}$ is the energy of particle i in the field of the other particles. The torque exerted by other particles on particle i is obtained from $\mathbf{T}_{m,i} = \mu_0\left(\mu_i \times \mathbf{H}_i\right)$, where the magnetic field $\mathbf{H}_i$ is given by $U_{dipole,i} = -\mu_0\left(\mu_i \cdot \mathbf{H}_i\right)$.

Brownian forces are represented by stochastic terms of the form $\mathbf{F}_{B,i} = \beta_i^t \cdot \mathbf{w}_i^t$, in which β_i^t and $\mathbf{w}_i^t$ have the same relation as Eqn (1.35) and Eqn (1.36) .

The translational and rotational Langevin equations of motion of particle i are given by

$$\begin{aligned} M_i\dot{\mathbf{v}}_i &= \mathbf{F}_i - \zeta_t\mathbf{v}_i + \mathbf{F}_{B,i}^t \\ \mathbf{I}_i \cdot \dot{\boldsymbol{\omega}}_i &= \mathbf{T}_i - \zeta_r\boldsymbol{\omega}_i + \mathbf{T}_{B,i}^r \end{aligned} \tag{5.4}$$

where M_i and $\mathbf{I}_i$ are the mass and inertia tensor of the particle, ζ_t and ζ_r are the translational and rotational friction constants, respectively. The Brownian force and torque follow the same properties as Eqn (1.34). The equations presented in Eqn (5.4) are the complete set of equations for the study of interacting and interacting magnetic particle suspensions.

Introducing the dipolar and short-range terms into Eqn (5.4) the dimensionless equations of motion can now be written as

$$\begin{aligned} \dot{\mathbf{v}}_i^* &= \sum_{j\neq i}\left(\mathbf{F}_{ij}^{dip*} + \mathbf{F}_{ij}^{LJ*} + \mathbf{F}_{ij}^{rf*}\right) - \zeta_t^* \mathbf{v}_i^* + \mathbf{F}_{B,i}^{t*}, \\ \mathbf{I}_i^* \cdot \dot{\boldsymbol{\omega}}_i^* &= \sum_{j\neq i}\left(\mathbf{T}_{ij}^{dip*}\right) + \mathbf{T}_{m,i}^* - \zeta_r^* \boldsymbol{\omega}_i^* + \mathbf{T}_{B,i}^{r*}. \end{aligned} \tag{5.5}$$

Here the variables are given in dimensionless form, reduced by the following units: length $r^* = r/\sigma$, dipole moment $m^{*2} = m^2/4\pi\mu_0 \in \sigma^3$, moment of inertia $I^* = I/(M\sigma^2)$, time $t^* = t\left(\in/M\sigma^2\right)^{1/2}$, the friction constants $\zeta_t^* = \zeta_t\left(\sigma^2/M\in\right)^{1/2}$, and $\zeta_r^* = \zeta_r\Big/\left(M\sigma^2\in\right)^{1/2}$, magnetic field $H^* = H\left(4\pi\mu_0\sigma^3/\in\right)^{1/2}$ as well as temperature $T^* = k_B T/\in$. The values of the dimensionless friction constant do not affect the equilibrium properties.

The investigated ferrofluid system consists of $N = 1000$ spherical particles of diameter σ distributed in a cubic simulation box of side length L. Each particle has a permanent point dipole moment $\mathbf{m}_i$ at its center. The solvent of the ferrofluid is not considered explicitly. Instead, it is assumed that collisions keep the particles in thermal equilibrium with the solvent. To model this effect, Brownian forces are added to the equations of motion. We used periodic boundary conditions in all space directions and the reaction field method explained. In this work focusing on the magnetic properties of the suspension, hydrodynamic interactions are neglected.

The simulations were performed at constant reduced temperature $T^* = 1$ and a reduced

time step $\Delta t^* = 0.0025$ .The runs were started from initial configurations with random particle positions and dipole moment orientations. For each case, the system was first equilibrated for a period of 50 000 time steps. The magnetization properties were then calculated from the data for another period of at least 500 000 steps. The volume fractions were in the range $0.001 < \phi < 0.07$.

6.3 RESULTS

Simulations were performed for a wide range of volume fractions varying between $0.001 < \phi < 0.07$ and different dipolar interactions. We compared the simulation results with the theoretical Langevin function. The magnetization of the magnetic suspensions for the equilibrium simulations are shown in **Figure 6.2**. Results are in good agreement with theory for low volume fractions which indicates that the algorithm is capable to describing the equilibrium properties of a suspension of interacting particles.

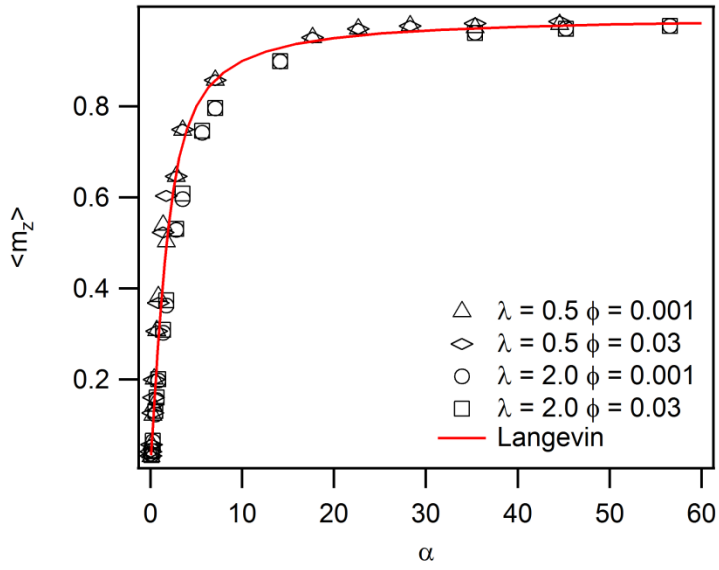

Figure 6.2 Reduced magnetization for interacting particle suspension compared with the Langevin function at different dipolar interaction strength and volume fraction.

6.4 PROPOSED WORK

In real ferrofluids the understanding of changing of specific properties such as microstructure or apparent density, viscosity, birefringence, among other due to the presence of an applied magnetic field has attracted considerable interest. However, there is no clear and definitive answer on several points, in particular the possible control of the formation of chains. Therefore, the role of the magnetic dipolar interactions in the structural and dynamic properties of these magnetic fluids becomes a possible area of study. One of the interests of this study is that it is possible to compare with experimental results obtained by the synthesized and characterization of particles by the same research group, which make a direct relation in the control parameter such as magnetic field, concentration, temperature, among others of both experiments and simulations.

Brownian dynamics simulations with particle interactions are able to provide not only the structural properties of the suspension but also the dynamical behavior of the particles. In addition, most of the theory of ferrohydrodynamics was developed for ferrofluids in the highly dilute limit, i.e. particle interaction is not considered. Then, simulations considering low dipolar interactions and low concentrations could study the limit at which theory is capable to predict ferrofluids behavior.

7

7 CONCLUDING REMARKS AND DISSERTATION CONTRIBUTION

The aim of this dissertation was to contribute to the understanding of the magnetic and rheological properties of dilute and semi-dilute suspensions of spherical magnetic nanoparticles suspended in Newtonian fluids and under applied shear and constant magnetic fields by rotational Brownian dynamics simulations. Prior work on modeling the behavior of ferrofluids has focused on using phenomenological suspension scale continuum equations, but there is a controversy regarding which equation correctly describes the rate of change of the ferrofluid magnetization. Our work found that for suspensions of spherical particles, excellent agreement was observed between predictions of the Martsenyuk, Raikher, and Shliomis (MRSh) relaxation equation and our direct simulations.

It was shown that the magnetoviscosity of dilute ferrofluids could be described using a newly defined rotational Mason number, which collapses the simulation results into a single master curve. Moreover, results also show that the assumed $\sin^2\beta$ dependence of the magnetoviscosity on the angle β between the vorticity and the magnetic field is only valid for low fields and high shear rates.

The Brownian dynamics simulation method was used to study the transient behavior in the magnetoviscosity of a dilute ferrofluid in response to step changes in shear rate and magnetic field. For comparison purposes, a simple mathematical analysis based on the ferrohydrodynamic equations in the linear magnetization limit was derived. In both, simulations and mathematical

solution, it was observed that the approach of the magnetoviscosity to the steady state value can be either monotonic or oscillatory depending on the particular values of magnetic field amplitude and shear rate. Such observations are relevant in the operation of devices which take advantage of the magnetoviscous effect, as oscillatory response can lead to instability in device performance.

The dynamic properties of dilute ferrofluids under oscillatory shear and constant magnetic fields were studied using Brownian dynamics simulations and continuum modeling using the ferrohydrodynamics equations. Results show that the in-phase and out-of-phase components of the complex magnetoviscosity depend on both magnetic field and frequency of the sinusoidal oscillatory shear wave. Even though we are considering the infinitely dilute limit in which there are negligible particle-particle interactions, and therefore no particle chaining, the results indicate an apparent elastic character to the rheology of these suspensions. At small rotational Péclet number a regular perturbation solution of the continuum equations shows that the response of the magnetoviscosity followed a Maxwell-like model with field dependent viscosity and characteristic time equal to the field-dependent transverse relaxation time. A numerical solution of the ferrohydrodynamics equations was also obtained and compared with simulation results, which shows that the magnetoviscosity obtained using the kinetic magnetization relaxation equation agrees with simulations for a wide range of Péclet number and Langevin parameter, but deviates from the simulations at high values of the Langevin parameter. In addition we determined if the Cox-Merz rule apply for dilute ferrofluids using an asymptotic analytical solution of the ferrohydrodynamics equations, valid for $Pe << 2$. It was demonstrated that the Cox-Merz rule applies for dilute ferrofluids under conditions of small shear rates but does not apply at higher shear rates even though ferrofluids shows an apparent viscoelastic property.

Because energy dissipation from ferrofluids depends upon their magnetic susceptibility,

Brownian dynamics simulations for magnetic nanoparticles subjected to an alternating magnetic field were performed. Simulation results, as well as numerical solution of the MRSh magnetization equation, showed that Rosensweig's original analysis is strictly limited to low magnetic field amplitude and frequency, owing to the limitations imposed by the use of Shliomis's magnetization relaxation equation. However, use of the more exact equation due to MRSh demonstrates that Rosensweig's expression provides an upper bound on the energy dissipation rate achieved at high field frequency and amplitude but more complex behavior is observed for intermediate values.

Finally, an algorithm that includes dipolar interaction was developed and shown to predict correctly the equilibrium properties of ferrofluids in a wide range of dipolar interaction parameters and volume fraction of particles. In addition, using this algorithm, it is proposed to study the validation of the constitutive magnetization equations as well as structure formations with and without applied magnetic fields.

APPENDIX A: PREDICTIONS OF THE VARIOUS MAGNETIZATION RELAXATION EQUATIONS

Differences between the magnetization relaxation equations are also manifested in their predictions for the relaxation from equilibrium magnetization in a quiescent ferrofluid after the external field is suddenly switched off. In that case the transient magnetization of the suspension is such that $\boldsymbol{\Omega} = 0$ and both $\mathbf{M}$ and $\mathbf{H}_e$ are always parallel to $\mathbf{H}$. Under these conditions Eqn (2.1) reduces to

$$\frac{dM}{dt} = -\frac{(M - M_0)}{\tau}, \tag{A.1}$$

whereas the MRSh Eqn (2.5) and the Sh'01 Eqn (2.7) reduce to

$$\frac{dM}{dt} = -\left(1 - \frac{H}{H_e}\right)\frac{M}{\tau}, \tag{A.2}$$

$$\frac{dH_e}{dt} = -\frac{\left(H_e - H\right)}{\tau}, \tag{A.3}$$

respectively. These equations were integrated numerically and the predicted relaxation is shown in **Figure A.1.** For Eqn (A.1) and Eqn (A.2) the decay in reduced magnetization follows exponential behavior, while Eqn (A.3) only predicts exponential behavior in the limit of $\alpha \ll 1$. Direct solution of the particle orientational distribution function for the case of non-interacting particles yields exponential decay regardless of the magnitude of the initial field [159], hence indicating that the Sh'01 equation incorrectly predicts the dynamic response of dilute ferrofluids to a step decrease in the magnetic field strength.

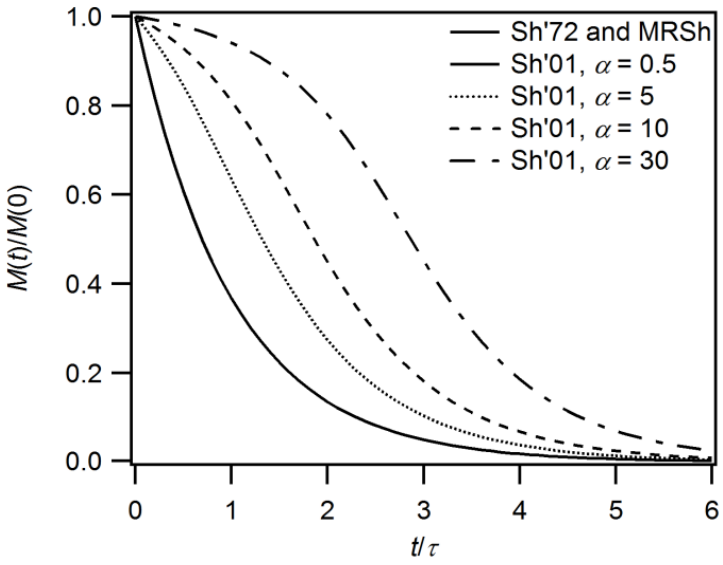

Figure A.0.1-Transient magnetization for an infinitely dilute ferrofluid according to the Sh'72, MRSh, and Sh'01 magnetization relaxation equations. The Sh'72 and MRSh equations both predict exponential decay regardless of the magnitude of the initial equilibrium magnetic field, whereas the Sh'01 equation only predicts exponential decay for small values of the initial equilibrium magnetic field (small values of α).

REFERENCES

[1] R. E. Rosensweig, *Ferrohydrodynamics*. New York: Cambridge University Press, 1985.

[2] C. Rinaldi, T. Franklin, M. Zahn, and T. Cader, "Magnetic nanoparticles in fluid suspension: Ferrofluid applications," in *Encyclopedia of Nanoscience and Nanotechnology*, ed: Marcel Dekker, Inc., 2004, pp. 1-18.

[3] K. Raj, B. Moskowitz, and R. Casciari, "Advances in ferrofluid technology," *Journal of Magnetism and Magnetic Materials,* vol. 149, pp. 174-180, 1995.

[4] K. Raj and R. Moskowitz, "Commercial applications of ferrofluids," *Journal of Magnetism and Magnetic Materials,* vol. 85, pp. 233-245, 1990.

[5] A. P. Singh, M. Mishra, A. Chandra, and S. K. Dhawan, "Graphene oxide/ferrofluid/cement composites for electromagnetic interference shielding application," *Nanotechnology,* vol. 22, p. 465701, 2011.

[6] R. Ravaud, G. Lemarquand, and V. Lemarquand, "Mechanical properties of ferrofluid applications: Centering effect and capacity of a seal," *Tribology International,* vol. 43, pp. 76-82, 2010.

[7] J. Chen, Z. Yan, R. Liu, N. Wang, J. Li, and Z. Wang, "Magnetic fluid-modeled microgravity: A novel way to treat tumor," *Medical Hypotheses,* vol. 77, pp. 953-955, 2011.

[8] L.-Y. Zhang, H.-C. Gu, and X.-M. Wang, "Magnetite ferrofluid with high specific absorption rate for application in hyperthermia," *Journal of Magnetism and Magnetic Materials,* vol. 311, pp. 228-233, 2007.

[9] M. Latorre-Esteves, A. Cortes, M. Torres-Lugo, and C. Rinaldi, "Synthesis and characterization of carboxymethyl dextran-coated Mn/Zn ferrite for biomedical applications," *Journal of Magnetism and Magnetic Materials,* vol. 321, pp. 3061-3066, Oct 2009.

[10] T.-Y. Liu, S.-H. Hu, S.-H. Hu, S.-P. Tsai, and S.-Y. Chen, "Preparation and characterization of thermal-sensitive ferrofluids for drug delivery application," *Journal of Magnetism and Magnetic Materials,* vol. 310, pp. 2850-2852, 2007.

[11] C. Bussy, C. Alexiou, R. A. Petros, A. M. Nyström, L. Methven, and K. Kostarelos, "Chapter 16 - Therapeutic Applications," in *Adverse Effects of Engineered Nanomaterials*, ed Boston: Academic Press, 2012, pp. 285-313.

[12] A. Chaves, C. Rinaldi, S. Elborai, X. He, and M. Zahn, "Bulk flow in ferrofluids in a uniform rotating magnetic field," *Physical Review Letters,* vol. 96, p. 194501, 2006.

[13] V. L. Calero-DdelC, C. Rinaldi, and M. Zahn, "Magnetic fluids and nanoparticle based sensors," in *Encyclopedia of Sensors*. vol. 5, C. A. Grimes, E. C. Dickey, and M. V. Pishko, Eds., ed: American Scientific Publishers, 2006, pp. 389-401.

[14] C. Rinaldi, F. Gutman, X. He, A. D. Rosenthal, and M. Zahn, "Torque measurements on ferrofluid cylinders in rotating magnetic fields," *Journal of Magnetism and Magnetic Materials,* vol. 289, pp. 307-310, 2005.

[15] S. R. Strand and S. Kim, "Dynamics and rheology of a dilute suspension of dipolar nonspherical particles in an external field: Part 1. Steady shear flows.," *Rheologica Acta,* vol. 31, pp. 94-117, 1992.

[16] D. Borin, A. Zubarev, D. Chirikov, R. Müller, and S. Odenbach, "Ferrofluid with clustered iron nanoparticles: Slow relaxation of rheological properties under joint action of shear

flow and magnetic field," *Journal of Magnetism and Magnetic Materials,* vol. 323, pp. 1273-1277, 2011.
[17] O. Volkova, S. Cutillas, P. Carletto, G. Bossis, A. Cebers, and A. Meunier, "Flow-induced structures in magnetorheological suspensions," *Journal of Magnetism and Magnetic Materials,* vol. 201, pp. 66-69, 1999.
[18] C. Rinaldi, A. Chaves, S. Elborai, X. He, and M. Zahn, "Magnetic fluid rheology and flows," *Current Opinion in Colloid and Interface Science,* vol. 10, pp. 141-157, 2005.
[19] P. Ilg and M. Kröger, "Magnetization dynamics, rheology, and an effective description of ferromagnetic units in dilute suspension," *Physical Review E,* vol. 66, p. 021501, 2002.
[20] L. M. Pop, S. Odenbach, A. Wiedenmann, N. Matoussevitch, and H. Bönnemann, "Microstructure and rheology of ferrofluids," *Journal of Magnetism and Magnetic Materials,* vol. 289, pp. 303-306, 2005.
[21] A. Yu Zubarev and L. Yu Iskakova, "On the theory of rheological properties of magnetic suspensions," *Physica A: Statistical Mechanics and its Applications,* vol. 382, pp. 378-388, 2007.
[22] R. Y. Hong, Z. Q. Ren, Y. P. Han, H. Z. Li, Y. Zheng, and J. Ding, "Rheological properties of water-based Fe3O4 ferrofluids," *Chemical Engineering Science,* vol. 62, pp. 5912-5924, 2007.
[23] P. Rajinder, *Rheology of particulate dispersions and composites* vol. 136. Boca Raton: CRC Press, 2007.
[24] G. Bossis, E. Lemaire, C. Mathis, Z. Mimouni, and C. Paparoditis, "Magnetoviscosity of colloidal suspensions," *Progress in Colloid and Polymer Science,* vol. 81, p. 251, 1990.
[25] X. He, S. Elborai, D. Kim, S. Lee, and M. Zahn, "Effective magnetoviscosity of planar-Couette magnetic fluid flow," *Journal of Applied Physics,* vol. 97, p. 10Q302, 2005.
[26] A. Zeuner, R. Richter, and I. Rehberg, "Experiments on negative and positive magnetoviscosity in an alternating magnetic field," *Physical Review E,* vol. 58, p. 6287, 1998.
[27] M. I. Shliomis and K. I. Morozov, "Negative viscosity of ferrofluid under alternating magnetic field," *Physics of Fluids,* vol. 6, pp. 2855-2861, 1994.
[28] J. C. Bacri, R. Perzynski, M. I. Shliomis, and G. I. Burde, ""Negative-viscosity" effect in a magnetic fluid," *Physical Review Letters,* vol. 75, pp. 2128-2131, 1995.
[29] H. Morimoto, T. Maekawa, and Y. Matsumoto, "Nonequilibrium Brownian dynamics analysis of negative viscosity induced in a magnetic fluid subjected to both ac magnetic and shear flow fields," *Physical Review E,* vol. 65, p. 061508, 2002.
[30] R. E. Rosensweig, J. Popplewell, and R. J. Johnston, "Magnetic fluid motion in rotating field," *Journal of Magnetism and Magnetic Materials,* vol. 85, pp. 171-180, 1990.
[31] C. Rinaldi, A. Chaves, S. Elborai, X. W. He, and M. Zahn, "Magnetic fluid rheology and flows," *Current Opinion in Colloid & Interface Science,* vol. 10, pp. 141-157, Oct 2005.
[32] J. P. Embs, S. May, C. Wagner, A. V. Kityk, A. Leschhorn, and M. L. Lücke, "Measuring the transverse magnetization of rotating ferrofluids," *Physical Review E,* vol. 73, p. 036302, 2006.
[33] A. Chaves, I. Torres-Diaz, and C. Rinaldi, "Flow of ferrofluid in an annular gap in a rotating magnetic field," *Physics of Fluids,* vol. 22, Sep 2010.
[34] P. C. Fannin and S. W. Charles, "The study of ferrofluid exhibiting both Brownian and Néel relaxation," *Journal of Physics D: Applied Physics,* vol. 22, p. 187, 1989.
[35] R. Mazo, *Brownian Motion: Fluctuations, Dynamics and Applications* vol. 112. New

York: Oxford University Press, 2002.
[36] M. I. Shliomis and V. I. Stepanov, "Rotational viscosity of magnetic fluids: contribution of the Brownian and Néel relaxational processes," *Journal of Magnetism and Magnetic Materials,* vol. 122, pp. 196-199, 1993.
[37] M. I. Shliomis and V. I. Stepanov, "Theory of the Dynamic Susceptibility of Magnetic Fluids," in *Advances in Chemical Physics*, ed: John Wiley & Sons, Inc., 2007, pp. 1-30.
[38] C. Scherer and H.-G. Matuttis, "Rotational dynamics of magnetic particles in suspensions," *Physical Review E,* vol. 63, p. 011504, 2000.
[39] W. T. Coffey and P. C. Fannin, "Internal and Brownian mode-coupling effects in the theory of magnetic relaxation and ferromagnetic resonance of ferrofluids," *Journal of Physics: Condensed Matter,* vol. 14, p. 3677, 2002.
[40] R. Kötitz, W. Weitschies, L. Trahms, and W. Semmler, "Investigation of Brownian and Néel relaxation in magnetic fluids," *Journal of Magnetism and Magnetic Materials,* vol. 201, pp. 102-104, 1999.
[41] A. B. Pakhomov, Y. Bao, and K. M. Krishnan, "Effects of surfactant friction on Brownian magnetic relaxation in nanoparticle ferrofluids," *Journal of Applied Physics,* vol. 97, p. 10Q305, 2005.
[42] A. S. Almusallam and D. S. Sholl, "Brownian dynamics simulations of copolymer-stabilized nanoparticles in the presence of an oil–water interface," *Journal of Colloid and Interface Science,* vol. 313, pp. 345-352, 2007.
[43] D. L. Ermak and J. A. McCammon, "Brownian dynamics with hydrodynamics interactions," *Journal of Chemical Physics,* vol. 69, pp. 1352-1359, 1978.
[44] A. S. Almusallam and D. S. Sholl, "Brownian dynamics study of polymer-stabilized nanoparticles," *Nanotechnology,* vol. 16, p. S409, 2005.
[45] G. Mériguet, M. Jardat, and P. Turq, "Brownian dynamics investigation of magnetization and birefringence relaxation in ferrofluids," *Journal of Chemical Physics,* vol. 123, p. 144915, 2005.
[46] R. E. Rosensweig, R. Kaiser, and G. Miskolczy, "Viscosity of magnetic fluid in a magnetic field," *Journal of Colloid and Interface Science,* vol. 29, pp. 680-686, 1969.
[47] J. P. McTague, "Magnetoviscosity of magnetic colloids," *Journal of Chemical Physics,* vol. 51, pp. 133-136, 1969.
[48] M. A. Martsenyuk, Y. L. Raikher, and M. I. Shliomis, "On the kinetics of magnetization of suspensions of ferromagnetic particles," *Soviet Physics JETP,* vol. 38, p. 413, 1974.
[49] M. I. Shliomis, "Effective viscosity of magnetic suspensions," *Soviet Physics JETP,* vol. 34, pp. 1291-1294, 1972.
[50] M. I. Shliomis, "Comment on "Magnetoviscosity and relaxation in ferrofluids"," *Physical Review E,* vol. 64, pp. 063501-1, 2001.
[51] M. I. Shliomis, "Ferrohydrodynamics: Testing a third magnetization equation," *Physical Review E,* vol. 64, p. 060501, 2001.
[52] E. Blums, A. Cebers, and M. M. Maiorov, *Magnetic Fluids*. Berlin: Walter de Gruyter, 1997.
[53] S. Odenbach, *Magnetoviscous effects in ferrofluids*. Berlin: Springer, 2002.
[54] S. Odenbach, *Ferrofluids*. Berlin: Springer, 2002.
[55] S. Odenbach and K. H. J. Buschow, "chapter 3 Ferrofluids," in *Handbook of Magnetic Materials*. vol. Volume 16, ed: Elsevier, 2006, pp. 127-208.
[56] M. P. Allen and D. J. Tildesley, *Computer Simulation of Liquids*. London: Academic Press,

1987.
[57] A. Hijazi and M. Zoaeter, "Brownian dynamics simulation for rod-like particles in dilute flowing solutions," *European Polymer Journal,* vol. 38, pp. 2207-2211, 2002.
[58] A. O. Ivanov, S. S. Kantorovich, E. N. Reznikov, C. Holm, A. F. Pshenichnikov, A. V. Lebedev, A. Chremos, and P. J. Camp, "Magnetic properties of polydisperse ferrofluids: A critical comparison between experiment, theory, and computer simulation," *Physical Review E,* vol. 75, p. 061405, 2007.
[59] J. H. Sanchez and C. Rinaldi, "Magnetoviscosity of dilute suspensions of magnetic ellipsoids obtained through rotational Brownian dynamics simulations," *Journal of Colloid and Interface Science,* vol. 331, p. 500, 2009.
[60] C. Scherer, "Computer simulation of the stochastic dynamics of super-paramagnetic particles in ferrofluids," *Brazilian Journal of Physics,* vol. 36, pp. 676-681, 2006.
[61] D. Soto-Aquino and C. Rinaldi, "Magnetoviscosity in dilute ferrofluids from rotational Brownian dynamics simulations," *Physical Review E,* vol. 82, Oct 2010.
[62] A. O. Tsebers, "Numerical experiments on the simulation of the rotational brownian motion of a ferromagnetic particle in a field," *Magnetohydrodynamics,* vol. 20, p. 343, 1985.
[63] S. Yamamoto and T. Matsuoka, "Viscosity of dilute suspensions of rodlike particles: A numerical simulation method," *Journal of Chemical Physics,* vol. 100, pp. 3317-3324, 1994.
[64] H. Goldstein, C. Poole, and J. Safko, *Classical Mechanics,* Third ed. San Francisco: Addison Wesley, 2002.
[65] E. Dickinson, "Brownian dynamics with rotation-translation coupling," *Journal of the Chemical Society, Faraday Transactions 2,* vol. 81, pp. 591-601, 1985.
[66] H. Brenner and D. W. Condiff, "Transport mechanics in systems of orientable particles III. Arbitrary particles," *Journal of Colloid and Interface Science,* vol. 41, pp. 228-274, 1972.
[67] B. U. Felderhof, "Magnetoviscosity and relaxation in ferrofluids," *Physical Review E,* vol. 62, p. 3848, 2000.
[68] P. Ilg, "Importance of depletion interactions for structure and dynamics of ferrofluids," *European Physical Journal E,* vol. 26, p. 169, 2008.
[69] H. C. Weng, C.-L. Chen, and C. o.-K. Chen, "Non-Newtonian flow of dilute ferrofluids in a uniform magnetic field," *Physical Review E,* vol. 78, p. 056305, 2008.
[70] H. W. Müller and M. Liu, "Structure of ferrofluid dynamics," *Physical Review E,* vol. 64, p. 061405, 2001.
[71] S. Odenbach and H. Stork, "Shear dependence of field-induced contributions to the viscosity of magnetic fluids at low shear rates," *Journal of Magnetism and Magnetic Materials,* vol. 183, p. 188, 1998.
[72] L. M. Pop, J. Hilljegerdes, S. Odenbach, and A. Wiedenmann, "The microstructure of frerrofluids and their rheological properties," *Applied Organometallic Chemistry,* vol. 18, p. 523, 2004.
[73] L. Vekas, D. Bica, I. Potencz, D. Gheorghe, O. Balu, and M. Raisa, "Concentration and composition dependence of rheological and magnetorheological properties of some magnetic fluids," *Progress in Colloid and Polymer Science,* vol. 117, p. 104, 2001.
[74] J. Vicente, M. T. López, J. D. G. Durán, and F. C. González, "Shear flow behavior of confined magnetorheological fluids at low magnetic fieldstrenghts," *Rheologica Acta,* vol. 44, p. 94, 2004.

[75] A. R. Altenberger and J. S. Dahler, "A renormalization group calculation of the viscosity of a hard-sphere suspension," *Journal of Colloid and Interface Science,* vol. 189, p. 379, 1997.
[76] N. Andhariya, B. Chudasama, R. Patel, R. V. Upadhyay, and R. V. Mehta, "Field induced rotational viscosity of ferrofluid: Effect of capillary size and magnetic field direction," *Journal of Colloid and Interface Science,* vol. 323, p. 153, 2008.
[77] R. Patel, R. V. Upadhyay, and R. V. Mehta, "Viscosity measurements of a ferrofluid: comparison with various hydrodynamics equations," *Journal of Colloid and Interface Science,* vol. 263, p. 661, 2003.
[78] A. Chaves, M. Zahn, and C. Rinaldi, "Spin-up flow of ferrofluids: Asymptotic theory and experimental measurements," *Physics of Fluids,* vol. 20, p. 053102, 2008.
[79] A. Satoh and M. Ozaki, "Transport coefficients and orientational distributions of spheroidal particles with magnetic moment normal to the particle axis (Analysis for an applied magnetic field normal to the shear plane)," *Journal of Colloid and Interface Science,* vol. 298, p. 957, 2006.
[80] A. Satoh, "Rheological properties and orientational distribution of dilute ferromagnetics spherocylinders particles dispersions," *Journal of Colloid and Interface Science,* vol. 234, pp. 425-433, 2001.
[81] J. H. Sanchez and C. Rinaldi, "Magnetoviscosity of dilute magnetic fluids in oscillating and rotating magnetic fields," *Physics of Fluids,* vol. 22, p. 043304, 2010.
[82] ed, See EPAPS Document No. [number will be inserted by publisher] for calculated values of the magnetoviscosity over a range of values of the Langevin parameter and rotational Peclet number. For more information on EPAPS, see http://www.aip.org/pubservs/epaps.html.
[83] M. I. Shliomis, "On "Maxwell's equations and vorticity: A note on the viscosity of magnetic fluids"," *Journal of Magnetism and Magnetic Materials,* vol. 159, pp. 236-237, 1996.
[84] D. J. Klingenberg, "Mason Number for Magnetorheology," *J. Rheol.,* vol. 51, p. 883, 2007.
[85] B.-J. d. Gans, H. Hoekstra, and J. Mellema, "Non-linear magnetorheological behaviour of an inverse ferrofluid," *Faraday Discuss,* vol. 112, p. 209, 1999.
[86] D. J. Klingenberg, J. C.Ulicny, and M. A. Golden, "Mason number for magnetorheology," *Journal of Rheology,* vol. 51, p. 883, 2007.
[87] M. T. L. López, J. D. G. Durán, Á. V. Delgado, and F. G. Caballero, "Scaling between viscosity and hydrodynamic / magnetic forces in magnetic fluids," *Croatica Chemica Acta,* vol. 80, p. 445, 2007.
[88] O. G. Calderón and S. Melle, "Dynamics of simple magnetorheological suspensions under rotating magnetic fields with modulated Mason number," *Journal of Physics D: Applied Physics,* vol. 35, p. 2492, 2002.
[89] J. H. Sánchez and C. Rinaldi, "Magnetoviscosity of dilute suspensions of magnetic ellipsoids obtained through rotational Brownian dynamics simulations," *Journal of Colloid and Interface Science,* vol. 331, pp. 500-506, 2009.
[90] A. O. Ivanov, S. S. Kantorovich, E. N. Reznikov, C. Holm, A. F. Pshenichnikov, A. V. Lebedev, A. Chremos, and P. J. Camp, "Magnetic properties of polydisperse ferrofluids: A critical comparison between experiment, theory, and computer simulation," *Physical Review E* vol. 75, p. 061405 2007.

[91] D. Y. Borin and S. Odenbach, "Magnetic measurements on frozen ferrofluids as a method for estimating the magnetoviscous effect," *Journal of Physics: Condensed Matter,* vol. 21, p. 246002, 2009.
[92] H. Shahnazian and S. Odenbach, "Rheological investigations of ferrofluids with a shear stress controlled rheometer," *Journal of Physics: Condensed Matter,* vol. 20, p. 204137, 2008.
[93] Y. L. Raikher and M. I. Shliomis, "On the kinetics of establishment of the equilibrium concentration in a magnetic suspension," *Journal of Magnetism and Magnetic Materials,* vol. 122, pp. 93-97, 1993.
[94] A. Zubarev and L. Y. Iskakova, "On the theory of structural transformations in magnetic fluids," *Colloid Journal,* vol. 65, p. 703, 2003.
[95] J. A. Kupriyanova and A. V. Zatovsky, "On the theory of the orientation Brownian motion of anisotropic particles in the Couette flow," *Journal of Molecular Liquids,* vol. 127, pp. 102-104, 2006.
[96] D. Soto-Aquino and C. Rinaldi, "Magnetoviscosity in dilute ferrofluids from rotational Brownian dynamics simulations," *Physical Review E,* vol. 82, p. 046310.
[97] B. U. Felderhof, "Magnetoviscosity of a ferrofluid in an oscilating field," *Magnetohydrodynamics,* vol. 36, p. 307, 2001.
[98] H. Brenner, "Rheology of a dilute suspension of dipolar spherical particles in an external field," *Journal of Colloid and Interface Science,* vol. 32, pp. 141-158, 1970.
[99] H. Brenner and M. H. Weissman, "Rheology of a dilute suspension of dipolar spherical particles in an external field. II. Effects of rotary Brownian motion," *Journal of Colloid and Interface Science,* vol. 41, pp. 499-531, 1972.
[100] V. M. Zaitsev and M. I. Shliomis, "Entrainment of ferromagnetic suspension by a rotating field," *Journal of Applied Mechanics and Technical Physics,* vol. 10, pp. 696-700, 1969.
[101] S. Rhodes, X. He, S. Elborai, S.-H. Lee, and M. Zahn, "Magnetic fluid behavior in uniform DC, AC, and rotating magnetic fields," *Journal of Electrostatics,* vol. 64, p. 513, 2006.
[102] D. Soto-Aquino and C. Rinaldi, "Transient magnetoviscosity of dilute ferrofluids," *Journal of Magnetism and Magnetic Materials,* vol. 323, pp. 1319-1323.
[103] R. G. Larson, *The Structure and Rheology of Complex Fluids*: Oxford University Press, USA, November 1998.
[104] C. Collaboration, "Time reconstruction and performance of the CMS electromagnetic calorimeter," *Journal of Instrumentation,* vol. 5, p. T03011, 2010.
[105] J. Claracq, J. Sarrazin, and J.-P. Montfort, "Viscoelastic properties of magnetorheological fluids," *Rheologica Acta,* vol. 43, pp. 38-49, 2004.
[106] D. J. Klingenberg, "Simulation of the dynamic oscillatory response of electrorheological suspensions: Demonstration of a relaxation mechanism," *Journal of Rheology,* vol. 37, pp. 199-214, 1993.
[107] M. Parthasarathy and D. J. Klingenberg, "Electrorheology: Mechanisms and models," *Materials Science and Engineering: R: Reports,* vol. 17, pp. 57-103, 1996.
[108] H. Kanai and T. Amari, "Strain-thickening transition in ferric-oxide suspensions under oscillatory shear," *Rheologica Acta,* vol. 32, pp. 539-549, 1993.
[109] W. H. Li, H. Du, and N. Q. Guo, "Dynamic behavior of MR suspensions at moderate flux densities," *Materials Science and Engineering: A,* vol. 371, pp. 9-15, 2004.
[110] B. J. de Gans, C. Blom, A. P. Philipse, and J. Mellema, "Linear viscoelasticity of an

inverse ferrofluid," *Physical Review E,* vol. 60, pp. 4518-4527, 1999.
[111] J. Ramos, J. de Vicente, and R. Hidalgo-Alvarez, "Small-Amplitude Oscillatory Shear Magnetorheology of Inverse Ferrofluids," *Langmuir,* vol. 26, pp. 9334-9341.
[112] S. T. Milner, "Relating the shear-thinning curve to the molecular weight distribution in linear polymer melts," *Journal of Rheology,* vol. 40, pp. 303-315, 1996.
[113] B. S. Chae, A. M. Lane, and J. M. Wiest, "On the Cox-Merz rule for magnetic dispersions," *Rheologica Acta,* vol. 40, pp. 599-602, 2001.
[114] M. Pinho, B. Brouard, J. M. Génevaux, N. Dauchez, O. Volkova, H. Mézière, and P. Collas, "Investigation into ferrofluid magnetoviscous effects under an oscillating shear flow," *Journal of Magnetism and Magnetic Materials,* vol. 323, pp. 2386-2390, 2011.
[115] R. Moskowitz and R. E. Rosensweig, "Nonmechanical torque-driven flow of a ferromagnetic fluid by an electromagnetic field," *Applied Physics Letters,* vol. 11, pp. 301-303, 1967.
[116] S. Khushrushahi and M. Zahn, "Ultrasound velocimetry of ferrofluid spin-up flow measurements using a spherical coil assembly to impose a uniform rotating magnetic field," *Journal of Magnetism and Magnetic Materials,* vol. 323, pp. 1302-1308, 2011.
[117] M. M., H. H., N. T., K. R., and U. H., "Frequency Characteristics of Stiffness and Damping Effect of a Ferrofluid Bearing," *Tribology Letters,* vol. 15, pp. 97-105, 2003.
[118] W. P. Cox and E. H. Merz, "Correlation of dynamic and steady flow viscosities," *Journal of Polymer Science,* vol. 28, pp. 619-622, 1958.
[119] P. J. Blennerhassett, F. Lin, and P. J. Stiles, "Heat Transfer through Strongly Magnetized Ferrofluids," *Proc. R. Soc. Lond. A,* vol. 433, 1991
[120] R. Hergt, R. Hiergeist, M. Zeisberger, G. Glöckl, W. Weitschies, L. P. Ramirez, I. Hilger, and W. A. Kaiser, "Enhancement of AC-losses of magnetic nanoparticles for heating applications," *Journal of Magnetism and Magnetic Materials,* vol. 280, pp. 358-368, 2004.
[121] I. Hilger, W. Andr√§, R. Hergt, R. Hiergeist, H. Schubert, and W. A. Kaiser, "Electromagnetic Heating of Breast Tumors in Interventional Radiology: In Vitro and in Vivo Studies in Human Cadavers and Mice1," *Radiology,* vol. 218, pp. 570-575, February 1, 2001 2001.
[122] I. Baker, Q. Zeng, W. Li, and C. R. Sullivan, "Heat deposition in iron oxide and iron nanoparticles for localized hyperthermia," *Journal of Applied Physics,* vol. 99, pp. 08H106-3, 2006.
[123] P. Cantillon-Murphy, L. L. Wald, E. Adalsteinsson, and M. Zahn, "Heating in the MRI environment due to superparamagnetic fluid suspensions in a rotating magnetic field," *Journal of Magnetism and Magnetic Materials,* vol. 322, pp. 727-733.
[124] M. A. Giordano, G. Gutierrez, and C. Rinaldi, "Fundamental solutions to the bioheat equation and their application to magnetic fluid hyperthermia," *International Journal of Hyperthermia,* vol. 26, pp. 475-484, 2010.
[125] A. Jordan, R. Scholz, P. Wust, H. Fahling, and R. Felix, "Magnetic fluid hyperthermia (MHF): cancer treatment with AC magnetic field induced excitation of biocompatible superparamagnetic nanoparticles," *Journal of Magnetism and Magnetic Materials,* vol. 201, p. 413, 1999.
[126] A. Jordan, R. Scholza, K. Maier-Hauffb, M. Johannsenc, P. Wusta, J. Nadobnya, H. Schirrad, H. Schmidtd, S. Degerc, S. Loeningc, W. Lankschb, and R. Felixa, "Presentation of a new magnetic field therapy system for the treatment of human solid tumors with magnetic fluid hyperthermia " *Journal of Magnetism and Magnetic Materials,* vol. 225, p.

118 2001.
[127] R. Kappiyoor, "The effects of magnetic nanoparticle properties on magnetic fluid hyperthermia," *Journal of Applied Physics,* vol. 108, p. 094702, 2010.
[128] M. Latorre and C. Rinaldi, "Applications of Magnetic Nanoparticles in Medicine: Magnetic Fluid Hyperthermia," *Puerto Rico Health Sciences Journal,* vol. 28, pp. 227-238, 2009.
[129] H. L. Rodriguez-Luccioni, M. Latorre-Esteves, J. Mendez-Vega, O. Soto, A. R. Rodriguez, C. Rinaldi, and M. Torres-Lugo, "Enhanced reduction in cell viability by hyperthermia induced by magnetic nanoparticles," *International Journal of Nanomedicine,* vol. 6, pp. 373-380, 2011.
[130] B. Thiesen and A. Jordan, "Clinical applications of magnetic nanoparticles for hyperthermia," *International Journal of Hyperthermia,* vol. 24, pp. 467-474, 2008.
[131] Y. S. Kim and Y. H. Kim, "Application of ferro-cobalt magnetic fluid for oil sealing," *Journal of Magnetism and Magnetic Materials,* vol. 267, p. 105, 2003.
[132] R. Ravaud, G. Lemarquand, and V. Lemarquand, "Mechanical properties of ferrofluid applications: Centering effect and capacity of a seal," *Tribology International,* vol. 43, pp. 76-82.
[133] K. Raj and R. Moskowitz, "A review of damping applications of ferrofluids " *IEEE Transactions on Magnetics,* vol. 16, p. 5, 2003.
[134] J. Barclay, "Use of a ferrofluid as the heat exchange fluid in a magnetic refrigerator," *Journal of Applied Physics,* vol. 53, 1982.
[135] R. E. Rosensweig, "Heating magnetic fluid with alternating magnetic field," *Journal of Magnetism and Magnetic Materials,* vol. 252, pp. 370-374, 2002.
[136] M. Lajvardi, J. Moghimi-Rad, I. Hadi, A. Gavili, T. Dallali Isfahani, F. Zabihi, and J. Sabbaghzadeh, "Experimental investigation for enhanced ferrofluid heat transfer under magnetic field effect," *Journal of Magnetism and Magnetic Materials,* vol. 322, pp. 3508-3513, 2010.
[137] C. H. Li, P. Hodgins, and G. P. Peterson, "Experimental study of fundamental mechanisms in inductive heating of ferromagnetic nanoparticles suspension (Fe[sub 3]O[sub 4] Iron Oxide Ferrofluid)," *Journal of Applied Physics,* vol. 110, p. 054303, 2011.
[138] P. P. Vaishnava, R. Tackett, A. Dixit, C. Sudakar, R. Naik, and G. Lawes, "Magnetic relaxation and dissipative heating in ferrofluids," *Journal of Applied Physics,* vol. 102, p. 063914, 2007.
[139] P. C. Fannin, "Investigating magnetic fluids by means of complex susceptibility measurements," *Journal of Magnetism and Magnetic Materials,* vol. 258-259, pp. 446-451, 2003.
[140] P. C. Fannin, "Characterisation of magnetic fluids," *Journal of Alloys and Compounds,* vol. 369, pp. 43-51, 2004.
[141] P. C. Fannin, S. W. Charles, C. Mac Oireachtaigh, and S. Odenbach, "Investigation of possible hysteresis effects arising from frequency- and field-dependent complex susceptibility measurements of magnetic fluids," *Journal of Magnetism and Magnetic Materials,* vol. 302, pp. 1-6, 2006.
[142] P. C. Fannin, B. K. P. Scaife, A. T. Giannitsis, and S. W. Charles, "Determination of the radius of nano-particles in a magnetic fluid by means of a constant frequency measurement technique," *Journal of Physics D: Applied Physics,* vol. 35, pp. 1305-1310, 2002.

[143] K. Okawa, M. Sekine, M. Maeda, M. Tada, M. Abe, N. Matsushita, K. Nishio, and H. Handa, "Heating ability of magnetite nanobeads with various sizes for magnetic hyperthermia at 120 kHz, a noninvasive frequency," *Journal of Applied Physics,* vol. 99, pp. 08H102-3, 2006.
[144] R. R.E, "Heating magnetic fluid with alternating magnetic field," *Journal of Magnetism and Magnetic Materials,* vol. 252, pp. 370-374, 2002.
[145] Y. L. Raikher and V. I. Stepanov, "Absorption of AC field energy in a suspension of magnetic dipoles," *Journal of Magnetism and Magnetic Materials,* vol. 320, pp. 2692-2695, 2008.
[146] D. Soto-Aquino, D. Rosso, and C. Rinaldi, "Oscillatory shear response of dilute ferrofluids: Predictions from rotational Brownian dynamics simulations and ferrohydrodynamics modeling," *Physical Review E,* vol. 84, Nov 2011.
[147] R. Müller, R. Hergt, M. Zeisberger, and W. Gawalek, "Preparation of magnetic nanoparticles with large specific loss power for heating applications," *Journal of Magnetism and Magnetic Materials,* vol. 289, pp. 13-16, 2005.
[148] A. F. Pshenichnikov, "Equilibrium magnetization of concentrated ferrocolloids," *Journal of Magnetism and Magnetic Materials,* vol. 145, pp. 319-326, 1995.
[149] A. Zeuner, R. Richter, and I. Rehberg, "On the consistency of the standard model for magnetoviscosity in an alternating magnetic field," *Journal of Magnetism and Magnetic Materials,* vol. 201, pp. 191-194, 1999.
[150] E. Pyanzina, S. Kantorovich, J. J. Cerdà, and C. Holm, "Structure factor of ferrofluids with chain aggregates: Theory and computer simulations," *Journal of Magnetism and Magnetic Materials,* vol. 323, pp. 1263-1268, 2011.
[151] A. Y. Zubarev and L. Y. Iskakova, "Rheological properties of ferrofluids with drop-like aggregates," *Physica A: Statistical Mechanics and its Applications,* vol. 376, pp. 38-50, 2007.
[152] A. Y. Zubarev, J. Fleischer, and S. Odenbach, "Towards a theory of dynamical properties of polydisperse magnetic fluids: Effect of chain-like aggregates," *Physica A: Statistical Mechanics and its Applications,* vol. 358, pp. 475-491, 2005.
[153] A. Y. Zubarev, S. Odenbach, and J. Fleischer, "Rheological properties of dense ferrofluids. Effect of chain-like aggregates," *Journal of Magnetism and Magnetic Materials,* vol. 252, pp. 241-243, 2002.
[154] A. O. Ivanov and A. Y. Zubarev, "Non-linear evolution of a system of elongated droplike aggregates in a metastable magnetic fluid," *Physica A: Statistical Mechanics and its Applications,* vol. 251, pp. 348-367, 1998.
[155] A. Zubarev, "Statistical physics of non-dilute ferrofluids," in *Ferrofluids, Magnetically Controllable Fluids and Their Applications*, Springer, Ed., ed Berlin: S. Odenbach, 2002, pp. 202-230.
[156] D. V. Berkov, L. Y. Iskakova, and A. Y. Zubarev, "Theoretical study of the magnetization dynamics of nondilute ferrofluids," *Physical Review E,* vol. 79, p. 021407, 2009.
[157] G. Mériguet, M. Jardat, and P. Turq, "Structural properties of charge-stabilized ferrofluids under a magnetic field: A Brownian dynamics study," *Journal of Chemical Physics,* vol. 121, p. 6078, 2004.
[158] D. Frenkel and B. Smit, *Understanding Molecular Simulation*. San Diego: Academic Press, 2002.
[159] Y. P. Kalmykov and S. V. Titov, "Anisotropic rotational diffusion and transient nonlinear

responses of rigid macromolecules in a strong external electric field," *Journal of Chemical Physics*, vol. 126, p. 174903, 2007.